The Role of HMGB1 in Myocardial Infarction



Carl (Tzung Yuan) Lee

New College

A thesis submitted for the degree of

Doctor of Philosophy

Trinity 2024

Acknowledgements

I am deeply grateful to my parents and sisters for their unwavering support and guidance, which have been instrumental in shaping me into the person I am today.

I would especially like to thank my partner, Jia-Ling, for her help and support throughout my academic journey. Without her, I would not have made it this far.

Additionally, I extend my gratitude to the colleagues I have had the privilege of working alongside at VA Medical Hospital in Seattle. In particular, I am deeply indebted to Charlies Keelin, Dr. Kurt Strand, and Ben Brainard, among many others, for their invaluable contributions to my academic journey. Each of you has played a significant role in my success.

Furthermore, I would like to thank my PI and mentor, Professor Jagdeep Nanchahal, for his incredible guidance and support throughout my DPhil experience, which I will never forget. Under his countless hours of mentorship, I have developed immensely as a researcher. I would also like to thank Professor Mark Coles, who helped me gain admission to Oxford; without him, I would not have received this scholarship.

I'd like to express my appreciation to everyone at Kennedy for their wonderful friendship and support throughout the years. I am also grateful to

Dr. Kristoffer Petersson, Dr. David Johnson, Professor Carolyn Carr, Professor Paul Riley, and Professor Joseph Wu for their time, feedback, guidance, and friendship during my DPhil.

Finally, I'd like to thank Ana, Thea, Ray, Isolde, Kaitlyn, Shihong, Shiyan, Lynn, Nan, Matthias, Mathilde, Yonggang, and Alvaro for their friendship.

To the rest of the Kennedy faculty and staff, thank you for making the last few years an unforgettable and worthwhile experience.

Abstract

Coronary artery disease remains the leading cause of morbidity and mortality worldwide, and approximately 100,000 people in the UK suffer myocardial infarction (MI) every year. The mainstay of treatment for MI remains reperfusion. However, despite the therapeutic advances, approximately one-third of patients go on to develop heart failure. Animal models of MI have their limitations and *in vitro* models based on human cardiomyocytes provide additional valuable mechanistic insights. In this thesis, I describe how I developed a method to generate mature cardiomyocytes from human embryonic stem cells by culturing them in glucose-depleted and fatty acid-enriched media together with electrical stimulation. Next, I optimised an *in vitro* model of repeated cycles of hypoxia followed by normoxia to emulate ischaemia reperfusion injury and investigated the effects of fully reduced HMGB1 (FR-HMGB1) using this system. I found that HMGB1 reduced injury and improved cell survival by upregulating mitochondrial pathways in a mammalian target of rapamycin complex (mTORC) and peroxisome proliferator-activated receptor γ coactivator-1α-dependent manner. I also found that FR-HMGB1 reversed doxorubicin-induced cardiotoxicity, again through upregulation of mitochondrial pathways. Finally, I investigated the efficacy of a non-oxidisable HMGB1 construct (double Box B – dBB) and found that it was more effective than FR-HMGB1 in ameliorating the effects repeated cycles of hypoxia and doxorubicin. Taken together, my results show that HMGB1 constructs could be used to treat ischaemia-reperfusion injury following MI and doxorubicin-induced cardiotoxicity.

Table of Contents

ABBREVIATION 8

CHAPTER 1. INTRODUCTION 11

1.1. Introduction 11

1.1.1. The Social and Economic Burden of Cardiovascular Disease. 11

1.1.2. Pathophysiology of Myocardial Infarction 11

1.1.3. Mitochondria 12

1.1.4. Peroxisome Proliferator-Activated Receptor γ Coactivator-1α (PGC-1 α) 13

1.1.5. Therapeutic Challenges and Strategies 13

1.1.5.1. Exogenous Stem Cell Therapy 14

1.1.5.2. Targeting Endogenous Repair Mechanisms 14

1.1.6. High Mobility Group Box 1 (HMGB1) 15

1.1.6.1. FR-HMGB1 16

1.1.6.2. DS-HMGB1 16

17

1.1.6.3. Engineered HMGB1 18

1.1.6.4. Potential Mechanism of Action of Beneficial Effects of HMGB1 in MI 18

1.1.7. Stem Cells 21

1.2. Aim 21

CHAPTER 2. METHODS 22

2.2. Methods 22

2.2.1. HMGB1 and dBB 22

2.2.2. Cell Culture and Preparation of hESC-CM 22

2.2.3. hESC-CM Purification 23

2.2.4. hESC-CM Maturation 23

2.2.4. Contraction Assay and Phase-Contrast Imaging 23

2.2.5. Cardiac-Differentiation Efficiency 24

2.2.6. Hypoxia-Normoxia Cycle 24

2.2.7. Doxorubicin Cardiotoxicity Assay 24

2.2.8. siRNA Knockdown 25

2.2.9. Membrane Microarray Assay, ELISA Assay, and other Cellular Assays 26
2.2.10. Seahorse Analysis 28
2.2.11. Western Blots 28
2.2.12. Bulk RNA Sequencing 29
2.2.13. Measurement of PFA 30
2.2.14. Proinflammatory Cytokine Assay 30
2.2.15. hESC-Cardiomyocytes Immunofluorescent Staining 31
2.2.16. Rapamycin Treatment 31
2.2.17. Gene Expression Analysis 31
2.2.18. Statistical Analysis 33

CHAPTER 3. OPTIMISATION OF HUMAN EMBRYONIC STEM CELL-DERIVED CARDIOMYOCYTES **34**

3.1. Introduction **34**
3.1.1. Mouse Models of Myocardial Infarction 34
3.1.2. Human Cardiomyocyte Models 35
3.1.3. Limitations of Immature hESC and hiPSC and How They Can be Overcome 36

3.2. Results **37**
3.2.1. Phenotypic Analysis of Standard hESC-CM Culture Method 37
3.2.2. Immature hESC-CM are Unresponsive to Hypoxia 39
40
3.2.3. Maturation Using Fatty-acid Enriched Medium and Prolonged Culture Times 40
42
3.2.4. Impact of Electrical Stimulation on hESC-CM Maturity 42

44

3.3. Discussion **44**
3.3.1. Genetic and Metabolic Maturation Landscape of hESC-CM 44
3.3.2. Advancements in hESC-CM Maturation through Electrical Stimulation 46
3.3.3. Integrating Insights and Addressing Challenges in Cardiomyocyte Maturation 47

CHAPTER 4. THE EFFECT OF HMGB1 ON ISCHAEMIA-REPERFUSION (IR) INJURY. **48**

4.1. Introduction **48**
4.1.1. Ischaemia-Reperfusion 48
4.1.2. *In Vitro* Models of Emulating Ischaemia-Reperfusion (I/R) Injury 48
4.1.3. Severity of Hypoxia 49
4.1.4. Duration of Hypoxia and Normoxia 49
4.1.5. Multiple Cycles of Hypoxia-Reoxygenation 50
4.1.6. Alternative Methods for Inducing Hypoxia 50

4.2. Results **51**
4.2.1. Effect of Multiple Hypoxia-Normoxia Cycles on Cardiomyocytes 51
4.2.2. HMGB1 Reduces Hypoxia-Induced Injury 53
4.2.3. HMGB1 Facilitation of Energy Production Shift and Mitochondrial Function 56
4.2.4. Confirmation of the Role of mTOR in HMGB1-Regulated Pathways 58

59

4.3. Discussion **59**
4.3.1. Cardiomyocyte Responses to Multiple Cycles of Hypoxia-Normoxia 59
4.3.2. Effects of HMGB1 on Cardiomyocytes Subjected to Four Cycles of Hypoxia-Normoxia 61
4.3.3. Effects of HMGB1 on Cardiomyocyte Energy Dynamics 62
4.3.4. The Role of mTOR Pathway in the Heart 62

4.4. Conclusion **64**

CHAPTER 5. THE EFFECT OF HMGB1 AND DBB IN ISCHAEMIA-REPERFUSION (I/R) INJURY AND DOXORUBICIN-INDUCED CARDIOTOXICITY (DIC) **66**

5.1. Introduction **66**
5.1.1. Mechanism of Doxorubicin-Induced Cardiotoxicity (DIC) 67
5.1.2. Engineered HMGB1 67

5.2. Results **68**
5.2.1. dBB Retains Full Regenerative Capacity While Remaining Non-Oxidisable 68
5.2.2. HMGB1 Reduces Doxorubicin-Induced Cardiotoxicity (DIC) 71
73

5.2.3. dBB Demonstrates Comparable or Superior Efficacy in Reducing Hypoxia-Induced Injury Relative to HMGB1 73
5.2.4. dBB Facilitates Shifts of Energy Production and Enhances Mitochondrial Function 75

5.3. Discussion **77**
5.3.1. Engineered HMGB1 Variant, dBB 78
5.3.2. Doxorubicin-Induced Cardiotoxicity 79
5.3.3. dBB in Hypoxia Induced Injury 80

5.4. Conclusion **84**

CHAPTER 6. CONCLUDING DISCUSSION **85**

6.1. Discussion **85**
6.1.1. Summary 85
6.1.2. Limitation and Ethical Issue Relating to The Use of Human Embryonic Stem Cells 87
6.1.3. Future Work. 88

CHAPTER 7. REFERENCE **91**

Abbreviation

3D	three dimensional
3S-HMGB1	nonoxidisable HMGB1 mutant with serines replace all cysteines
Akt	protein kinase B
ATF	activating transcription factor
ATP	adenosine triphosphate
ATP2A2	ATPase sarcoplasmic/endoplasmic reticulum Ca2+ transporting 2
Bnip3L	Bcl-2/E1B 19 kDa-interacting protein 3-like protein
BOC	body-on-a-chip
BZ	border zone
CAD	coronary artery disease
CALM	calmodulin
$CoCl_2$	cobalt chloride
CXCL	chemokine (C-X-C motif) ligand
cTnI	cardiac troponin I
cTnT	cardiac troponin T
dBB	double box B
DMOG	dimethyloxalylglycine
DIC	doxorubicin-induced cardiotoxicity
DS-HMGB1	disulfide HMGB1
ELISA	enzyme-linked immunosorbent assay
ERK	extracellular signal-regulated kinase
ERR	estrogen-related receptors
FOXO1	forkhead Box O1
FR-HMGB1	fully reduced high mobility group box 1
G_0	quiescent phase
G_{Alert}	alert phase
GATA	GATA binding protein
GLUT1/4	glucose transporter-1/4
GR	glucocorticoid receptor
hESC	human embryonic stem cell
HFrEF	heart failure with reduced ejection fraction

HFpEF	heart failure with preserved ejection fraction
HIF1a	hypoxia inducible factor 1-alpha
hiPSC	human induced pluripotent stem cell
HMGB1	high mobility group box 1
HNF	hepatocyte nuclear factor
hESC-CM	human embryonic stem cell-derived cardiomyocytes
hiPSC-CM	human induced pluripotent stem cell-derived cardiomyocytes
IGF	insulin-like growth factor
IZ	ischaemic zone
I/R	ischaemia reperfusion
JNK	Jun N-terminal kinase
KCNJ2	potassium inwardly rectifying channel subfamily J member 2
KDR	kinase insert domain receptor
LAD	left anterior descending artery
MAP	microtubule associated protein
MEK	mitogen-activated protein kinase kinase
MI	myocardial infarction
MKK	MAP kinase kinase
mPTP	mitochondrial membrane pore
mTOR	mammalian target of rapamycin
mTORC	mammalian target of rapamycin complex
MYH	myosin heavy chain
MYL	myosin light chain
NAD	nicotinamide adenine dinucleotide
NADPH	nicotinamide adenine dinucleotide phosphate hydrogen
NF-κB	nuclear factor kappa B
Nkx2.5	NK2 Homeobox 5
NOX4	NADPH oxidase 4
NPPA	natriuretic peptide A
NRF1/2	nuclear respiratory factor 1/2
NSTEMI	non-ST segment elevation myocardial infarction
OCRs	oxygen consumption rates
OPA1	optic Atrophy 1

PCI	percutaneous intervention
PGC-1α/1b	peroxisome proliferator-activated receptor-gamma coactivator 1-alpha/beta
PHD	prolyl hydroxylase domain
PI3K	phosphatidylinositol 3-kinase
PL	permanent ligation
pO_2	oxygen partial pressure
PPAR	peroxisome proliferator-activated receptors
PPARGC1A	peroxisome proliferator-activated receptor gamma coactivator 1-alpha
RAGE	receptor for advanced glycation end products
ROS	reactive oxygen species
siRNA	small interfering RNA
SIRT1/3	sirtuin 1/3
STEMI	ST segment elevation myocardial infarction
TAC	thoracic artery constriction
TLR	Toll-like receptor
TNNT2	troponin T2
TOP1MT	DNA topoisomerase 1 mitochondrial
TOP2B	DNA topoisomerase 2 beta
TR	thyroid hormone receptors
TRIB3	tribbles homolog 3
YAP	yes-associated protein 1

Chapter 1. Introduction

1.1. Introduction

1.1.1. The Social and Economic Burden of Cardiovascular Disease.

Coronary artery disease (CAD) remains the leading cause of morbidity and mortality globally, with myocardial infarction (MI) representing the most severe manifestation. Every year, nearly 805,000 individuals suffer from MI in the United States, with an estimated 100,000 affected in the UK [1], [2-4]. These large numbers not only represent a significant health challenge but also have a profound socio-economic impact. Many patients suffer from long-term disabilities that lead to extended work absences or even premature retirement, resulting in an annual economic burden of approximately €282 billion in the European Union, encompassing healthcare costs, lost productivity, and related expenses [5].

Despite recent advancements in medical treatments for MI, including revascularisation through percutaneous intervention [6-8], around 30% of patients go on to develop heart failure, underscoring the need for more effective interventions [5, 9]. In the United States, healthcare costs associated with heart failure have reached $31 billion, while the five-year survival rate lingers at approximately 50% [4, 10]. This figure is notably lower than that for many cancers, emphasising the limited efficacy of current treatments [10-12].

1.1.2. Pathophysiology of Myocardial Infarction

MI can be broadly classified into ST elevation MI (STEMI) and non-ST elevation MI (NSTEMI). Since the mid-1990s, there has been a progressive decline in numbers of patients suffering STEMI and increase in the numbers with NSTEMI [1]. The pathogenesis of MI typically involves the rupture of a vulnerable atherosclerotic plaque within a coronary artery, exposing thrombogenic surfaces that activate local platelets and initiate thrombosis, culminating in vessel lumen occlusion. The extent of the resultant ischaemia depends on whether the occlusion is complete or partial, leading to oxygen and nutrient deprivation of the cardiac muscle and subsequent necrosis [13]. The severity and magnitude of the injury are determined by the duration of occlusion and the size of the ischaemic area. Patients suffering STEMI are now routinely treated by percutaneous coronary intervention (PCI)

whereby the circulation is restored. NSTEMI patients are often initially treated with antithrombotics to restore blood flow followed by PCI. However, reperfusion itself leads to reperfusion injury [13].

The progression to heart failure post-MI involves a complex interplay between biological and biomechanical factors, predominantly influenced by infarct expansion [14]. The initial event is death of cardiomyocytes in the ischaemic zone (IZ), followed by inflammation and remodelling, where damaged muscle is replaced by fibrous tissue [15, 16]. The myocardium adjacent to the ischaemic zone, known as the border zone (BZ), is subject to abnormal stress and strain due to the adjacent non-contractile tissue in the IZ. This in turn results in oxidative stress in the cardiomyocytes and activation of pro-inflammatory pathways in the border zone. Loss of functioning cardiomyocytes in the BZ leads to expansion of the infarct, with further decline in cardiac function, and eventual heart failure.

1.1.3. Mitochondria

Mitochondria occupy around 40% of the volume of cardiomyocytes, generating the 6 kg/day of ATP required by the heart each day [17, 18]. Following MI, cardiomyocytes switch from mitochondrial oxidative phosphorylation to anaerobic glycolysis [19]. Ischaemia also results in the accumulation of the citric acid cycle intermediate succinate as a result of reversal of succinic dehydrogenase. Whilst reperfusion following STEMI results in improved outcomes and is now standard of care [20], it leads to the rapid reoxidation of the succinate by succinic dehydrogenase, leading to the generation of Reactive Oxygen Species (ROS) by reverse electron transport at Mitochondrial Complex I [21]. Whilst the precise mechanism of cardiomyocyte necrosis is not fully understood, the following mechanism has been proposed. The switch to anaerobic respiration leads to build up of lactic acid. This results in intracellular acidosis, which the cell tries to correct by exchanging intracellular H^+ for extracellular Na^+. The high intracellular Na^+ triggers the Na^+/Ca^{2+} exchanger, leading to a build up of intracellular Ca^{2+}. The high intracellular Ca^{2+} leads to opening of the inner mitochondrial membrane pore (mPTP). Opening of the mPTP results in loss of the proton gradient across the inner mitochondrial membrane, causing cessation of ATP production. In addition, opening of the pore results in ingress of water into the mitochondria down the osmotic gradient, resulting in mitochondrial swelling, followed by mitochondrial rupture and cell necrosis [22]. Therefore, a number of strategies have been developed to target mitochondria,

including protection, promoting biogenesis, modulating mitochondrial dynamics and enhancing quality control [23]. The crucial role of mitochondria following MI has prompted clinical trials for the use of cyclosporin A to block mPTP [23]. Despite promising phase 2 data, the phase 3 trial in patients with STEMI cyclosporine A did not lead to improved outcomes compared to placebo [24]. Currently there is no approved therapeutic for protecting mitochondrial function following MI.

1.1.4. Peroxisome Proliferator-Activated Receptor γ Coactivator-1α (PGC-1 α)

The transcriptional coactivator PGC-1α plays a pivotal role in cell metabolism and is central to several mitochondrial pathways. It is involved in controlling a number of genes, including those related to fatty acid metabolism. PGC-1α also upregulates the activity of transcription factors for nuclear respiratory factors 1 and 2 (NRF1, NRF2) and estrogen-related receptor α (ERRα), which in turn upregulate expression of nuclear encoded genes necessary for mitochondrial oxidative phosphorylation [25]. PGC-1α also acts as a master regulator of mitochondrial biogenesis through coactivation of mitochondrial transcription factor A (Tfam), leading to the transcription and replication of mitochondrial DNA and nuclear genes related to mitochondria [26, 27]. mTORC1 increases expression of genes related to mitochondrial biogenesis through activation of the Ying Yang 1/ PGC-1α complex [28-30]. Cardiac-specific transgenic overexpression of PGC-1α resulted in markedly enhanced mitochondrial biogenesis [31]. Genetic deletion of PGC-1α did not lead to abnormalities of mitochondrial function under normal conditions, although it resulted in accelerated loss of cardiac function following pressure overload [32]. Surprisingly, PGC-1α transgenic overexpression was also detrimental in mouse models of heart failure induced by thoracic artery constriction [33], suggesting that PGC-1α expression is finely tuned in both magnitude and temporally [34].

1.1.5. Therapeutic Challenges and Strategies

Despite the improvement in primary prevention strategies and secondary intervention for MI [35] around a third of patients develop heart failure due to lack of approved therapeutics to prevent cardiomyocyte death and expansion of infarct. Hence, several strategies have been investigated to improve outcomes.

1.1.5.1. Exogenous Stem Cell Therapy

Over the past few decades, numerous attempts have been made to harness the repair and renewal potential of stem cells to overcome the cell death and fibrosis that usually occurs following tissue injury [36] [36]. However, whilst stem cell therapy has become the standard of care for some haematological disorders, there has been disappointing and conflicting clinicial results on enhancing the regeneration of solid organs, including the heart [37] [38, 39], despite the continuing scientific and public interest [40]. Strategies that rely on exogenously administered stem cells have found that they tend not to repopulate and repair the damaged and disease area due to the hostile inflammatory and fibrotic microenvironment [41, 42]. The few autologous stem cells that implant in the scarred host bed led to little improvement in overall function [43, 44]. In a mouse model of MI, two types of stem cells (fractionated bone marrow mononuclear cells or c-kit+ mesenchymal cells) that had been killed by freezing and thawing were found to be as 'effective' as live cells, the limited improvement being attributed to upregulation of the acute inflammatory wound healing response [45]. Studies in subhuman primates and clinical trials have reported significant adverse events, including arrhythmias following stem cell therapies for MI [38, 46, 47]. Even if the challenges associated with autologous stem cell therapies could be overcome, the costs would be prohibitive. Allogeneic cells could potentially address some of the issues of availability and cost. However, their use would entail immunosuppressive therapy[48], and safety concerns remain about induced pluripotent stem cells [41, 49].

1.1.5.2. Targeting Endogenous Repair Mechanisms

An alternative strategy, which overcomes many of the limitations described above of stem cell therapy for solid organs, is to promote repair by harnessing the regenerative potential of resident cells from solid organs [50] , including the heart [43]. The adult heart is generally considered a terminally differentiated organ and multiple studies have shown that only ~1% of cardiomyocytes replicate per year [51-53]. Whilst contribution of c-kit+ cardiac cells to regeneration has now been largely discounted [37], a small epicardial progenitor population has been identified [43]. However, their small numbers are unlikely to make a significant contribution to cardiac repair following MI [37]. Interestingly, the adult heart can repair and the available data would suggest that following injury, adult cardiomyocytes are capable of de-differentiation, proliferation and increase in the rate of cell cycling [54, 55] [56] [57] to

contribute to tissue healing. This capacity makes cardiomyocytes an ideal therapeutic target for promoting endogenous repair. By focusing on enhancing the regenerative potential of resident cardiac cells, this strategy offers a promising alternative to traditional stem cell therapies for cardiac repair [43, 50].

Due to our improved understanding of the signalling pathways that contribute to cardiac repair, a few strategies have emerged to target these endogenous repair pathways [58]. Cardiomyocyte proliferation has been shown to be controlled by the microRNA network [59-62] and the Hippo signalling pathway [63]. A recent attempt to promote cardiac repair by overexpression of microRNA-199a resulted in improved function in a pig model of MI [64]. However, uncontrolled proliferation of cardiomyocytes resulted in sudden death from arrhythmias after 7-8 weeks [64]. In addition to modulating cycling cardiomyocytes, alternative strategies targeting the CXCL12 or growth factors have also shown promise by stimulating angiogenesis and thereby reducing cardiomyocyte death [65]. To date, proangiogenic cytokines including vascular endothelial growth factor [66], hepatocyte growth factor [67], and CXCL12 [68] have shown encouraging pre-clinical results, but failed to result in significant clinical improvement [69]. Nonetheless, these studies show that the adult mammalian heart is capable of repairing through promoting cardiomyocyte proliferation or angiogenesis.

1.1.6. High Mobility Group Box 1 (HMGB1)

High mobility group box 1 (HMGB1) is the most abundant non-histone protein in the nucleus, with about one million copies per cells. Here it regulates transcription, DNA replication and repair. It belongs to a class of molecules called alarmins which when it is released into the extracellular space have additional signalling roles and HMGB1 has long been known as a mediator of inflammatory organ damage[70]. HMGB1 release is recognised as a danger signal upon cell death and tissue injury, binding to Toll-like receptor 4 (TLR-4), Toll-like receptor 2 (TLR-2), and receptor for advanced glycation end-products (RAGE) to promote inflammatory signalling [71, 72]. Consistent with this, several studies have shown that the administration of exogenous HMGB1 leads to increase in infarct size and deterioration of cardiac function in permanent ligation (PL) and ischaemia reperfusion (I/R) models of MI in mice [73]. However, other studies suggest that HMGB1 may have a protective role following I/R injury [74, 75]. The apparent discrepancy between the findings from these studies by be

explained by the redox state of HMGB1. Fully reduced HMGB1 (FR-HMGB1) has been shown to promote chemotaxis, whereas the partially oxidised disulfide form HMGB1 (DS-HMGB1) is proinflammatory [76].

1.1.6.1. FR-HMGB1

The redox status of HMGB1 determines the confirmation of the molecule and hence the receptors to which it binds. The HMGB1 in the nucleus is the fully-reduced form. Interestingly, cardiac specific transgenic overexpression of HMGB1 resulted in decreased infarct size and improved cardiac function [77]. Our group has previously shown that FR-HMGB1 forms a heterocomplex with CXCL12. This heterocomplex binds to the cell surface receptor CXCR4. Exogenous administration of FR-HMGB1 resulted in accelerated the repair of multiple tissues (bone, skeletal muscle, blood) by transitioning CXCR4-expressing endogenous stem cells to a state termed G_{Alert}, which is intermediate between the deeply quiescent G_0 and fully activated G_1 [78]. Several other studies have also shown that the CXCL12-CXCR4 axis plays an important role in tissue repair [79] [80] [81, 82]. Our group subsequently found that administration of FR-HMGB1 iv at the time of injury resulted in ~60% improvement in ejection fraction over a 5-week period and a similar decrease in infarct size in a murine model using permanent ligation of the left anterior descending artery (Fig. 1). Together these studies illustrate the potential utility of FR-HMGB1 to preserve function following MI.

1.1.6.2. DS-HMGB1

FR-HMGB1 can be oxidised to DS-HMGB1 in an inflammatory environment with the formation of a disulfide bond forms between C23 to C45 in the Box A domain [76, 83]. DS-HMGB1 can also be secreted by inflammatory immune cells [70]. Unlike FR-HMGB1, DS-HMGB1 has a higher affinity for TLR-2, TLR-4, and RAGE, resulting in release of pro-inflammatory cytokines via the NF-κB pathway [70, 84]. Several studies examining the effects of HMGB1 on the heart failed to report the redox status of the molecule. Based on our current understanding, it is likely that those reporting a deleterious effect are likely to be using DS-HMGB1 [85, 86].

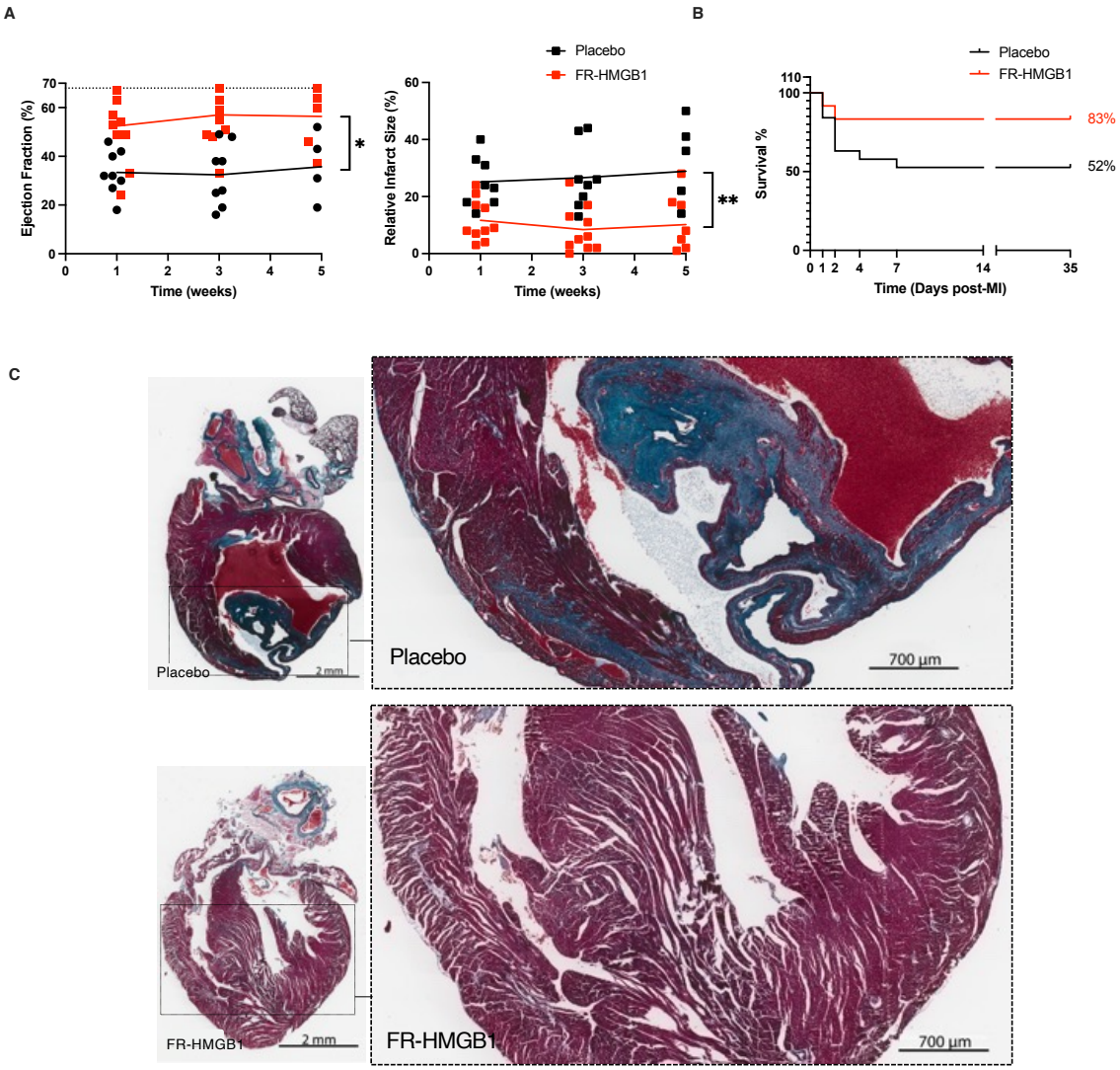

Figure 1. FR-HMGB1 Treatment Improves Cardiac Function and Survival After Myocardial Infarction

(A) Ejection fraction and relative infarct size over 5 weeks following permanent coronary artery ligation in C57BL/6 mice treated with a single intravenous dose of 1.2 mg/kg FR-HMGB1 or saline (placebo) at the time of injury. Individual data points are shown with connecting lines for means. Dotted line in the ejection fraction graph indicates normal ejection fraction in uninjured mice. **(B)** Kaplan-Meier survival curve for FR-HMGB1 and placebo-treated mice over 35 days post-myocardial infarction (MI), showing 83% and 52% survival rates, respectively. **(C)** Representative Masson's trichrome-stained heart sections at 5 weeks post-injury (muscle in red, fibrous tissue/scar in blue). Saline solution (placebo) treated hearts show thin, attenuated infarcts, while FR-HMGB1-treated hearts exhibit less scarring and preserved myocardium. Scale bars: 2 mm (left panels) and 700 µm (right panels). n = 8 for placebo group, n = 10 for FR-HMGB1 group. Statistical significance was determined by two-way ANOVA followed by the Sidak post-hoc test. For the survival study, Kaplan-Meier analysis was used. *p = 0.046 for ejection fraction at 5 weeks, **P = 0.004 for infarct size at 5 weeks.

1.1.6.3. Engineered HMGB1

The redox status of HMGB1 between reduced and disulfide forms of HMGB1 is reversible, depending on the level of oxidative stress during inflammatory responses and tissue repair. Therefore, to harness the regenerative potential of FR-HMGB1 and avoid inflammatory signalling, attempts have been made to engineer HMGB1 constructs that cannot be oxidised. One example involved replacing three cysteines in FR-HMGB1 with serines (3S-HMGB1), preventing the formation of disulfide bonds in the Box A domain. Exogenous administration of 3S-HMGB1 promoted regeneration of skeletal muscle and enhanced cell replication in the liver following injury [87]. Our group showed that like FR-HMGB1, exogenous administration of 3S-HMGB1 resulted in accelerated healing of bone, skeletal muscle and blood through transition of resident stem cells from G_0 to G_{Alert} [78]. However, in the heart, whilst intracardiac injection of FR-HMGB1 in the border zone 4 h after MI in a mouse model resulted in improved outcomes, 3S-HMGB1 was detrimental and resulted in increased fibrosis compared to placebo. Here 3S-HMGB1 was shown to promote cardiac fibroblast migration by the receptor CXCR4 without the involvement of CXCL12, unlike FR-HMGB1 [88]. DS-HMGB1 has also been shown to be a potent activator of platelets and thrombosis via RAGE [89].

1.1.6.4. Potential Mechanism of Action of Beneficial Effects of HMGB1 in MI

A number of studies have reported beneficial effects of intramyocardial injection after MI in mice [85, 90], rats [91, 92] and sheep [93], and also following intravenous administration in rats [94]. Whilst the majority of intramyocardial injections were administered 4 h after MI [95, 96], in one study beneficial effects were observed following administration 3 wk after MI [91]and another where the HMGB1 was injected 1 h before MI [97]. The reported mechanism of action varied across the studies.

1.1.6.4.1. Bone Marrow Derived c-kit$^+$ Cells

Following reports of self-renewing, multipotent c-kit$^+$ stem cells in the adult heart capable of giving rise to cardiomyocytes, smooth muscle and endothelial cells [98], it was reported in a murine model of MI that HMGB1 resulted in an increase in Ki67$^+$ cardiomyocyte population

due to the recruitment of bone marrow c-kit+ cells, implying de novo cardiomyogenesis from c-kit$^+$ cells [95]. In a follow up study, the same authors using a transcriptomics approach reported the role of upregulation of Notch signalling in the activation of the c-kit$^+$ cells [96]. A similar increase in Ki67+ cardiomyocytes and expression of c-kit was reported in a sheep model of MI [93]. However, cardiomyogenesis from c-kit+ cells have now been largely discounted [37, 99-102]. Using genetic lineage tracing, it has been shown that c-kit$^+$ cells contribute to less than 1 in 10,000 cells to the process of cardiomyogenesis following MI. It is likely that a subset of mature cardiomyocytes expressing c-kit may have explained the previous false positive results.

1.1.6.4.2. Bone Marrow-Derived PDGFRα_+ cells

Intravenous administration of HMGB1 for four consecutive days following MI in a rat model was reported to lead to enhanced outcomes as a result of recruitment of PDGFRα^+ cells from the bone marrow to the peri-infarct areas, leading to enhanced angiogenesis [103].

1.1.6.4.3. Angiogenesis

Angiogenesis is an important factor in recovery following MI, especially in the border zone [104]. A study in rats demonstrated that intravenous injection of HMGB1 prior to I/R enhanced cardiac function [94]. This improvement was attributed to protection against oxidative stress protection and increased VEGF expression [94]. In a sheep model, intramyocardial injection of HMGB1 4 h after MI was reported also reported to lead to upregulation of VEGF expression and vascular density [93]. In a mouse model of MI induced by permanent ligation of the left anterior descending artery, intramyocardial injection of HMGB1 1 hour before injury was reported to lead to enhanced cardiac function in part because of upregulation of HIF1α-induced angiogenesis as a result of the HMGB1 signalling via TLR-9 [97].

1.1.6.4.4. Cycling Cells

It has been shown that the adult mammalian heart can undergo repair through the contribution of pre-existing cardiomyocytes, which can be induced to proliferate through systemic hypoxaemia [105]. The authors studying the effects of HMGB1 in the sheep model of MI showed increased Ki67$^+$ cycling cardiomyocytes [93]. They also reported that HMGB1

led to enhanced expression of genes typically associated with cardiomyocyte progenitors, including *Tbx20, Nkx2.5*, and *Gata4*. This raises the intriguing possibility that HMGB1 can promote the re-entry of cardiomyocytes into the cell cycle and promote the progression of dedifferentiated cardiomyocytes into progenitor stages, which in turn can contribute to myocardial repair through the generation of additional mature cardiomyocytes.

1.1.6.4.5. Intracellular Signalling Pathways

A number of intracellular signalling pathways have been implicated in the positive effects reported in the heart following MI.

The MAP kinase pathway has four main branches, ERK, c-JNK, p38/MAPK and ERK5 [106]. Together they modulate a variety of pathways in the context of MI, including proliferation, growth and differentiation of resident cells. Activation of p38 can lead to apoptosis, inflammation and fibrosis. HMGB1 has been shown to reduce levels of phosphorylated p38, with concomitant reduction in levels of IL-6 and TNF in the circulation [107]. PI3K leads to activation of Akt, which in turn upregulates the proangiogenic pathways induced by VEGF and eNOS and downregulates FOXO, GSK3β and mTORC1 [106]. In a rat model of ischaemia reperfusion injury, HMGB1 resulted in reduced levels of phosphorylated PI3K and increased levels of HIF-1α [107]. The authors suggested that the enhanced levels of HIF-1α may be cardioprotective analogous to the effects of ischaemic preconditioning. It is difficult to reconcile the lower levels of phosphorylated PI3K and the expected subsequent downregulation of VEGF with the reports by others of higher levels of VEGF.

1.1.6.4.6. CXCL12

It has been well documented that FR-HMGB1 acts by forming a heterocomplex with CXCL12 [108]. Interestingly, a phase 2 clinical trial focusing on the over-expression of CXCL12 by direct endomyocardial delivery of a CXCL12-expressing plasmid in patients with established heart failure, while safe, failed to reach the primary endpoint of improvement in composite scores of heart function [68]. There was, however, a trend towards improvement both in the functional scores and left ventricular ejection fraction. Our group found that in a mouse model of fracture healing, exogenous administration of CXCL12 resulted in exuberant but disordered callus formation and no increase in breaking strength [78]. Taken together, these

results suggest that CXCL12 alone is unlikely to result in significant improvement in outcomes.

1.1.7. Stem Cells

At present, the isolated primary human cardiomyocytes cannot be cultured over a prolonged period, and human heart tissue is scarce [109]. Therefore, the human embryonic stem cell-derived cardiomyocytes (hESC-CM) and human induced pluripotent stem cell-derived cardiomyocytes (hiPSC-CM) are being increasingly used to study cardiac disease because of their availability, well-defined genetics, and being more representative of human biology than rodent models. Human embryonic stem cells and their cells derived have been extensively used to study cardiac disease in a controllable setting [110, 111]. Hence, I utilised the hESC-CM to elucidate the mechanism of action of HMGB1 *in vitro*.

1.2. Aim

Several studies have examined the effects of FR-HMGB1 on *in vivo* MI models and proposed a variety of mechanisms of action, but no study has been conducted to date using human cardiomyocytes. While mouse models provide invaluable insights into the *in vivo* processes over time, they do not model all aspects of the human condition. Therefore, it is essential to complement the findings from these models with *in vitro* data obtained using human cardiomyocytes. Furthermore, studies on cardiomyocytes permit a reductive approach to allow a detailed understanding of the mechanism of action.

My overall aim is to elucidate the mechanism of action of FR-HMGB1 using human cardiomyocytes.

Chapter 2. Methods

2.2. Methods

2.2.1. HMGB1 and dBB

High Mobility Group Box 1 (HMGB1) protein and its engineered variant, dBB, were produced in collaboration with the Centre for Medicines Discovery (CMD) at the University of Oxford. The production methods and molecular designs for HMGB1 and dBB have been patented by our research group (international publication number: WO 2021/094983 A1).

HMGB1 was expressed in *E. coli* and purified using a series of chromatographic steps, including affinity chromatography and size exclusion chromatography, to ensure high purity and biological activity. The dBB variant was engineered through site-directed mutagenesis of the HMGB1 sequence, with modifications designed to alter its redox sensitivity and receptor binding properties. Both proteins were characterized using mass spectrometry to confirm their molecular weights and purity. Their biological activities were verified using *in vitro* assays before use in experiments. Endotoxin levels were assessed using the Limulus Amebocyte Lysate (LAL) assay and confirmed to be below 0.1 EU/µg protein. For all experiments, HMGB1 and dBB were used at a final concentration of 1 µM unless otherwise stated. Protein solutions were prepared fresh for each experiment by diluting stock solutions (1 mg/mL in PBS) into the appropriate cell culture medium or buffer.

2.2.2. Cell Culture and Preparation of hESC-CM

Human Embryonic Stem Cell-Derived Cardiomyocytes (hESC-CM) were generated from hESC with a modified protocol of STEMdiff™ Cardiomyocyte Differentiation Kit (STEMCELL Tech, 05010). H9 hESC lines (WiCell, USA) were maintained on a feeder layer of irradiated mouse embryonic fibroblasts (Thermo Fisher) at 37°C, 5% CO2, and 95% humidity. Cells were passaged every 5-7 days and media was changed daily. Cells were then weaned off mouse embryonic fibroblasts for 2 to 4 passages on Matrigel (Corning, 354277) with mTeSR Plus medium (STEMCELL Tech, 100-0276). For differentiation, cells were dissociated into

single cells using Accutase (STEMCELL Tech) and seeded at $7x10^5$/well on Matrigel coated 12 well plates in mTeSR Plus medium containing 10 μM ROCK inhibitor Y-27632 (STEMCELL Tech, 72304). Cardiomyocyte differentiation was initiated the following day (day 0) using the STEMdiff™ Cardiomyocyte Differentiation Kit. Spontaneously contracting cardiomyocytes were typically observed from day 7 of differentiation.

2.2.3. hESC-CM Purification

To enhance hESC-CM purity, cells underwent glucose-deprivation from day 10 of differentiation. Cells were cultured in glucose-free RPMI 1640 medium supplemented with B27 (Thermo Fisher) for three days, followed by one day in standard RPMI 1640 with B27, and then three additional days in glucose-free RPMI 1640 with B27. On day 18, hESC-CM were dissociated using the STEMdiff™ Cardiomyocyte Dissociation Kit (STEMCELL Tech) and seeded onto Matrigel-coated 6-well plates at $2x10^6$ cells per well. Cells were maintained in RPMI 1640/B27+ medium with 10 μM ROCK inhibitor Y-27632 for 2 days to enhance recovery.

2.2.4. hESC-CM Maturation

For maturation, hESC-CM were cultured for up to 100 days. Cells were detached and reseeded on Matrigel-coated plates in RPMI/B27+ containing 10 μM ROCK inhibitor Y-27632 for the first 2 days. Subsequently, cells were cultured in hESC-CM maturation medium (RPMI 1640 without glucose + B27 + Chemically Defined Lipid Mixture 1 (Merck)). Cells underwent daily electrical stimulation (2 Hz, 5V/cm, 5 ms pulse) using a C-Pace EP Culture Pacer (IonOptix) for 6 hours per day.

2.2.4. Contraction Assay and Phase-Contrast Imaging

Phase-contrast images and contraction data were captured using a Leica DM IL LED Fluo microscope with a Leica DFC7000T camera. Videos were recorded at 100 frames per second for 10 seconds. Data were analysed with Leica Application Suite X (version 3.7) and ImageJ (version 1.53c) using the particle image velocimetry (PIV) and MUSCLEMOTION plugins for contraction analysis.

2.2.5. Cardiac-Differentiation Efficiency

Flow cytometry assessed cardiac-differentiation efficiency and maturation markers. At days 9, 13, 15, 17, 19, 30, 37, 60, 87, and 100 of differentiation, cells were dissociated with Accutase or STEMdiff™ Cardiomyocyte Dissociation Kit for 7 min at 37°C. Cells were fixed with 4% PFA for 10 min, permeabilised with 0.7% saponin for 15 min, and stained with PE mouse monoclonal IgG1 to rabbit monoclonal IgG to NKX 2.5 (Cell Signaling, 8792) or cTnT (BD Biosciences, 564767) for 30 min at room temperature. Secondary staining used PE goat Anti-Rabbit IgG (Abcam, ab72465). Isotype controls were PE conjugated rabbit IgG (Abcam, ab172730) and mouse IgG1 (BD Biosciences, 555749). A minimum of 10,000 events were analyzed per sample using an Attune NxT (Thermo Fisher) with a 100 µm nozzle. Data were analysed using FlowJo 10 (FlowJo), with gating based on forward and side scatter to exclude debris and doublets.

2.2.6. Hypoxia-Normoxia Cycle

Cells were dissociated and plated in appropriate formats. After recovery, hypoxia-designated cells were transferred to a HypoxyLab™ (Oxford Optronix) hypoxia workstation maintained at 1% O2 (8 mmHg), 37°C, and 5% CO2. Normoxia cycles used ambient conditions (~20% O2). Each cycle consisted of 24 hours hypoxia followed by 24 hours normoxia, repeated four times. For treatment groups, hESC-CM were pre-treated with 1 µM of either fully reduced high mobility group box 1 (HMGB1) or the dBB variant for 24 hours at the start of the normoxia cycle, after which treatments were removed.

2.2.7. Doxorubicin Cardiotoxicity Assay

Cells were dissociated using STEMdiff™ Cardiomyocyte Dissociation Kit for 7 min at 37°C, centrifuged at 500 g for 5 min. Live cells were counted using acridine orange and propidium iodide (AO/PI) staining with a LUNA-FL Dual Fluorescence cell counter (Logos Biosystems). Cells were plated onto Eppendorf cell image plates (24-well, 7.5x104/well) in STEMdiff™ Cardiomyocyte medium with 10 μM ROCK inhibitor Y-27632. Doxorubicin hydrochloride was prepared as a 1 mM stock solution in distilled water. hESC-CM were treated with 1 µM doxorubicin for 2 hours. For HMGB1 and dBB groups, hESC-CM were pre-treated with 1 µM FR-HMGB1 for 24 hours before doxorubicin exposure. Cardiac Troponin I in

supernatants was measured at 24-, 48-, and 72-hours post-treatment using a Human Cardiac Troponin I ELISA kit (Abcam, ab200016).

2.2.8. siRNA Knockdown

siRNA Transfection: RNA interference was used to knockdown PPARGC1α (PGC-1α) expression in hESC-CM. Cells were transfected with Silencer Select Pre-designed siRNA targeting PPARGC1α (Thermo Fisher, s21394) or Silencer Select Negative Control No. 1 siRNA (Thermo Fisher, 4390843) using Lipofectamine RNAiMAX Transfection Reagent (Invitrogen, 13778150).

hESC-CM were seeded in 6-well plates at a density of 2 x 10^5 cells per well 7 days prior to transfection and supplemented with Rock inhibitor for the first 24 hours. For each well, 9 µL of Lipofectamine RNAiMAX was diluted in 150 µL of Opti-MEM Medium (Gibco, 31985062), and 30 pmol of siRNA was diluted in 150 µL of Opti-MEM Medium. The diluted siRNA was added to the diluted Lipofectamine RNAiMAX (1:1 ratio) and incubated for 5 minutes at room temperature. The siRNA-lipid complex (250 µL) was added to each well containing cells in 2 mL of antibiotic-free culture medium, resulting in a final siRNA concentration of 50 nM.

Cells were incubated with the transfection mixture for 24 hours at 37°C in a 5% CO2 incubator, after which the medium was replaced with fresh complete growth medium.

Knockdown Verification: The efficiency of PPARGC1α knockdown was assessed at 48 hours, 3 days, and 5 days post-transfection using both qPCR and Western blot analysis.

qPCR Analysis: RNA extraction and qPCR were performed as described in the "Gene Expression Analysis" section. The following primers were used for PPARGC1α:

Gene	Forward Primer (5' → 3')	Reverse Primer (5' → 3')
PPARGC1α	CCAAAGGATGCGCTCTCGTTCA	CGGTGTCTGTAGTGGCTTGACT

Western Blot Analysis: Protein extraction and Western blot were performed as described in the "Western Blot Analysis" section. The primary antibody used was anti-PGC-1α (Abcam, Cat. No. ab54481, 1:500 dilution).

2.2.9. Membrane Microarray Assay, ELISA Assay, and other Cellular Assays

All assays were performed according to manufacturers' protocols with specific modifications as detailed below:

Human MAPK Phosphorylation Antibody Array (Abcam, ab211061): Cell lysates were prepared from hESC-CM subjected to various treatments. 300 µg of total protein was incubated with the antibody array membrane overnight at 4°C with gentle rocking. After washing, membranes were incubated with biotinylated anti-cytokine antibodies, followed by HRP-conjugated streptavidin. Signals were detected using chemiluminescence and quantified by densitometry.

p38 MAPK alpha ELISA Kit (Abcam, ab221012): 100 µL of cell lysate (1 µg/µL) was added to each well of the microplate pre-coated with p38 MAPK alpha-specific antibody. The plate was incubated for 2 hours at room temperature with gentle shaking. After washing, detection antibody was added and incubated for 1 hour, followed by HRP-Streptavidin for 45 minutes. TMB substrate was then added, and absorbance was measured at 450 nm.

RealTime-Glo™ Extracellular ATP Assay (Promega, GA5010): hESC-CM were seeded in white-walled 96-well plates at 2x10^4 cells/well. The RealTime-Glo™ Extracellular ATP Detection Reagent was added to the cells, and luminescence was measured at 10-minute intervals for 1 hour using a GloMax® Navigator Microplate Luminometer (Promega).

CellTiter-Glo® 2.0 Cell Viability Assay (Promega, G9241): hESC-CM were plated in opaque-walled 96-well plates at 1x10^4 cells/well. Equal volumes of CellTiter-Glo® 2.0 Reagent and cell culture medium were added to each well. The plate was shaken for 2 minutes to induce cell lysis, followed by a 10-minute incubation at room temperature. Luminescence was then recorded.

ROS-Glo™ H2O2 Assay (Promega, G8820): hESC-CM were seeded in 96-well plates at $5x10^3$ cells/well. H2O2 substrate solution was added to the cells and incubated for 6 hours

under standard culture conditions. ROS-Glo™ Detection Solution was then added, and the plate was incubated for 20 minutes at room temperature before luminescence measurement.

Cellular ROS Assay Kit (Abcam, ab113851): hESC-CM were seeded in black-walled, clear-bottom 96-well plates at $2x10^4$ cells/well. Cells were stained with 25 µM DCFDA for 45 minutes at 37°C. After washing, cells were treated with test compounds and incubated for 1 hour. Fluorescence was measured at Ex/Em = 485/535 nm.

Human TNF alpha ELISA Kit (Abcam, ab181421): 100 µL of standards or samples were added to antibody-coated wells and incubated for 3 hours at room temperature with gentle shaking. After washing, biotinylated TNF alpha detection antibody was added for 1 hour, followed by HRP-Streptavidin for 45 minutes. TMB substrate was added, and absorbance was read at 450 nm.

Human Peroxisome Proliferator Activated Receptor Gamma Coactivator 1 Alpha ELISA Kit (abbexa, abx152808): 50 µL of standards or samples were added to antibody-coated wells along with HRP-conjugated detection antibody. The plate was sealed and incubated overnight at 4°C. After washing, TMB substrate was added, and absorbance was measured at 450 nm.

Human Hif1α + BNIP3 Hypoxia In Cell ELISA Kit (Abcam, ab129733): hESC-CM were subjected to 24-hour hypoxia treatment (1% O2) before the assay. Cells were then fixed, permeabilized, and incubated with primary antibodies against HIF1a and BNIP3 overnight at 4°C. After washing, HRP-conjugated secondary antibodies were added for 1 hour. TMB substrate was added, and absorbance was read at 450 nm.

Human HIF-1α Quantification by ELISA (Merck, RAB1057): hESC-CM were cultured under normoxic or hypoxic conditions as described in section 2.2.6. Cells were lysed using the cell extraction buffer provided in the kit, supplemented with protease and phosphatase inhibitors. Lysates were centrifuged at 10,000 x g for 10 minutes at 4°C, and the cell culture supernatants were also collected and used for analysis.

Phospho-Akt1 (Ser473) Antibody Sampler Kit (Cell Signaling Technology, 9916): Cell lysates were separated by SDS-PAGE and transferred to PVDF membranes. Membranes were blocked with 5% BSA for 1 hour, then incubated with primary antibodies against phospho-Akt1 (Ser473) overnight at 4°C with gentle rocking. After washing, membranes were incubated with HRP-conjugated secondary antibodies for 1 hour at room temperature. Signals were detected using ECL substrate and quantified by densitometry.

2.2.10. Seahorse Analysis

Mitochondrial function was assessed using the Seahorse XF96 Extracellular Flux Analyzer (Agilent Technologies). XF96 assay plates were coated with 70 μL of Matrigel (Corning, 354230) per well and incubated for one hour at 37°C prior to cell seeding. hESC-CM were seeded at a density of 100,000 cells per well in the Matrigel-coated XF96 assay plates. The Cell Mito Stress Test used 2.5 μM oligomycin, 2 μM FCCP, and 2.5 μM rotenone/antimycin A. The Real-Time ATP Rate Assay used 2.5 μM oligomycin and 2.5 μM rotenone/antimycin A. Basal respiration, maximal respiration, ATP production, and proton leak were calculated using Wave software (Agilent) and Prism 10. OCR values were normalized to protein amount per well, determined using the Pierce BCA Protein Assay Kit (Thermo Fisher, Cat. No. 23225). OCR was defined as the average values measured from time point 1 to 4 during the experiments. Maximal OCR was the OCR difference between uncoupler FCCP and (rotenone + antimycin A), with respiratory reserve capacity being the difference between FCCP and baseline OCR values.

2.2.11. Western Blots

hESC-CM were washed with cold DPBS and lysed using RIPA buffer (Thermo Fisher, 89900) supplemented with 10X PhosStop (Roche, 4906845001) and 10X complete protease inhibitor cocktail (Roche, 11697498001) for 30 minutes on ice. Protein concentrations were determined using the BCA Protein Assay. Equal amounts of protein (20 µg) were loaded into 4-12% Bis-Tris gels (Invitrogen). Proteins were transferred to PVDF membranes using a Trans-Blot Turbo Transfer System (Bio-Rad). Membranes were blocked for one hour in 5% skim milk in TBST and then incubated with primary antibodies against PGC-1α (Abcam, ab54481, 1:500 dilution) or Beta-Actin (1:5000, Merck) overnight while shaking at 4°C. After washing, membranes were incubated with HRP-conjugated

secondary antibodies (1:5000, Cell Signaling Technology) for 1 hour at room temperature. Protein bands were visualized using ECL substrate (Bio-Rad) and a ChemiDoc imaging system (Bio-Rad).

2.2.12. Bulk RNA Sequencing

Sample Preparation: Human embryonic stem cell-derived cardiomyocytes (hESC-CM) were cultured as described in section 2.2.2, 2.2.3, and 2.2.4. Cells were harvested at selected dates for RNA sequencing. Three biological replicates were prepared for each experimental condition (control, hypoxia-treated, HMGB1-treated, and dBB-treated).

RNA Extraction: Total RNA was extracted from hESC-CM using the Direct-zol RNA MicroPrep Kit (Zymo Research, R2060) according to the manufacturer's instructions. Briefly, cells were lysed directly in the culture plate using 1 mL of TRI Reagent (Zymo Research, R2050-1-200) per 10 cm^2 of culture dish area. The lysate was immediately flash-frozen in liquid nitrogen and stored at –80°C. On-column DNase I treatment was performed to eliminate genomic DNA contamination.

RNA Quality Control: RNA quantity and quality were assessed using Agilent 2100 Bioanalyzer with the RNA 6000 Nano Kit (Agilent, 5067-1511), respectively. Only RNA samples with an RNA Integrity Number (RIN) > 7 were used for further analysis.

Library Preparation: mRNA library preparation was performed using the TruSeq Stranded mRNA Library Prep Kit (Illumina, 20020594) following the manufacturer's protocol. 1 µg of total RNA was used for each library. The resulting libraries were quantified using the Qubit dsDNA HS Assay Kit (Invitrogen, Q32851) and quality-checked using the Agilent 2100 Bioanalyzer with the High Sensitivity DNA Kit (Agilent, 5067-4626).

Sequencing: Sequencing was conducted on an Illumina NovaSeq X Plus platform at the Single Cell Discoveries. Paired-end sequencing (2 x 150 bp) was performed, generating approximately 30 million read pairs per sample.

Data Analysis: Raw sequencing data were processed and analyzed using the Galaxy web platform (version 21.05). The following tools and versions were used in the analysis pipeline: FastQC (v0.72+galaxy1): Quality control of raw sequencing reads; Trimmomatic

(v0.38.0): Adapter trimming and quality filtering; HISAT2 (v2.1.0+galaxy7): Alignment of reads to the human reference genome (GRCh38); featureCounts (v1.6.4+galaxy1): Quantification of gene expression; DESeq2 (v2.11.40.6+galaxy1): Differential expression analysis; GOEnrichment (v3.0.1): Gene Ontology enrichment analysis; KEGG Pathway (v1.0.0): KEGG pathway enrichment analysis

Significantly differentially expressed genes were defined as those with an adjusted p-value < 0.01 and absolute log2 fold change > 1.

Data Visualization: Volcano plots and heatmaps were generated using the Plot with ggplot2 tool (v3.3.5+galaxy0) in Galaxy. Principal Component Analysis (PCA) was performed using the PCA tool (v3.0.0) in Galaxy.

Statistical Analysis: Statistical analysis of differential gene expression was performed within the DESeq2 framework in Galaxy. The Benjamini-Hochberg method was used for multiple testing correction. For GO and KEGG pathway enrichment analyses, a hypergeometric test was applied, with p-values adjusted using the false discovery rate (FDR) method. An adjusted p-value < 0.01 was considered statistically significant for enrichment analyse.

2.2.13. Measurement of PFA

Whole blood samples (2.7 mL) were collected in 3.2% sodium citrate tubes. Samples were incubated for 30 minutes with 1 µM dBB, HMGB1, or DS-HMGB1 at room temperature. Platelet function was evaluated using the Innovance PFA-200 system (Siemens Healthcare Diagnostics Products). Three cartridges were used: COL/EPI, COL/ADP, and P2Y, with closure times recorded for each.

2.2.14. Proinflammatory Cytokine Assay

All protocols were approved by the local ethical committees and performed in accordance with national guidelines and regulations. PBMCs were isolated from anonymized human buffy coats using SepMate™ PBMC Isolation Tubes (STEMCELL Tech). CD14+ monocytes were extracted using CD14 MicroBeads (Miltenyi Biotec) according to the manufacturer's protocol. Monocytes ($1x10^6$ cells/mL) were treated with 100 nM of dBB, HMGB1, or DS-

HMGB1 for 24 hours. Some samples received co-stimulation with 10 ng/ml lipoteichoic acid (LTA) or 50 ng/ml lipopolysaccharide (LPS). TNF-α production was quantified using a Human TNF alpha ELISA Kit (Abcam). Additional cytokines (IL-1β, IL-6) were measured using a Human Inflammatory Cytokine Kit (BD Biosciences).

2.2.15. hESC-Cardiomyocytes Immunofluorescent Staining

H7 and H9 cells were grown and differentiated in glass-bottomed 35 mm dishes (iBidi). Cells were fixed with 4% paraformaldehyde for 15 minutes and permeabilized with 0.1% Triton X-100 for 10 minutes. Primary antibodies (rabbit anti-NKX 2.5 and mouse anti-Tnnt2, 1:200 dilution) were applied overnight at 4°C. Secondary antibodies (1:500 dilution) were applied for 1 hour at room temperature. Nuclei were counterstained with DAPI (1:1000). VECTSHIELD Antifade Mountant (Vector Laboratories) was used for mounting. Images were acquired using a Leica DM IL LED/Fl microscope with a 40x objective and processed using LAS X software (version 3.7).

2.2.16. Rapamycin Treatment

To inhibit mTORC1 signaling, hESC-CM were treated with 20 nM rapamycin (Merck) for 24 hours prior to HMGB1 or dBB treatment. The effectiveness of mTORC1 inhibition was confirmed by Western blot analysis of phosphorylated S6 kinase levels.

2.2.17. Gene Expression Analysis

Total RNA was extracted from hESC-CM using the Direct-zol RNA MicroPrep Kit (Zymo Research, R2060) according to the manufacturer's instructions. Briefly, cells were lysed directly in TRI Reagent, and RNA was purified using the Zymo-Spin IC Columns. On-column DNase I treatment was performed using the DNase I Set (Zymo Research, E1010) to eliminate genomic DNA contamination. RNA quantity and quality were assessed using a NanoDrop 2000 spectrophotometer (Thermo Fisher) and Agilent 2100 Bioanalyzer (Agilent Technologies). Only RNA samples with an A260/A280 ratio between 1.8 and 2.0 and an RNA Integrity Number (RIN) > 7 were used for further analysis.

cDNA Synthesis: First-strand cDNA was synthesized from 1 µg of total RNA using the SuperScript IV First-Strand Synthesis System (Invitrogen, 18091050) following the

manufacturer's protocol. The reaction mixture contained 50 µM oligo(dT)20 primer, 10 mM dNTP mix, 5X SSIV Buffer, 100 mM DTT, RNaseOUT Recombinant RNase Inhibitor, and SuperScript IV Reverse Transcriptase. The synthesis reaction was carried out at 50°C for 10 minutes, followed by 80°C for 10 minutes to inactivate the enzyme. The resulting cDNA was diluted 1:10 with nuclease-free water (Thermo Fisher) before use in qPCR.

Quantitative PCR (qPCR): qPCR was performed using the PowerUp SYBR Green Master Mix (Applied Biosystems, Cat. No. A25742) on a QuantStudio 5 Real-Time PCR System (Applied Biosystems). Each 20 µL reaction contained 10 µL of 2X PowerUp SYBR Green Master Mix, 1 µL of each primer (forward and reverse, 10 µM), 4 µL of diluted cDNA template, and 4 µL of nuclease-free water. The cycling conditions were as follows: UDG activation at 50°C for 2 minutes, Dual-Lock DNA polymerase activation at 95°C for 2 minutes, followed by 40 cycles of denaturation at 95°C for 15 seconds and annealing/extension at 60°C for 1 minute. A melting curve analysis was performed after each run to confirm the specificity of the amplification.

Primers: Primers were used for the following genes: TNNT2, MYH6, MYH7, KDR, GATA4, MYL7, KCNJ2, GLUT1, GLUT4, and MYL2 (Thermo Fisher). GAPDH (Thermo Fisher) was used as an endogenous control.

Gene	**Forward Primer (5' → 3')**	**Reverse Primer (5' → 3')**
TNNT2	AAGAGGCAGACTGAGCGGGAAA	AGATGCTCTGCCACAGCTCCTT
MYH6	GGAAGACAAGGTCAACAGCCTG	TCCAGTTTCCGCTTTGCTCGCT
MYH7	GGAGTTCACACGCCTCAAAGAG	TCCTCAGCATCTGCCAGGTTGT
KDR	GGAACCTCACTATCCGCAGAGT	CCAAGTTCGTCTTTTCCTGGGC
GATA4	GCGGTGCTTCCAGCAACTCCA	GACATCGCACTGACTGAGAACG
MYL7	CGACCAGAATCGTGATGGCATC	CAAAGAGCGTGAGGAAGACGGT
KCNJ2	AACAGTGCAGGAGCCGCTTTGT	AGGACGAAAGCCAGGCAGAAGA
GLUT1	TTGCAGGCTTCTCCAACTGGAC	CAGAACCAGGAGCACAGTGAAG

GLUT4	CCATCCTGATGACTGTGGCTCT	GCCACGATGAACCAAGGAATGG
MYL2	CGGAGAGGTTTTCCAAGGAGGA	CTCTTCTCCGTGGGTGATGATG
GAPDH	GTCTCCTCTGACTTCAACAGCG	ACCACCCTGTTGCTGTAGCCAA

Relative gene expression was calculated using the 2^-ΔΔCt method.

2.2.18. Statistical Analysis

Statistical analysis was performed using Excel (Microsoft Office) and Prism 10 (GraphPad). Each experiment was performed in triplicate and repeated at least three times. Data are presented as mean ± SD. Statistical analysis was performed using unpaired Student's t-test to compare data from two groups. For more than two groups, one-way ANOVA or two-way ANOVA was used with Tukey's, Geisser-Greenhouse's, or Sidak's correction for multiple comparisons. Results were considered statistically significant when $p<0.05$. Significance levels are denoted as *$p<0.05$, **$p<0.01$, ***$p<0.001$, and ****$p<0.000$.

Chapter 3. Optimisation of human embryonic stem cell-derived cardiomyocytes

3.1. Introduction

3.1.1. Mouse Models of Myocardial Infarction

In vivo murine models of myocardial infarction (MI) can be broadly divided into those involving permanent ligation (PL) of the left anterior descending (LAD) coronary artery or ischaemia and reperfusion (I/R). The PL model emulates the effects in 15-25% of patients following MI in whom timely reperfusion does not occur or reperfusion fails [112-114]. Typically, PL in mice results in irreversible ischaemia, hypoxia of the affected segment of the left ventricle, followed by contractile dysfunction, cardiomyocyte cell death and scar tissue formation [115]. The PL model is particularly suited to the study of the processes relating to cardiac remodelling after MI and investigating the efficacy of novel therapies over an extended period. However, reproducibility of the infarct size can be operator-dependent [113], and is largely determined by the level of ligation of the anterior descending artery, more proximal ligation resulting in larger infarcts [116].

The I/R model more closely emulates the clinical scenario on most patients who suffer an MI [117]. Timely reperfusion following ischaemia limits the infarct size, maintaining left ventricular function [118]. However, reperfusion also leads to a second reperfusion injury following the injury induced by the initial ischaemia [119]. While reperfusion injury in IR in mice more closely mimics the clinical scenario in humans, the infarct size can vary depending on the duration of coronary occlusion before reperfusion [120]. In mice, coronary artery occlusion for more than 90 minutes leads to an acute inflammatory response and irreversible injury [121-123]. In contrast, acute MI in humans usually occurs in the background of the gradual narrowing of coronary arteries with resulting collateral circulation rather than the acute and total temporary occlusion observed in the normal myocardium in mice subjected to I/R.

The genetic background of the experimental mice has a profound influence on the outcomes following MI. Studies have highlighted that post-MI survival rates, particularly in relation to

infarct rupture, show significant variation between mouse strains, highlighting some of the limitations of data derived from mouse models [121, 124]. For example, the 129S6 strain exhibits a considerably lower survival rate following MI compared to the widely used C57Bl/6 strain. In contrast, cardiac dilation, a crucial aspect of post-MI remodelling, appears less severe in 129S6 mice than in C57Bl/6 mice [124]. Despite these challenges, mouse models yield invaluable insights into *in vivo* processes over time. However, they fall short of encapsulating the full spectrum of human pathology. Therefore, it is imperative to augment findings from animal model with *in vitro* data derived from human cardiomyocytes, to achieve a comprehensive understanding of the processes associated with MI and the underlying mechanisms.

3.1.2. Human Cardiomyocyte Models

The most widely used *in vitro* models are based on either freshly isolated cardiomyocytes of or stem cell-derived cardiomyocytes. Typically, ischaemia is emulated by hypoxia, with or without depletion of nutrients, followed by reperfusion modelled by re-oxygenation and nutrient restoration [125]. *In vitro* models are especially useful as they allow a reductive approach through the ability to manipulate individual conditions and processes on a pure population of human cardiomyocytes without other effects of other cell types or systemic responses. In addition to the effects of hypoxia, cardiomyocyte cultures can also be used to study the cardiotoxic effects of drugs such as the anthracycline doxorubicin [126].

The supply of primary adult human cardiomyocytes relies on surgical biopsies or hearts not suitable for transplant. Consequently, they are scarce. Furthermore, they are difficult to maintain in culture long-term. Over time, the rod-shaped cardiomyocytes flatten, lose sarcomere organisation, and undergo dedifferentiation. Consequently, whilst they permit the study of hypoxia and reoxygenation in short-term experiments, they are not suitable for longer-term studies on the intracellular processes that involve overexpression or knock-down of key components of the pathways of interest [125].

Investigators have tried to address some of these limitations using immortalised cardiomyocyte cell lines, such as AT-1 cells from a mouse atrial tumour [127], and transformation of fetal cardiomyocytes with the SV40 oncogene [128]. These overcome the problems associated with long-term culture due to their ability to proliferate. However,

transformed cell lines have several disadvantages, such as the lack of a distinctive cardiomyocyte phenotypic structure and de-differentiation in some cases [129].

Therefore, the human embryonic stem cell-derived cardiomyocytes (hESC-CM) and human induced pluripotent stem cell-derived cardiomyocytes (hiPSC-CM) are being increasingly used to study cardiac disease because their availability, well-defined genetics, and being more representative of human biology than *in vitro* rodent models [130, 131]. The application of hiPSC-CM has also been expanded to study chemotherapy-mediated cardiotoxicity. A study of hiPSC-CM from patients suffering from doxorubicin-induced cardiotoxicity were more sensitive to the anthracycline drug *in vitro* compared to the hiPSC-CM from healthy patients [110]. This work demonstrates the utility of hiPSC-CM to model disease and study treatment options on individual patients [132].

3.1.3. Limitations of Immature hESC and hiPSC and How They Can be Overcome

The hiPSC are very similar to hESC in terms of their morphology, surface marker expression and *in vivo* teratoma formation capacity [133]. Despite their similarities, there are differences and hiPSC have been shown to exhibit greater variability in yield of mature cardiomyocytes and tendency to dedifferentiate compared to hESC [134]. Hence, hESC-derived cardiomyocytes have been used extensively to model disease and for drug screening, such as screening inhibitors for SARS-CoV-2[135], and drug-induced arrhythmias [136]. However, use of materials derived from human embryos remains controversial in some countries such as the USA.

Whilst cardiomyocytes derived from hESC-CM or hiPSC have several advantages as they recapitulate the underlying physiology of human cardiomyocytes, such as action potential in excitation-contraction coupling and relaxation [110], an important limitation is their immaturity compared to freshly isolated human or mouse cardiomyocytes [137]. For example, the early-stage cardiomyocytes derived from hESC-CM or hiPSC-CM tend to proliferate due to their persistent fetal characteristics in terms of structure, electrophysiology, gene, and metabolic profiles [138, 139].

In order to overcome these limitations, numerous strategies have been investigated to promote maturation, including 3D culture, organ-on-a-chip, electrophysiological stimulation

and induction of genes associated with cardiomyocyte maturation [140] [141, 142]. More recently, there has been increasing interest in promoting maturation through metabolic stimuli by altering the constituents of the culture medium [143]. Each of these strategies used individually have achieved limited success. Therefore, investigators have turned to using them in combination [144].

In this chapter I will describe the strategies I used to optimise the production of consistent batches of mature cardiomyocytes from hESC.

3.2. Results

3.2.1. Phenotypic Analysis of Standard hESC-CM Culture Method

First, I assessed the phenotypic and morphological features of cardiomyocytes derived from the H9 hESC line using a monolayer-based cardiac differentiation protocol under chemically defined conditions. This method yielded a cell population with over 88.2% cardiomyocytes, as substantiated by flow cytometry analysis for cardiac Troponin T (cTnT) (Figure 2A). Following a glucose starvation purification step, the hESC-CM organized into spontaneously beating layers, achieving a purity exceeding 98.1% (Figure 2B-C). The contractile function of the hESC-CM was evaluated using particle image velocimetry, providing qualitative data (Fig. 2D).

At day 20 of differentiation, quantification of NKX2.5 and cTnT expression using flow cytometry revealed both higher levels of cTnT and NKX2.5, indicating progression towards terminal differentiation while retaining some early cardiac marker expression (Fig. 2E). Next, I assessed the maturity of the cardiomyocytes based on gene expression for markers representing various cardiac development stages, including *KDR* (cardiac mesoderm), *GATA4* (cardiac progenitor cells), *TNNT2, MYH6, MYL7* (terminal differentiated cardiomyocytes), and *MYH7* and *MYL2* (mature cardiomyocytes).

By day 30, there was a significant decrease in mRNA expression levels of *KDR* and *GATA4* compared to day 20 (Fig. 2F) ($p < 0.024$), suggesting progression towards greater cardiomyocyte maturity. However, the expression levels of *TNNT2, MYH6, MYH7*, and *MYL7* remained stable, with no significant difference between day 20 and day 30 (Fig. 2F).

Notably, *MYL2* gene expression was above standard Ct range at either time point with no significant between them (Fig. 2G), indicating a significant potential limitation for this differentiation protocol to obtain mature cardiomyocytes.

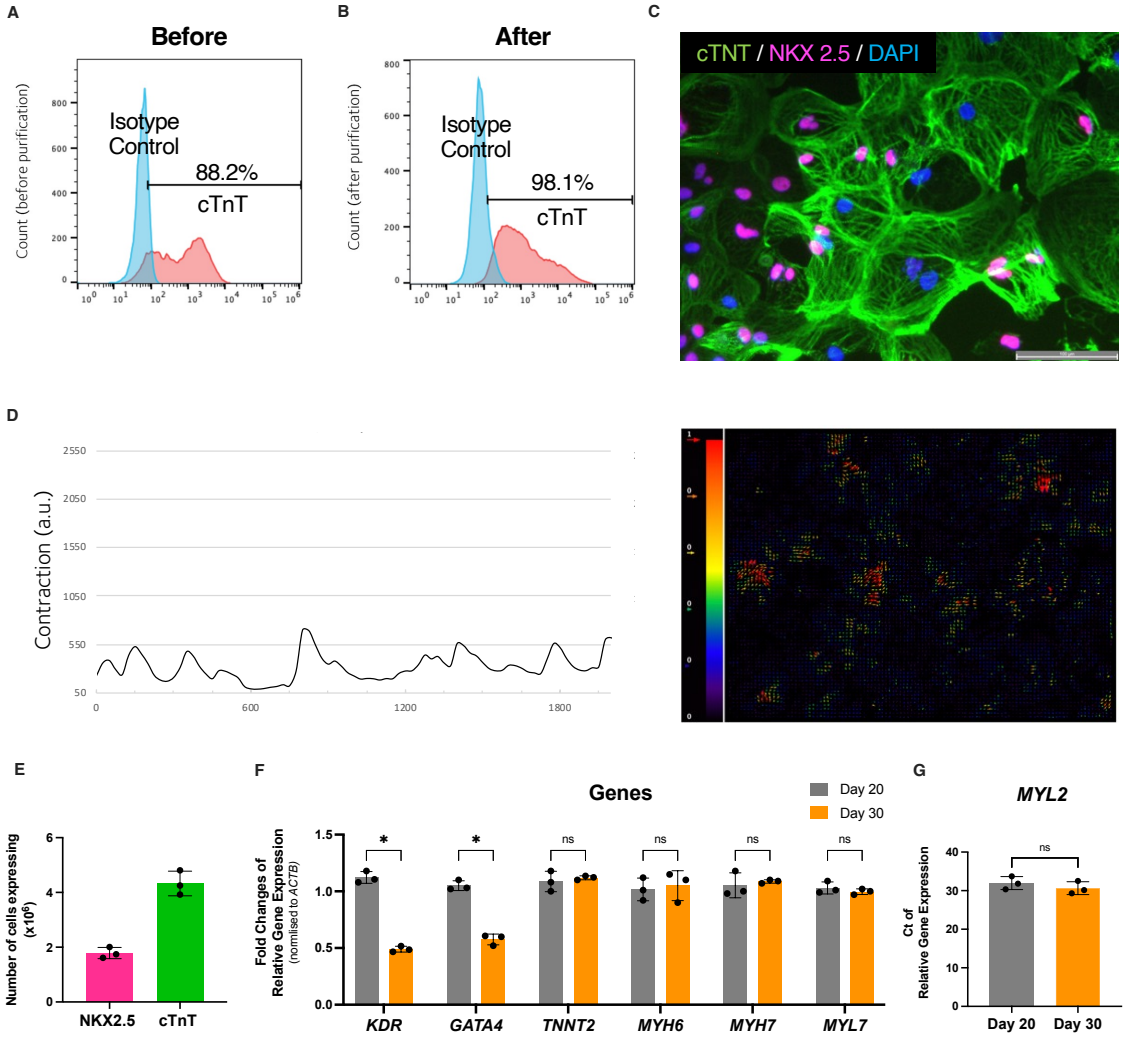

Figure 2. Characterization of hESC-derived cardiomyocytes.

(A) Cardiomyocytes derived from the H9 hESC line using a monolayer-based cardiac differentiation protocol under chemically defined conditions. Differentiation efficiency of H9-derived cardiomyocytes as demonstrated by cardiac Troponin T (cTnT, differentiated cardiomyocyte marker) flow cytometry before purification (88.2%) and **(B)** purification after glucose starvation showing 98.1% purity. **(C)** Representative immunofluorescence image of H9-derived cardiomyocytes; cTnT (green), early cardiomyocyte marker NKX2.5 (purple), nuclei stained with DAPI (blue). Scale bar not shown in image. **(D)** Representative plot of hESC-CM contraction (left) and particle image velocimetry analysis demonstrating the contraction amplitude of cardiomyocytes (right). **(E)** Quantification of NKX2.5 and cTnT positive cells by flow cytometry and cell counter, showing high expression of cTnT while retaining some early cardiac marker expression, NKX2.5, at day 20. **(F)** Comparison of gene expression at day

20 and day 30 of differentiation. Early cardiac development genes *KDR* and *GATA4* show significant decrease (*p < 0.024), while *TNNT2*, *MYH6*, *MYH7*, and *MYL7* show no significant change at day 30. **(G)** Expression of the mature cardiomyocyte gene *MYL2* at day 20 and day 30 were both above threshold of detection and showing no significant difference. n = 3, mean ± SD. Statistical significance was determined by paired t-test. ns: not significant, *p < 0.05.

3.2.2. Immature hESC-CM are Unresponsive to Hypoxia

Next, I assessed the sensitivity of 30-day-old hESC-CM to oxygen deprivation before utilising them for the downstream studies. Following incubation in 1% O_2 for intervals of 24, 48, and 72 hours, cardiac troponin I (cTnI) levels were measured using an ELISA-based assay as an indicator of cardiac injury. Exposure to hypoxia did not result in increased cell death (Fig. 3A), consistent with the observation of the large number of cardiomyocytes observed with minimal detectable hypoxic damage in immature hESC-CM (Fig. 3B). Nonetheless, an increase in hypoxia-inducible factor-1 alpha (HIF-1α) protein levels was detected following 48 and 72 hours of oxygen deprivation (Fig. 3C) ($p < 0.02$). Mitochondrial bioenergetic function assessments, as quantified by oxygen consumption rates (OCRs) using the XF90 Extracellular Flux Analyzer indicated no change in mitochondrial proton leak and ATP irrespective of the duration of hypoxia exposure, although there was a suggestion of a trend towards be a slight decrease in ATP synthesis and a marginal increase in mitochondrial proton leak when compared to non-hypoxic controls (Fig. 3D and 3E). These findings suggest that immature hESC-CM exhibit are relatively insensitivity to hypoxic damage, emphasising the necessity for maturation of hESC-CM.

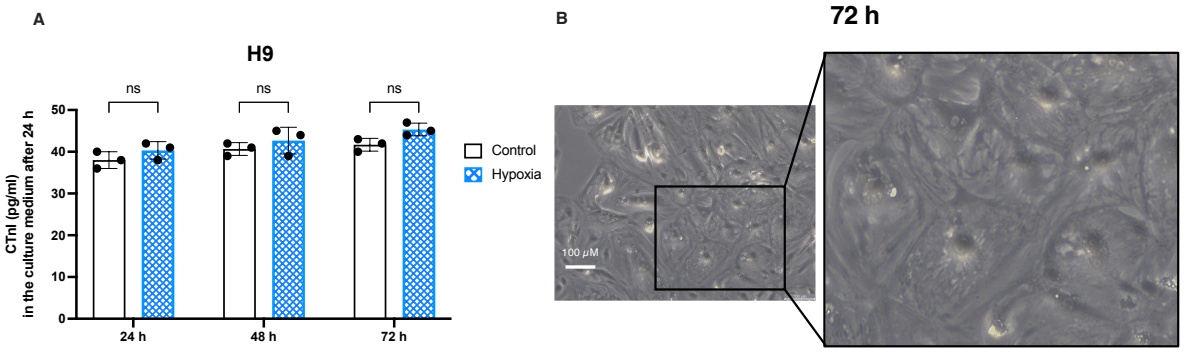

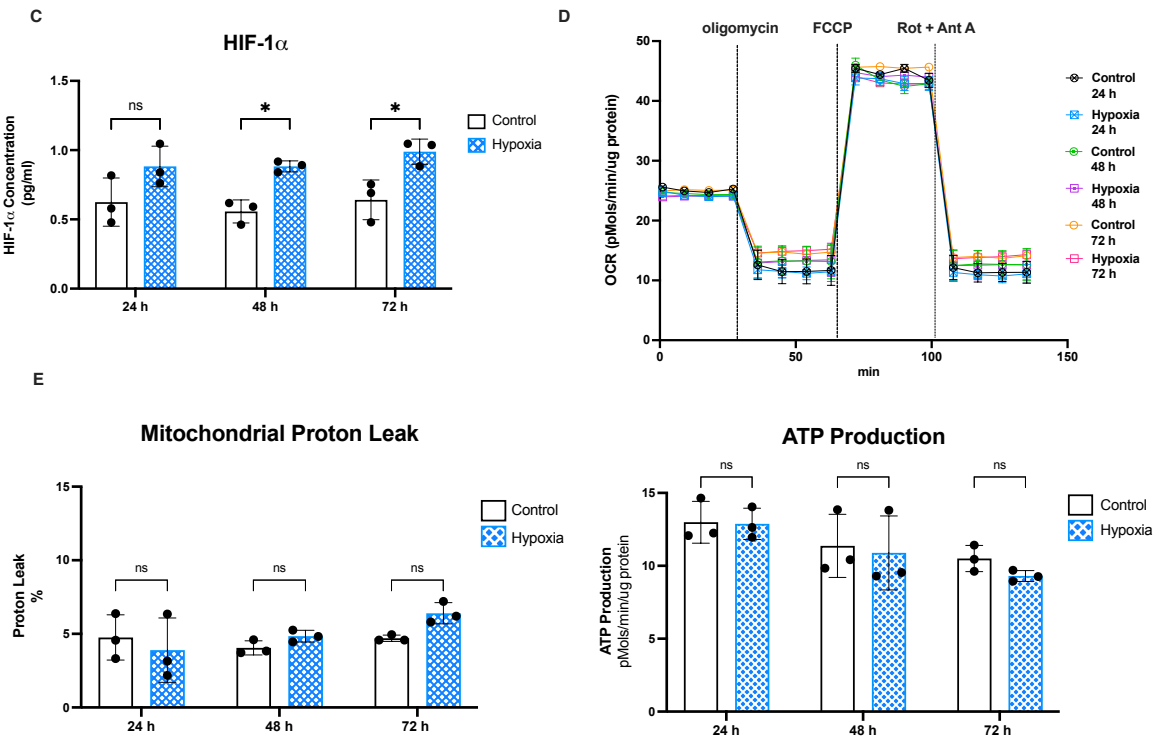

Figure 3. Immature hESC-CMs Show Resilience to Hypoxia

(A) Exposure to 24, 48 or 72 hours of hypoxia did not lead to a significant increase in cell death, as indicated by cTnI levels in the medium. **(B)** Representative microscopy images showing minimal morphological changes in H9-derived cardiomyocytes after 72-hour exposure to hypoxia. Scale bar 100 µm. **(C)** Hypoxia-inducible factor-1α (HIF-1α) protein levels increased significantly after 24, 48 and 72 hours of oxygen deprivation. **(D)** Real-time oxygen consumption rate (OCR) measurements of H9-derived cardiomyocytes cultured in RPMI/B27, assessed by Seahorse extracellular flux analyzer for both control and hypoxia conditions at 24, 48 and 72 hours. Cells were treated sequentially with oligomycin (ATP synthase inhibitor), FCCP (respiratory uncoupler) and rotenone + antimycin A (respiratory chain blockers). **(E)** Mitochondrial function assessment revealed no significant changes in mitochondrial proton leak (left) and ATP production (right) between control and hypoxia conditions at all time points. n = 3 independent batches, mean ± SD. Statistical significance determined by paired t-test. ns indicates not significant, *$p < 0.05$.

3.2.3. Maturation Using Fatty-acid Enriched Medium and Prolonged Culture Times

In order to further promote maturation of hESC-CM, I cultured them for an extended period (100 days) in the glucose-depleted, fatty-acid enriched medium. By day 100, a notable decrease in the relative gene expression of glucose transporters (*GLUT1* and *GLUT4*) was observed in comparison to day 30 (Fig. 4A) ($p < 0.034$), accompanied by a two-fold increase

in the expression of *TNNT2*, *MYH7*, and *MYL2* ($p < 0.047$). Flow cytometry analysis confirmed the absence of the early cardiomyocyte marker NKX2.5 by day 100 (Fig. 4B). Cellular function was further quantified, quantified by oxygen consumption rates (OCRs) using the XF90 Extracellular Flux Analyzer (Fig. 4C), revealing an increase in spare respiration capacity under glucose-free conditions at day 100 (Fig. 4D) ($p < 0.001$), and a significantly enhanced maximum respiration capacity in response to carbonylcyanide-p-trifluoromethoxyphenylhydrazone (FCCP) (Fig. 4D) ($p < 0.002$).

I tested the susceptibility of these matured hESC-CM to oxygen deprivation by incubating them in an environment comprising 1% O_2 for 24 hours. The matured hESC-CM exhibited a decrease in ATP levels and an increase in mitochondrial proton leak in comparison to their immature counterparts (Fig. 4E) ($p < 0.0001$), consistent with the appearance of hypoxic damage visualized using microscopy (Fig. 4F). These findings collectively underscore the importance of using extended culture in a fatty-acid enriched medium for enhancing the maturation of hESC-CM so they are better able to model cardiac responses to hypoxia.

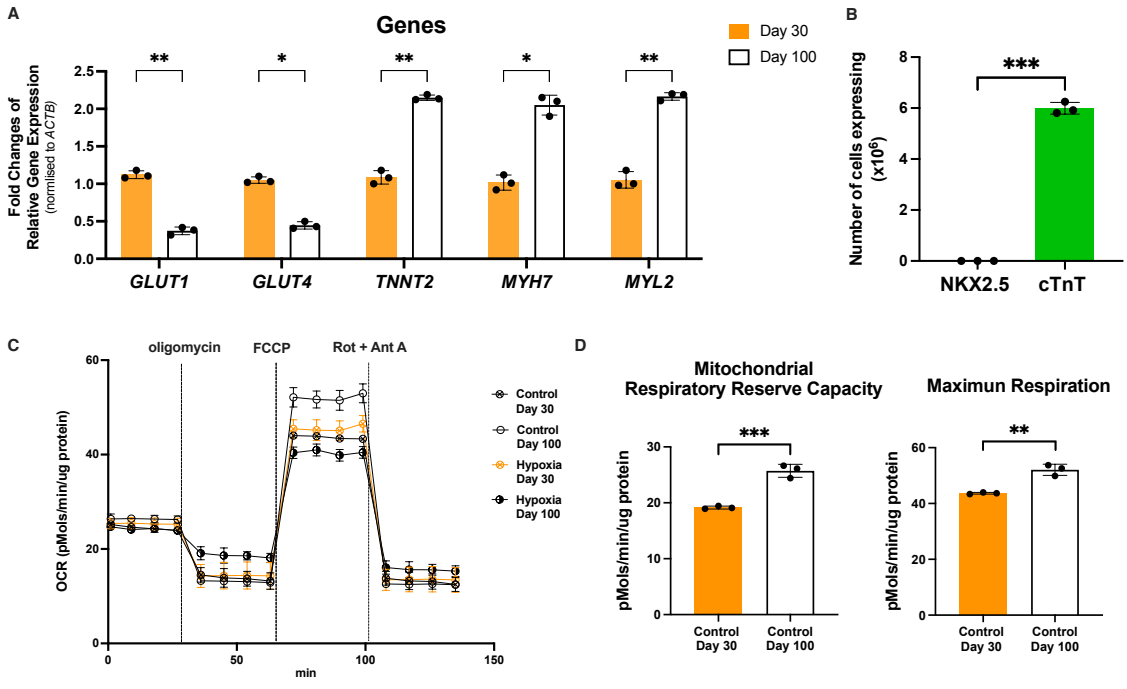

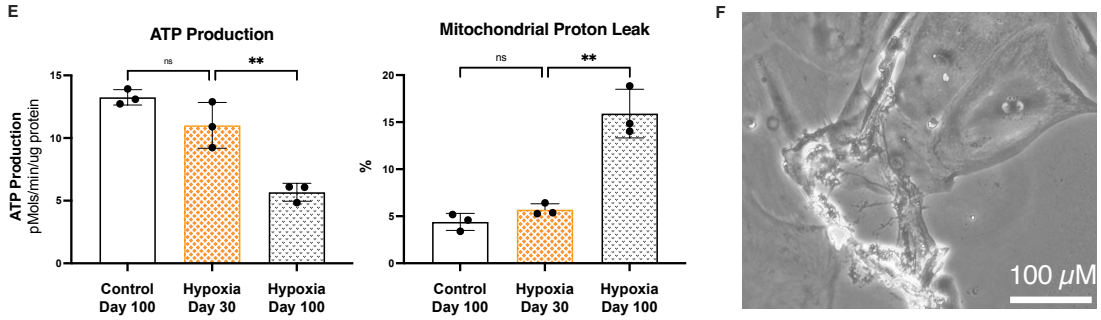

Figure 4. Enhanced Maturation of hESC-CM with Fatty Acid-Enriched Medium

(A) Gene expression comparison day 30 and day 100 hESC-CM. Results show decreased expression of glucose transporters *GLUT1* and *GLUT4* and increased expression of maturation-associated genes *TNNT2*, *MYH7* and *MYL2* by day 100. **(B)** Flow cytometry quantification demonstrating the absence of early cardiomyocyte marker NKX2.5 and high expression of cardiac Troponin T (cTnT) by day 100, indicating advanced maturation. **(C)** Real-time oxygen consumption rate (OCR) measurements of hESC-CM cultured under control and hypoxic conditions at day 30 and day 100, assessed by Seahorse extracellular flux analyzer. Cells were sequentially treated with oligomycin (ATP synthase inhibitor), FCCP (respiratory uncoupler),and rotenone + antimycin A (respiratory chain blockers). **(D)** Mitochondrial function analysis revealing improved respiratory reserve capacity and maximum respiration at day 100 compared to day 30, indicating enhanced metabolic maturation. **(E)** Comparison of ATP production and mitochondrial proton leak under control conditions and after 24-hour hypoxia exposure in day 30 and day 100 hESC-CM. Mature (day 100) hESC-CM showed decreased mitochondrial function under hypoxic conditions, suggesting increased sensitivity to oxygen deprivation. **(F)** Representative microscopy image of day 100 hESC-CM, exhibiting morphological changes consistent with hypoxic damage. Scale bar 100 µm. n = 3, mean ± SD. Statistical significance determined by one-way ANOVA (E) or paired t-test (A, B, D). ns indicates not significant, *p< 0.05, **p <0.01, ***p < 0.001.

3.2.4. Impact of Electrical Stimulation on hESC-CM Maturity

Culture periods extending over 100 days would significantly limit the number of experiments I could perform over the course of my DPhil. Therefore, I investigated whether electrical stimulation at a frequency of 2 Hz could be used to reduce the culture period whilst maintaining cell maturity. The mechanical stress imposed by the electrical stimulation significantly accelerated the maturation process at day 60 compared to non-stimulated controls, with the cardiomyocytes exhibiting alignment of their sarcomeres, as evidenced by high power brightfield image (Fig. 5A). Electrical stimulation also resulted in expression levels of mature cardiomyocyte markers such as *MYH7* and *MYL2* comparable to those observed in hESC-CM cultured for 100 days under glucose-deprived conditions (Fig. 5B). There was also a significant increase in the expression of the potassium inwardly-rectifying

channel gene (*KCNJ2*), which is essential for cell excitability and potassium homeostasis (Fig 5B) ($p < 0.0001$). When subjected to 24 h hypoxia, electrically stimulated hESC-CM cultured for 60 days exhibited a damage profile similar to mature hESC-CM cultured for 100 days, characterised by reduced ATP and increased mitochondrial proton leak compared to their immature counterparts (Fig. 5C) ($p < 0.0001$). Contractility assessments using particle image velocimetry analysis revealed that electrically stimulated hESC-CM had increased contraction amplitude and frequency (Fig. 5D). These findings collectively underscore the importance of mechanical cues for the efficient maturation of hESC-CM, with the added benefit of significantly reducing the culture period required to achieve a maturity level comparable to that obtained through extended culture durations under static conditions. Based on these data I used the maturation protocol based on fatty acid enrichment and electrical stimulation for all my subsequent experiments.

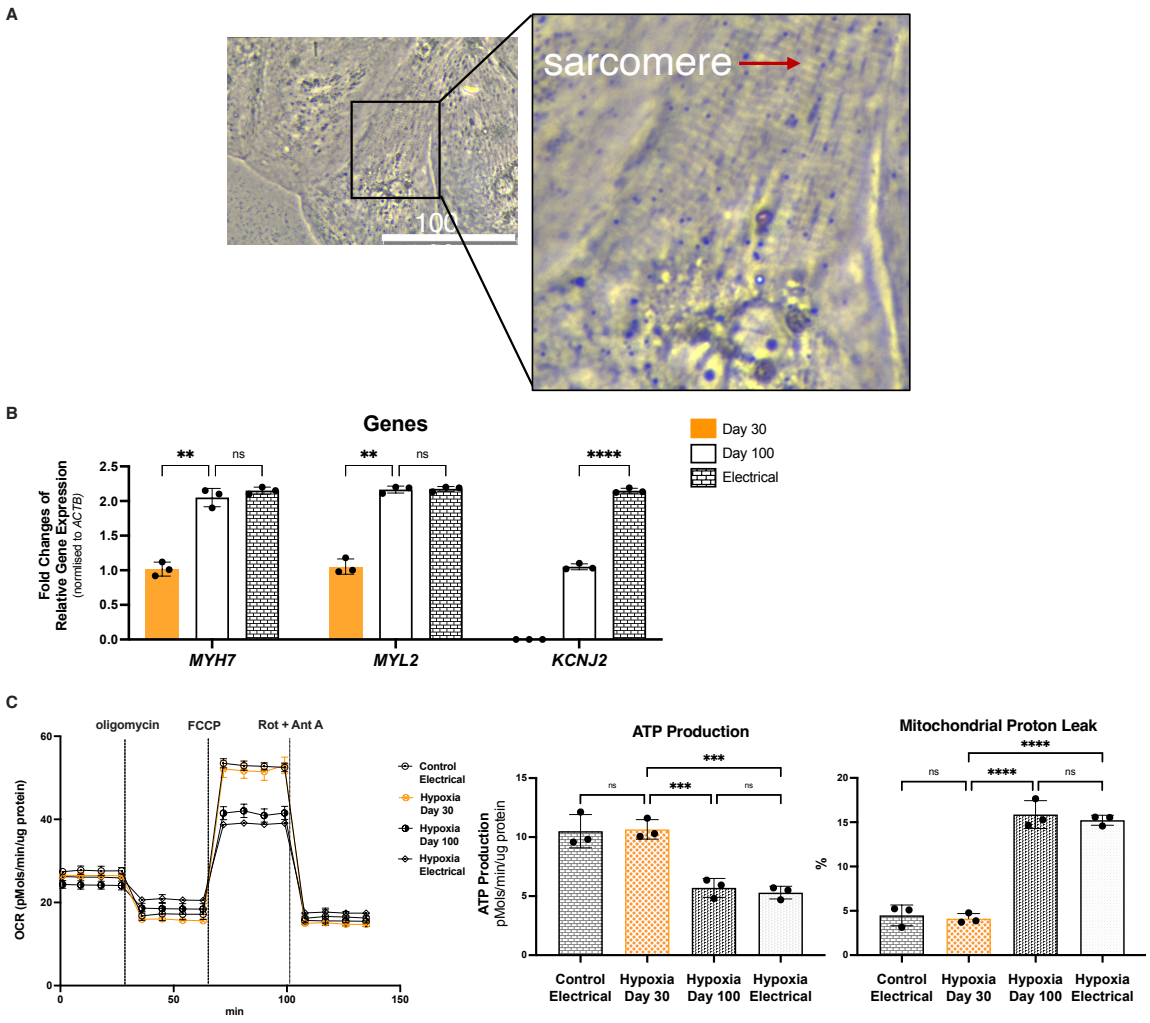

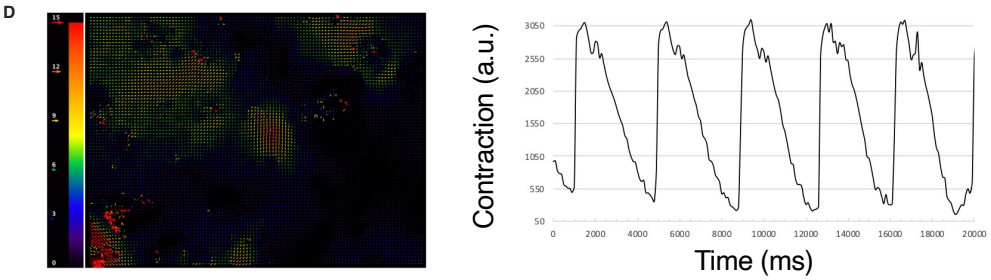

Figure 5. Electrical Stimulation Accelerates hESC-CM Maturation

(A) High-power brightfield imaging demonstrating sarcomere alignment in hESC-CM following 2 Hz electrical stimulation. Scale bar 100 µm. **(B)** Gene expression analysis comparing electrically stimulated hESC-CM to those cultured for 100 days under glucose-deprived conditions. Results show comparable expression levels of mature cardiomyocyte markers (*MYH7* and *MYL2*) and increased *KCNJ2* expression in electrically stimulated cells. **(C)** Mitochondrial function analysis after 24-hour hypoxia challenge, showing electrically stimulated hESC-CM exhibit susceptibility to mitochondrial damage comparable to mature hESC-CM cultured for 100 days. **(D)** Particle image velocimetry analysis demonstrating enhanced contraction amplitude and frequency in electrically stimulated hESC-CM. n = 3, mean ± SD. Statistical significance determined by one-way ANOVA (C) or paired t-test (B). ns indicates not significant, *p < 0.05, **p < 0.01, ***p < 0.001, ****p < 0.0001.

3.3. Discussion

The results shown in this chapter demonstrate the constraints of traditional differentiation approaches for human embryonic stem cell-derived cardiomyocytes (hESC-CM), particularly their reduced susceptibility to hypoxia-induced injury and death. Advances in maturation techniques, incorporating metabolic conditioning and prolonged culture durations, have significantly heightened their response to hypoxic conditions, thereby improving their suitability to emulate cardiac ischaemia. Moreover, the adoption of electrical stimulation emerged as a crucial strategy, significantly reducing the time required to achieve an enhanced state of maturation, paralleling the benefits observed with metabolic conditioning and extended culture periods.

3.3.1. Genetic and Metabolic Maturation Landscape of hESC-CM

My investigations revealed minimal variation in gene expression profiles comparing the maturity of hESC-CM aged 20 days with those cultured for 30 days. This is consistent with the report of persistently immature phenotype of human pluripotent stem cell-derived

cardiomyocytes cultured for between four and eight weeks [145]. The inherent resilience of immature hESC-CM to low oxygen conditions mirrors the tolerance seen in fetal cardiomyocytes. This adaptation is crucial during embryonic development, characterised by arterial oxygen saturation levels of around 3% [146]. This adaptability with a reliance on anaerobic metabolic pathways for development, is consistent with my observations that prolonged hypoxia induced only limited damage and did not significantly alter ATP production in immature hESC-CM at day 30. The small increase in HIF-1α maintained cardiomyocyte ATP levels and viability by promoting glycolytic metabolism under oxygen-limited conditions.

In an effort to overcome the challenges posed by the immature phenotype, several protocols have emerged, with some extending culture for up to a year [147] [148]. A comparison of hESC-CM cultured for 40 or 120 days found that the longer period was associated with the cells becoming significantly becoming larger, adopting a less spherical shape, and are more likely to be multinucleated [138]. My findings align with this transition, achieved using a patented culture cocktail medium to facilitate the maturation of hESC-CM [148].

These morphological changes were accompanied by upregulation of *MYH6,* and *MYH7*, gene expression without significant changes in *KCNJ2* expression, paralleling the results observed in my study. This pattern of gene expression suggests a shift towards a more mature cardiomyocyte phenotype, characterized by changes in myosin heavy chain isoforms, which are crucial for contractile function.

The transition to a more energy-efficient, oxidative phosphorylation-based metabolism is catalysed by the increased oxygen availability post-birth, leading to the destabilisation of the HIF-1α transcription factor complex [149]. My findings reflect this transition, with mature hESC-CM being markedly more susceptible to hypoxia-induced cell death and exhibiting diminished mitochondrial respiration after 24 hours of hypoxia. The improved maturation I observed on transitioning to fatty acid-enriched media aligns with a previous report [150], which showed that glycolysis-dependent ATP generation in glucose-rich medium shifted towards oxidative phosphorylation with glucose depletion and fatty acid supplementation. The metabolic shift towards oxidative phosphorylation following transitioning to glucose-depleted, fatty-acid enriched could in the future also be explored through advanced methodologies like Fluorescence Resonance Energy Transfer [151].

Whilst exposure of mature hESC-CM to 24-hour hypoxia induced detectable cellular damage, interestingly it did not damage all cell (Fig. 4F). This finding hints at a more subtle impact of hypoxia as opposed to reperfusion injury on cellular integrity, consistent with previous observations that compared to reperfusion injury, hypoxia exerts a lesser effect on calcium overload-related cellular damage in immature iPSC-CM [152]. This nuanced understanding merits reconsideration of the role of hypoxia and suggests consideration of a broader spectrum of experimental conditions to accurately replicate *in vivo* physiological states. I concluded that in subsequent studies cycles of hypoxia rather than a single period of prolonged hypoxic conditions to better capture the complex effects of oxygen levels on cardiomyocyte health and functionality.

3.3.2. Advancements in hESC-CM Maturation through Electrical Stimulation

The necessity to circumvent the constraints posed by prolonged culture durations led me to explore alternative avenues for expediting maturation, focusing on mechanical and electrical stimulation. Recent publications have highlighted the potential of mechanical and electrical stimulation for advancing cardiomyocyte maturation, with significant improvements in sarcomere structure, gene expression and contractile functionality [153, 154]. Specifically, protocols utilising high-intensity (6 Hz) electrical stimulation during the initial phases of cardiomyocyte differentiation have shown to yield cardiomyocytes with more mature characteristics, including enhanced calcium dynamics, sarcomere alignment, T-tubule formation and a robust force-frequency relationship—that mirror my observations [154].

Diverging from existing methodologies that typically employ adaptive frequencies ranging from 2 to 6 Hz on engineered cardiac tissues, my approach integrated a 2Hz electrical stimulation regimen in conjunction with a glucose-depleted, fatty-acid enriched culture medium directly applied to monolayer hESC-CM. This novel protocol demonstrated that electrically stimulated hESC-CM under these specific conditions exhibited damage profiles and maturation markers comparable to those observed in hESC-CM cultured for an extended period of 100 days. This finding not only highlights the efficacy of electrical stimulation in accelerating hESC-CM maturation but also provides a method that combines the benefits of metabolic conditioning with those of electrical cues.

Enhanced maturation of the hESC-CM is essential when investigating processes that impact mitochondria. Immature hESC-CM, characterised by a reduced mitochondrial count compared to their mature counterparts, may not fully capture the cardioprotective dynamics applicable to mature cardiomyocytes [154, 155]. Hence my optimised protocol would be especially well suited to the study of injuries that particularly impact mitochondria, such as hypoxia or exposure to doxorubicin.

3.3.3. Integrating Insights and Addressing Challenges in Cardiomyocyte Maturation

In summary, the data I have presented in this chapter show that mature hESC-CM exhibit an increased susceptibility to hypoxic injury, akin to the response of adult cardiomyocytes, positioning them as a superior *in vitro* model for exploring human ischaemic heart disease. However, while my optimised protocol represents a significant advance in hESC-CM maturation, it does not overcome other existing limitations such as the scalability of these protocols and the inherent challenge in fully replicating the entire spectrum of adult cardiomyocyte functions. Furthermore, variations among different hESC lines and induced pluripotent stem cells (iPSCs) can make comparisons between studies difficult.

Chapter 4. The effect of HMGB1 on Ischaemia-Reperfusion (IR) Injury.

4.1. Introduction

4.1.1. Ischaemia-Reperfusion

Patients who suffer myocardial infarction are broadly divided into those with ST segment elevation on ECG (ST segment elevation myocardial infarction, STEMI) or those without ST segment elevation (non-STEMI – NSTEMI). Over the last 30 years, there has been a steady decrease in the number of patients experiencing STEMI, with NSTEMI now comprising around 60-75% of all myocardial infarctions [1]. Typically, STEMI occurs following complete occlusion of a coronary artery whilst NSTEMI tends to occur after occlusion followed by spontaneous reperfusion of collateral blood flow from an adjacent artery [156]. It is recommended that following STEMI, patients should undergo reperfusion, usually with percutaneous intervention (PCI), within 60–90 minutes. NSTEMI patients should undergo PCI within 24 h, except those at low risk where it can be delayed for 48–72 hours [1]. Whilst reperfusion following MI has been shown to reduce mortality as well as other complications by 50–70% [156], the reperfusion also leads to additional injury. Therefore, when using *in vitro* systems, these events are emulated using normoxia followed by hypoxia to more accurately emulate the clinical scenarios.

4.1.2. *In Vitro* Models of Emulating Ischaemia-Reperfusion (I/R) Injury

Hypoxia chambers represent the most widely used method for inducing hypoxia in cardiomyocyte studies, offering precise control over oxygen concentrations. Typically, oxygen levels below 2% are considered hypoxic. However, in practice, the oxygen concentration is adjusted between 1% and 10%, tailored to specific experimental requirements and sensor limitations [157]. Despite the advantages afforded by the simplicity of standard hypoxia incubator, variations in oxygen concentration and reproducibility challenges have led to the adoption of more sophisticated systems like HypoxyLab. This apparatus enhances experimental accuracy by regulating the environment based on the direct measurement of oxygen partial pressure (pO_2) in mmHg [158].

The simulation of reperfusion, a critical component of clinical ischaemia-reperfusion, involves restoring oxygen levels to normoxic conditions, typically around 21% [125, 159]. It is important to recognise that the stabilisation of oxygen concentrations between cell culture media and the environment can require up to 24 hours[160]. Consequently, hypoxia chambers are particularly suited to studies extending beyond this timeframe as they allow for comprehensive examination of effects of hypoxia followed by reoxygenation, including overexpression or knockdown of specific signalling pathway components, thereby providing detailed information about cellular responses under controlled conditions [125, 159].

4.1.3. Severity of Hypoxia

The severity of hypoxia critically influences cellular responses, an essential factor when simulating ischaemia-reperfusion *in vitro*. Oxygen levels below 2% are generally considered hypoxic, yet specific thresholds and durations can activate distinct cellular pathways. For instance, severe hypoxia (1% O_2) tends to induce robust activation of hypoxia-inducible factors (HIFs), which can have dual effects—both protective and detrimental—on cellular functions [161]. Conversely, moderate hypoxia (5% O_2) typically triggers less severe stress responses, potentially enhancing survival pathways [162].

The impact of hypoxia also varies with the maturity of the cells in human pluripotent stem cell-derived cardiomyocyte (hPSC-CM) models. Immature hPSC-CM show considerable resistance to hypoxia, with minimal (less than 5%) cell death. In contrast, mature hPSC-CM are much more sensitive to fluctuations in oxygen levels, exhibiting up to about 30% cell death after hypoxia and subsequent reoxygenation [163, 164].

4.1.4. Duration of Hypoxia and Normoxia

The duration of hypoxia prior to reoxygenation is crucial. Short hypoxic exposures may fail to trigger comprehensive cellular adaptations seen after more extended periods, such as the upregulation of antioxidant defences, autophagy mechanisms and contractility [165, 166]. Conversely, prolonged hypoxia can lead to irreversible damage and cell death if not managed by appropriate reoxygenation strategies [165, 167]. Experimental setups show a wide range in the duration of hypoxia, from a few hours to a few days, which makes comparison between studies challenging [167].

The period of normoxia following hypoxia is equally critical. For instance, extending the reoxygenation period to 17 hours results in greater cardiomyocyte loss compared to a shorter, 2-hour reoxygenation phase [167]. Moreover, extending the reoxygenation time from 6 to 24 hours has been shown to alter the expression of genes like *VEGFA*, a well-known hypoxia-responsive gene, and *TRPV1*, which is implicated in ischaemia-reperfusion injury [168].

4.1.5. Multiple Cycles of Hypoxia-Reoxygenation

The benefits of extending hypoxia duration must be balanced against the number of viable cardiomyocytes available for downstream analysis. Multiple cycles of hypoxia followed by normoxia have been used to overcome this challenge in several studies [169-171]. Researchers found that repeated cycles induce pro-apoptotic endoplasmic reticulum (ER) stress and maintain elevated HIF-1α expression [172], phenomena not observed after a single cycle. Multiple cycles of hypoxia and normoxia *in vitro* also better model NSTEMI, which now comprises approximately 70% of all acute coronary artery syndrome events and is characterised by repeated episodes of ischaemia-reperfusion [1].

The number of cycles of hypoxia-normoxia is also important. A study of human-induced pluripotent stem cell-derived cardiac organoids found that whilst three cycles of hypoxia (0.1% oxygen) emulated many of the effects of MI *in vivo*, 4 cycles resulted in the formation of a fibrotic shell and an apoptotic core, with complete loss of cardiomyocytes [169]. These observations emphasise the critical need to finely balance hypoxic stress to maintain cellular health while still imposing sufficient stress to explore pathological processes and potential therapeutic strategies [173]. It is imperative to monitor and adjust the duration and intensity of each cycle, evaluating their collective and individual impacts on cell viability and function.

4.1.6. Alternative Methods for Inducing Hypoxia

Various chemical compounds such as cobalt chloride ($CoCl_2$) and dimethyloxalylglycine (DMOG) offer an alternative to hypoxia chambers to simulate hypoxic conditions by stabilising hypoxia-inducible factor 1-alpha (HIF-1α) [174]. This approach is not only simple and cost-effective but also facilitates the rapid induction of a cellular response akin to hypoxia [159]. While the precise mechanism through which $CoCl_2$ and DMOG stabilise HIFs

remains incompletely understood, available data suggest that they bind to the active site of HIF-prolyl hydroxylase domain enzymes (PHDs), thereby impeding proline hydroxylation, which leads to inactivation of HIFs [175]. These compounds might also directly bind to HIF-1α proteins to inhibit their ubiquitination [175]. However, the use of chemical compounds to emulate hypoxia has significant limitations. The most important of these is that stabilisation of HIFs only partially emulates the myriad cellular responses to hypoxia and reoxygenation [159]. This is highlighted by the significant difference in the gene expression induced by hypoxia and chemical treatment. Furthermore, $CoCl_2$ can lead to higher expression of p53 compared to methods using hypoxia chambers, suggesting an additional mechanism distinct from the HIF-1α-mediated response [176]. Additionally, there are concerns about the potential toxicity of these chemical compounds [159]. Taken together, these data show that chemical methods such as $CoCl_2$ do not accurately mimic the cellular pathways activated by hypoxia chambers.

In this chapter, I will describe the effects of HMGB1 following cycles of hypoxia-reoxygenation on hESC-CM *in vitro* to elucidate the mechanisms underlying HMGB1 action in ischaemia-reperfusion injury.

4.2. Results

4.2.1. Effect of Multiple Hypoxia-Normoxia Cycles on Cardiomyocytes

Initially, I sought to determine the optimal number of hypoxia-normoxia cycles by measuring levels of cardiac troponin I (cTnI), a biomarker of cardiomyocyte damage, in the culture medium. I noted increasing levels of cellular stress and damage beginning with the second cycle (Fig. 6A). The most pronounced rise in cTnI occurred between the second and third cycles, a 1.6-fold increase (Fig. 6A), with cTnI levels stabilising thereafter. There was no significant difference between the third and fourth cycles (Fig. 6A).

However, there was a marked reduction in cell viability between the third and fourth cycles, as evident on brightfield microscopy and viable cell counts (Fig. 6B and 6C) ($p = 0.0203$). The discrepancy between viable cell counts and the modest increase in cTnI levels from the third to the fourth cycle suggests that stressed cells may release cTnI while retaining potential for recovery upon restoration of normoxia.

This increased cell stress and decreased viability with successive cycles was mirrored in the progressive decline in ATP production, which was not significant until the fourth cycle, where a notable reduction was observed compared to the first cycle using the XF90 Extracellular Flux Analyzer (Fig. 6D and 6E) ($p = 0.0070$). Additionally, mitochondrial proton leak significantly increased after the third cycle compared to the first (Fig. 6F), whilst there was no difference in proton leak between the third and fourth cycle (Fig. 6F).

Levels of HIF-1α were significantly upregulated following cycles of hypoxia-normoxia, reflecting an adaptive cellular response to hypoxic stress (Fig. 6G). The increased expression of HIF-1α between the third and fourth cycles suggested a cumulative effect with successive cycles ($p = 0.0010$).

These findings highlight the importance of carefully monitoring the effects of successive hypoxia-normoxia cycles to induce hypoxia damage in hESC-CM to best emulate the effects seen *in vivo*.

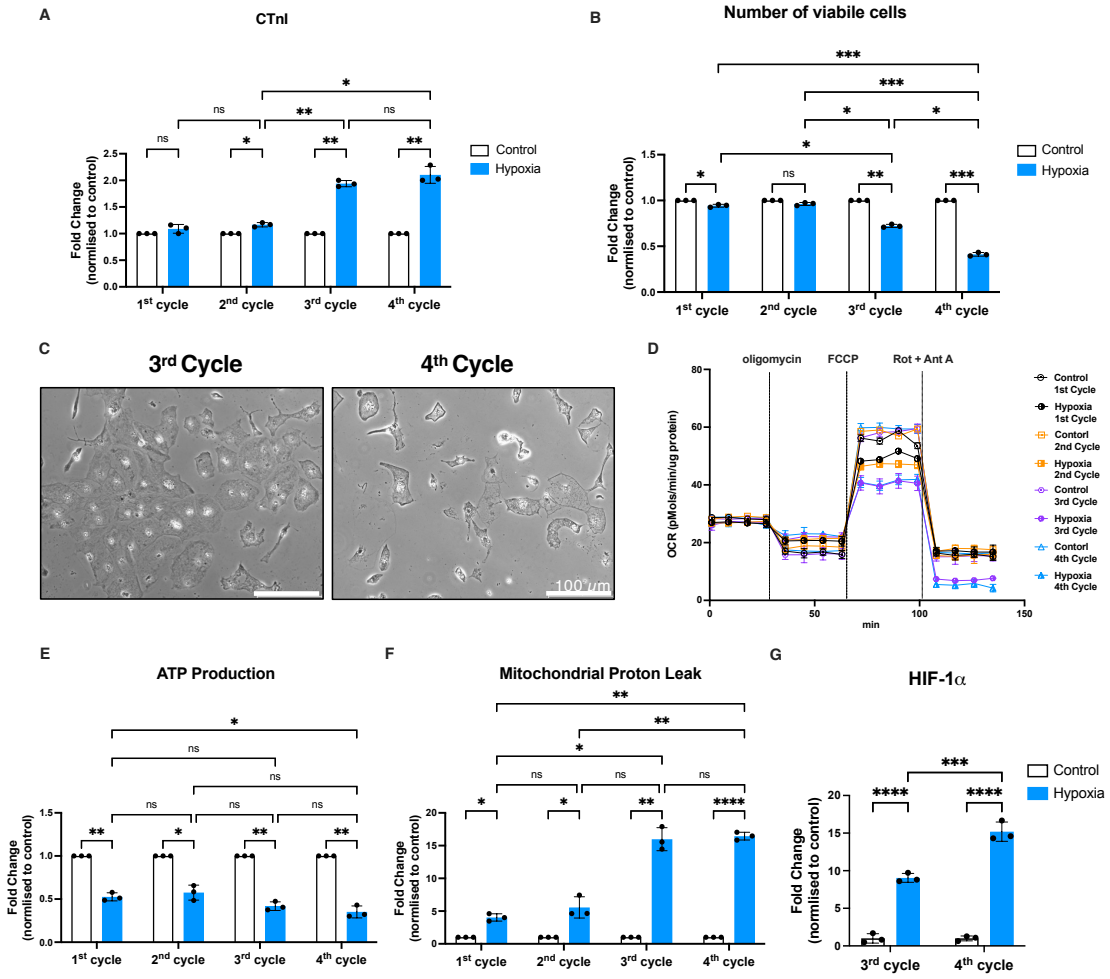

Figure 6. Effects of Repeated Hypoxia-Normoxia Cycles on hESC-CM Viability and Metabolism.

(A) Cardiac troponin I (cTnI) levels in the culture medium across four hypoxia-normoxia cycles. Significant elevations in cTnI are observed from the second cycle onwards, suggesting cumulative stress effects. **(B)** Cell viability assessment over successive cycles, showing a general trend of decreasing viability with each cycle, except for the second cycle. **(C)** Representative brightfield microscopy images comparing the third and fourth cycles, visually demonstrating the marked decrease in cell density and altered morphology by the fourth cycle. Scale bar 100 µm. **(D)** Real-time oxygen consumption rate (OCR) measurements of hESC-CMs under control and hypoxic conditions across all four cycles, assessed by Seahorse extracellular flux analyzer. Cells were sequentially treated with oligomycin (ATP synthase inhibitor), FCCP (respiratory uncoupler), and rotenone + antimycin A (respiratory chain blockers), revealing cycle-dependent changes in metabolic profiles. **(E)** ATP production analysis showing a progressive decline across cycles, with a significant difference observed between the first and fourth cycles, indicative of increasing cellular stress and metabolic dysfunction. **(F)** Mitochondrial proton leak measurements demonstrating a rising trend over successive cycles, suggesting escalating mitochondrial dysfunction as cycles progress. **(G)** HIF-1α expression levels in the third and fourth cycles, showing significantly elevated expression indicative of an intensifying hypoxic response with additional cycles. n=3 biological replicates, each in triplicate, mean ± SD. Statistical significance determined by 2-way ANOVA with baseline correction (A, B, E, F, G). ns: not significant, *p≤0.0316, **p≤0.0081, ***p≤0.001, ****p<0.0001.

4.2.2. HMGB1 Reduces Hypoxia-Induced Injury

Next, I investigated the impact of HMGB1 on cardiomyocytes after four cycles of hypoxia-normoxia (Fig. 7A) HMGB1 treatment led to a significant reduction in cTnI levels, suggesting a decrease in cellular stress and death (Fig. 7B). Additionally, HMGB1 treatment enhanced ATP production and reduced mitochondrial proton leak using XF90 Extracellular Flux Analyzer, indicating improved mitochondrial function (Figs. 7C, 7D and 7E).

Further analysis involved assessing the effects of HMGB1 on the gene expression profile of cardiomyocytes subjected to four cycles of hypoxia-normoxia. A volcano plot revealed differential gene expression, with upregulation of genes associated with cardiac mitochondrial function. Notable amongst those upregulated by HMGB1 were *ATF5*, which is involved in maintaining mitochondrial homeostasis; *NPPA*, which regulates mechanical stress; *ATP2A2*, responsible for calcium transport; and *PPARGC1α* (*PGC-1α*), critical for mitochondrial function and biogenesis (Fig. 7F). Conversely, genes associated with cell stress and death pathways, including *ATF3* and *TRIB3* (related to cellular stress and inflammatory responses), and *BNIP3L* (mitochondrial dysfunction), were downregulated by HMGB1 (Fig. 7F). Gene Ontology Enrichment Analysis supported these findings, with

upregulation of pathways associated with mitochondrial function and biogenesis and a concomitant downregulation of pathways involved in cell stress and death (Fig. 7F).

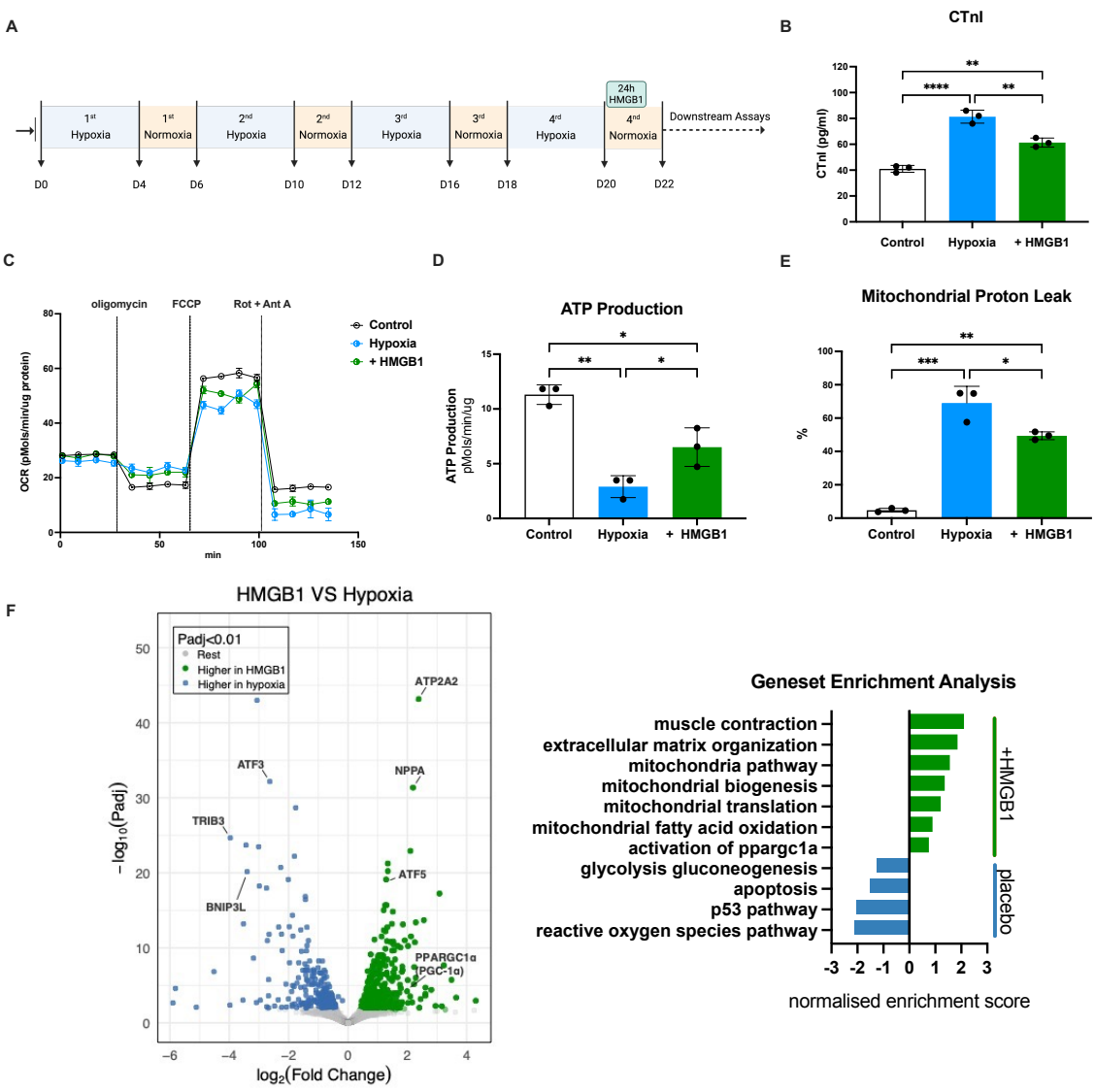

Figure 7. HMGB1 Improves Cardiomyocyte Viability and Function After Four Cycles of Hypoxia-Normoxia.

(A) Schematic representation of the experimental design, illustrating the timing of hypoxia-normoxia cycles and HMGB1 treatment. **(B)** HMGB1 treatment significantly reduces cell injury following four cycles of hypoxia-normoxia, as evidenced by lower cardiac Troponin I (cTnI) levels in the culture medium. **(C)** Real-time oxygen consumption rate (OCR) measurements of hESC-CMs under control conditions, hypoxia, and hypoxia with HMGB1 treatment, assessed by Seahorse extracellular flux analyzer. The graph shows sequential treatment with oligomycin, FCCP, and rotenone + antimycin A. **(D)** HMGB1 treatment significantly improved ATP production in hypoxic cardiomyocytes. **(E)**HMGB1 reduces mitochondrial proton leak, indicating improved mitochondrial function. **(F)** Left: Volcano plot displaying differential gene expression following HMGB1 treatment. Genes upregulated by HMGB1 are shown in green, downregulated genes in blue. Analysis was performed on bulk RNA-seq data using Galaxy. Right: Geneset Enrichment Analysis shows that HMGB1 treatment leads to upregulation of pathways associated with mitochondrial function and biogenesis, as well as fatty acid oxidation, while downregulating glycolysis, cell death, p53 pathway and reactive oxygen species pathways. Statistical significance was determined by one-way ANOVA (B, D, E). ns: not significant, *p≤0.0031, **p≤0.0064, ***p≤0.0002, ****p<0.0001. n = 3 biological replicates, each repeated in triplicate, data presented as mean ± SD.

4.2.3. HMGB1 Facilitation of Energy Production Shift and Mitochondrial Function

The Gene Ontology enrichment showed that HMGB1 upregulates mitochondrial fatty acid oxidation and downregulates glycolysis. I sought to confirm this using the Seahorse XF Real-Time ATP Rate Assay Kit to study the effects of HMGB1 on ATP derived from glycolysis and mitochondrial fatty acid oxidation over time (Fig. 8A). I found that HMGB1 restored mitochondrial fatty acid oxidation and reduced glycolysis-derived ATP production to near control levels at 7–10 hours, the effects being sustained up to 48 hours, with no statistical difference between HMGB1 and control group (Fig. 8B).

A key regulator of cardiomyocyte metabolism is the mammalian target of rapamycin complex (mTORC1/2), with phosphorylation associated with activation. I found that HMGB1 treatment of cardiomyocytes subjected to four cycles of hypoxia-normoxia resulted in upregulation of phospho-mTORC1 (Fig. 8C). Upstream regulators of mTORC include the MAP kinases MEK1 and ERK, as well as Akt [177]. HMGB1 treatment resulted in upregulation of MEK1, ERK1/2, and Akt (Fig. 8C).

In parallel, HMGB1 treatment downregulated pathways associated with cell stress (p53) and cell death (apoptosis) (Fig. 8D. I confirmed my findings from the gene expression at the protein level, with downregulation of p53 (Fig. 8D). In addition, there was downregulation of other pathways associated with cell stress, including JNK1/2, p38 and HIF-1α (Fig. 8D and 8E).

Gene Ontology enrichment also indicated that HMGB1 activation enhances pathways associated with PGC-1α. I confirmed that HMGB1 enhanced PGC-1α protein levels and also increased expression of YAP, with concomitant downregulation of BNIP3 and ROS (Fig. 8E).

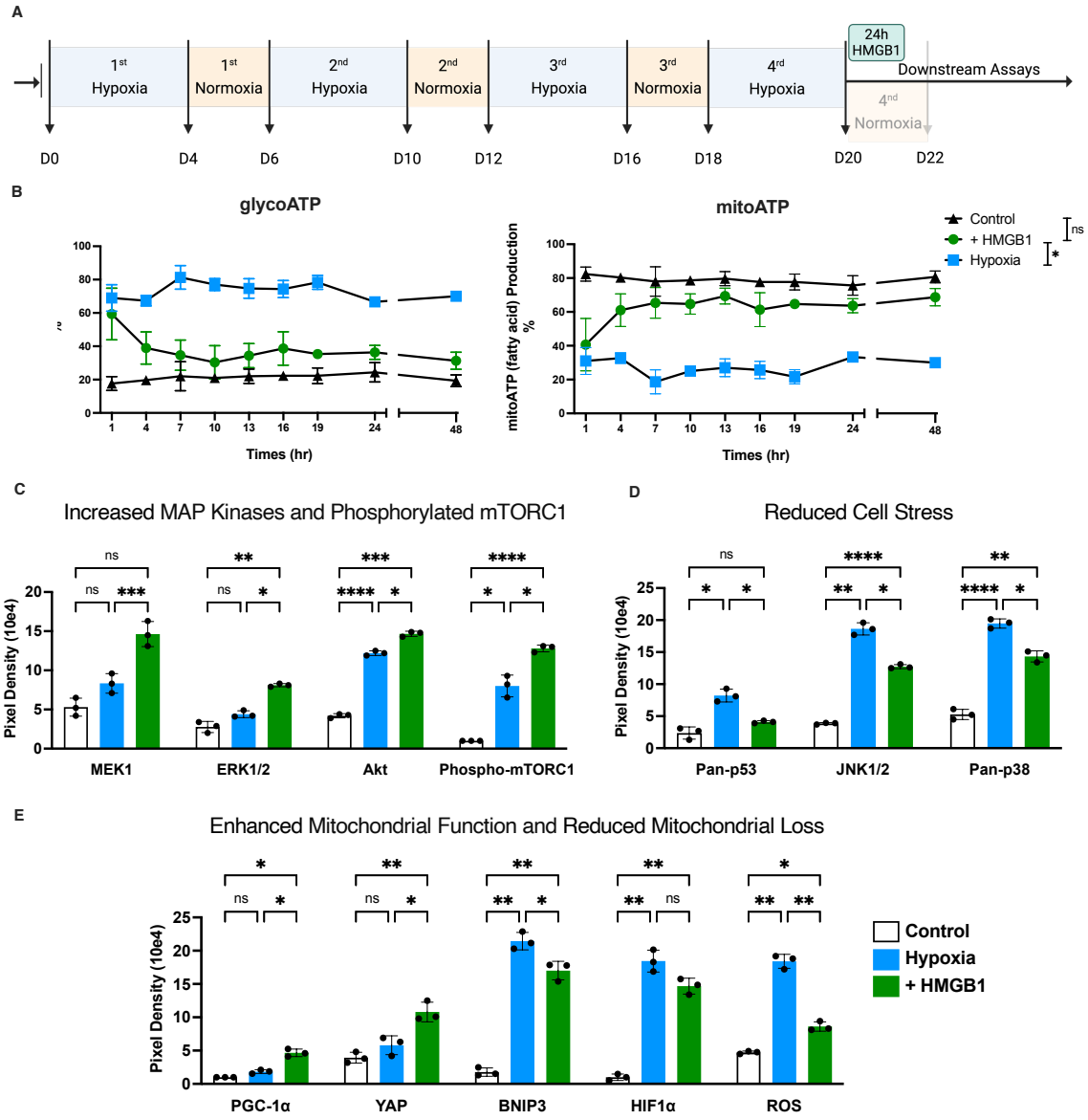

Figure 8. HMGB1 Restores Mitochondrial ATP Production and Modulates Cellular Pathways in Cardiomyocytes Exposed to Multiple Hypoxia-Normoxia Cycles

(A) Schematic representation of the experimental design, illustrating the timing of hypoxia-normoxia cycles and HMGB1 treatment. **(B)** HMGB1 shifts metabolism of cardiomyocytes exposed to four cycles of hypoxia-normoxia from glycolysis (glycoATP, left) back to mitochondrial fatty acid oxidation (mitoATP, right). Measurements taken at various time points over 48 hours. **(C)** HMGB1 upregulates phosphorylated mTORC1 and upstream MAP kinases (MEK1, ERK1/2) and Akt, indicating enhanced cellular growth and survival pathways. **(D)** HMGB1 downregulates proteins associated with cell stress (pan-p53, JNK1/2, pan-p38), suggesting reduced cellular stress response. **(E)** HMGB1 upregulates proteins associated with enhanced mitochondrial function (PGC-1α, YAP, BNIP3) and downregulates markers associated with mitochondrial loss (HIF1α, ROS), indicating improved mitochondrial health and reduced oxidative stress. Data presented as mean ± SD. Statistical significance was determined by one-way ANOVA (C, D, E). ns: not significant, *p ≤ 0.0376, **p ≤ 0.0095, ***p ≤ 0.00015, ****p ≤ 0.0001; n = 3 biological replicates, each repeated in triplicate.

4.2.4. Confirmation of the Role of mTOR in HMGB1-Regulated Pathways

Next, I sought to confirm my hypothesis that the effects of HMGB1 were mediated via mTOR (Fig. 9A). Addition of rapamycin, an mTOR inhibitor, abolished the effects of HMGB1 on ATP production (Fig. 9B). Our group has previously shown that HMGB1 transitions stem and progenitor cells from G_0 to G_{Alert} through an mTOR-dependent pathway and that G_{Alert} is characterised by increased levels of ATP and mitochondrial DNA [78].

Given that PGC-1α is a central regulator of mitochondrial function and biogenesis, I hypothesised that its modulation by HMGB1 could also be dependent on mTOR signalling. Addition of rapamycin suppressed the HMGB1-induced upregulation of PGC-1α in cardiomyocytes subjected to four cycles of hypoxia-normoxia ($p = 0.0030$) (Fig. 9C).

To further substantiate the critical role of PGC-1α, I employed siRNA-mediated knockdown of this protein in cardiomyocytes (Fig. 9D). PGC-1α expression was significantly reduced, reaching its lowest levels two days after siRNA treatment (Fig. 9E). However, due to the transient nature of siRNA effects, the experimental conditions were adjusted to only one cycle of hypoxia-normoxia instead of four. Under this condition, the knockdown of PGC-1α led to the complete loss of HMGB1-mediated increase in ATP production ($p = 0.0027$) (Fig. 9F).

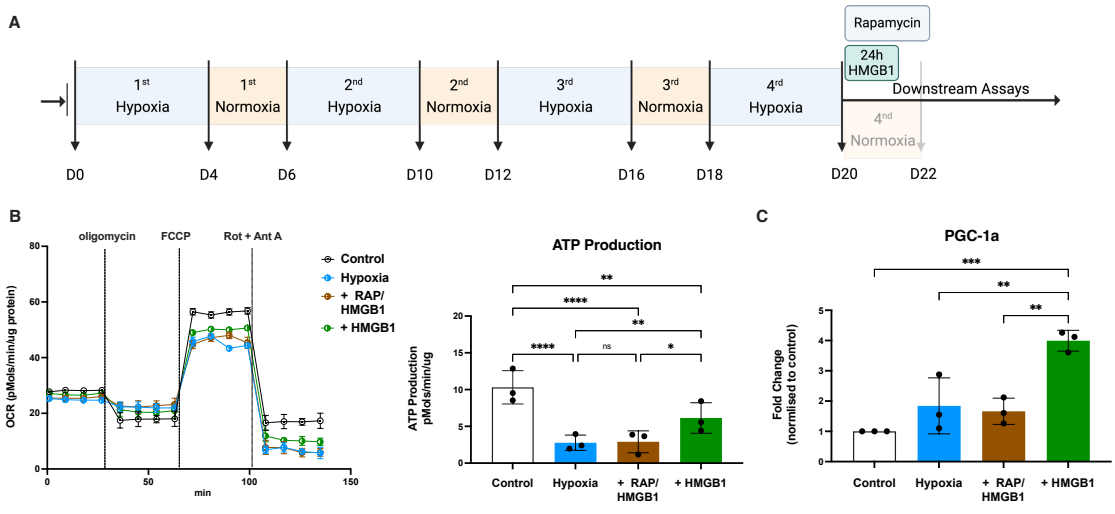

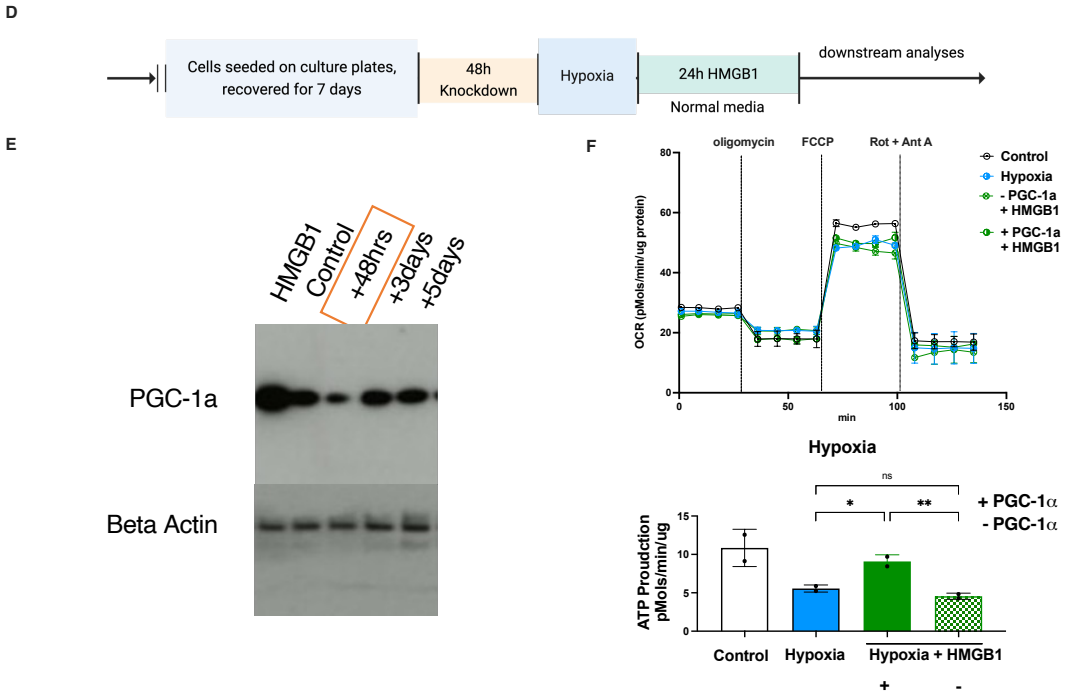

Figure 9. HMGB1 Effects on ATP Production and PGC-1α Are mTOR-Mediated.

(A) Schematic representation of the experimental design, illustrating the timing of hypoxia-normoxia cycles, rapamycin and HMGB1 treatment. **(B)** Rapamycin abolished the effects of HMGB1 on ATP production, as shown by OCR measurements (left) and quantification (right). **(C)** Rapamycin also abolished effect of HMGB1 on PGC-1α expression. **(D)** Experimental design for siRNA-mediated PGC-1α knockdown and subsequent HMGB1 treatment under hypoxic conditions. **(E)** Western blot showing siRNA-mediated knockdown maximally reduces PGC-1α levels at 48h, with 87% recovery after 5 days. HMGB1 treatment of healthy controls (positive control) showed higher PGC-1α expression compared to untreated control. **(F)** PGC-1α knockdown abolished effects of HMGB1 on upregulation of ATP production, demonstrated by OCR measurements (top) and quantification (bottom). Data presented as mean ± SD. Statistical significance determined by one-way ANOVA (B, C, F). ns: not significant *p=0.0468, **p<0.0030, ***p<0.0006, ****p<0.0001; n = 3 biological replicates for rapamycin experiments, n=2 for PGC-1α knockdown experiments, each repeated in triplicate.

4.3. Discussion

4.3.1. Cardiomyocyte Responses to Multiple Cycles of Hypoxia-Normoxia

In this chapter, I have described the effects of multiple hypoxia-normoxia cycles on cardiomyocytes. Multiple cycles emulate the repetitive ischaemia-reperfusion (I/R) insults that occur in NSTEMI [1, 13, 156, 178]. I assessed cellular stress and injury using several

markers: cTnI levels in the medium, cell viability, ATP production and mitochondrial proton leak. The data in Figure 6 reveal the progressive impact of successive hypoxia-normoxia cycles. cTnI levels showed significant increases from the second cycle onwards, indicating cumulative cellular damage. Cell viability decreased after the first cycle, with further significant reductions in the third and fourth cycles, visually confirmed by brightfield microscopy which showed marked morphological changes and reduced cell density in the fourth cycle. ATP production exhibited a declining trend across cycles, with a significant decrease observed between the first and fourth cycles, suggesting progressive metabolic dysfunction. Mitochondrial proton leak increased significantly in the third and fourth cycles compared to first cycle, indicating escalating mitochondrial dysfunction as cycles progressed. HIF-1α expression was significantly elevated following both the third and fourth cycles, with a marked increase from the third to the fourth cycle. These findings collectively suggest that while some effects of hypoxia-normoxia cycles are evident early, others become more pronounced with repeated cycles. The cumulative nature of the damage is particularly evident in the later cycles, with the fourth cycle showing the most severe effects across multiple parameters, especially HIF-1α expression and visible cell damage.

Expression of HIF-1α was found to be significantly increased within the infarct region during the early stages of myocardial infarction, whereas it was undetectable in the border zone [179]. HIF-1α has been shown to have multiple effects. It plays a crucial role in cardiac ischaemic preconditioning and eliminating HIF-1α through knockdown removes its protective effect, whereas inhibiting PHD2 or administering the HIF-1α activator dimethyloxalylglycine replicated its protective effects [179]. In contrast, other studies have demonstrated that a partial deficiency of HIF-1α significantly mitigates I/R injury in mice [180]. These apparently contradictory effects of HIF-1α may be explained by their dependence on levels and duration of HIF-1α expression. Whilst modest upregulation may be protective, prolonged activation of downstream signalling may be detrimental. For example, cardiac-specific overexpression of HIF-1α has been shown to induce myocardial hypertrophy and exacerbate cardiac dysfunction under conditions of pressure overload [181]. I found that HIF-1α levels were significantly increased between the third and fourth cycles of hypoxia and normoxia, mirroring the reduction in cell viability and reduction in

ATP production. Therefore, I used four cycles of hypoxia-normoxia for all my subsequent experiments, except where described otherwise.

4.3.2. Effects of HMGB1 on Cardiomyocytes Subjected to Four Cycles of Hypoxia-Normoxia

Mitochondrial morphology, dynamics, and function are known to be adversely affected during I/R injury, leading to a reduced capacity for ATP production and increased ROS generation [182, 183]. Chouchani et al. [21] further investigated this phenomenon, demonstrating that accumulated succinate is rapidly re-oxidised by succinate dehydrogenase during reperfusion, resulting in excessive ROS generation. This process exacerbates cellular damage and contributes significantly to the overall impact of I/R injury. Despite the growing understanding of these mechanisms, there is currently no approved therapeutic for limiting ischemia-reperfusion-induced injury, highlighting a critical need for further research in this area.

Treatment of cardiomyocytes with HMGB1 exposed to four cycles of hypoxia and normoxia resulted in reduced levels of cTnI in the media, indicating decreased cell stress and death. This was accompanied by improved mitochondrial function, as evidenced by an increase in ATP levels and a reduction in mitochondrial proton leak. These changes were further supported by the upregulation of genes associated with mitochondrial function and biogenesis, coupled with the downregulation of genes associated with cell stress, apoptosis, and loss of mitochondrial function. One of the genes most highly upregulated by HMGB1 was *ATP2A2*, which encodes an enzyme essential for transporting calcium ions for muscle contraction in an ATP-dependent manner [184, 185]. This finding aligns with the upregulation of muscle contraction observed in the Gene Set Enrichment Analysis.

HMGB1 also increased the expression of *ATF5*, which reduces mitochondrial stress [186], and upregulated *PPARGC1A*, the gene that encodes PGC-1α. In response to greater energy demands during stress, mitochondrial biogenesis is triggered within cardiomyocytes to increase ATP production and restore mitochondrial homeostasis, a process largely regulated by PGC-1α [187]. PGC-1α is a critical regulator of mitochondrial function and biogenesis, activating nuclear receptors and transcription factors such as NRF1/2, PPARs, thyroid hormone receptors (TR), estrogen-related receptors (ERR), hepatocyte nuclear

factor (HNF) 4α, FOXO1, and glucocorticoid receptor (GR) [188, 189]. Increased expression of PGC-1α can enhance the contractile function of cardiomyocytes by improving calcium handling (clearance) while maintaining calcium homeostasis [190]. This enhancement is consistent with the observed upregulation of muscle contraction and mitochondrial biogenesis. Overexpression of PGC-1α in cardiomyocytes also markedly increases fatty acid oxidation both in cell culture and *in vivo* [31].

4.3.3. Effects of HMGB1 on Cardiomyocyte Energy Dynamics

In the healthy heart, over 95% of the ATP consumed is generated through mitochondrial oxidative phosphorylation, with 50-70% derived from fatty acid oxidation and the remaining 5% supplied by glycolysis [191, 192]. However, during I/R, there is an orchestrated shift in cardiac metabolism under the regulation of HIF-1α, favouring increased glucose utilisation. This metabolic shift results in a lower ATP yield relative to oxygen consumption when glucose rather than fatty acids is metabolised, a critical adaptation to maintain cardiomyocyte viability during severe ischaemia [163, 164]. Furthermore, in conditions such as uncompensated hypertrophy and various forms of heart failure, characterised by elevated energy demands, there is a marked increase in glucose uptake and utilisation. This alteration in metabolism is accompanied by changes in anaerobic metabolism-related genes and adjustments in calcium handling [193].

Geneset Enrichment Analysis showed that HMGB1 upregulated genes associated with mitochondrial fatty acid oxidation and downregulated those associated with glycolysis. I confirmed that HMGB1 reversed the shift to glycolysis induced by four cycles of hypoxia-normoxia cardiomyocytes and restored the reliance of cardiomyocytes on fatty acid oxidation for ATP production. This is consistent with the improvement in other parameters of mitochondrial function and downregulation in HIF-1α.

4.3.4. The Role of mTOR Pathway in the Heart

mTOR is crucial for maintaining cardiovascular homeostasis and adapting to stress [194]. Activation of mTORC1 is essential for developing adaptive cardiac hypertrophy in response to mechanical overload [195]. Similarly, mTORC2 plays a vital role in normal cardiac physiology, promoting cardiomyocyte survival under conditions of pressure overload, as

evidenced by studies involving cardiac-specific gene knockdown [196]. Although preclinical studies have demonstrated that pharmacological inhibition of mTORC1 can reduce cardiac remodelling and mitigate heart failure symptoms in models of pressure overload and chronic myocardial infarction, these findings have not successfully translated into clinical application [197, 198].

I observed that MAP kinases exhibit increased activity in cardiomyocytes exposed to hypoxia as part of a complex cellular response to low oxygen stress. This activation serves multiple roles, including initiating stress response pathways, mediating ROS signaling, promoting cell survival, regulating key transcription factors like HIF-1α, facilitating mitochondrial adaptation, and activating antioxidant defences [199, 200]. Specifically, p38 MAPK is activated by hypoxia-induced mitochondrial ROS, further amplifying the stress response [200]. The ERK1/2 and JNK pathways are also activated during hypoxia, contributing to survival signalling and potentially to profibrotic responses in prolonged hypoxia condition [201, 202]. This multifaceted activation of MAP kinases aims to help cardiomyocytes adapt to and survive hypoxic conditions [203]. However, the balance and duration of this activation are critical, as prolonged or excessive MAP kinase activity can lead to maladaptive responses and contribute to pathological changes in the heart [204], as illustrated by my data.

Intriguingly, Dhingra et al. [205] have shown that mTOR overexpression reduces cardiomyocyte death under hypoxic conditions through NF-κB activation and Bnip3 downregulation [205]. This suggests that the protective effects noted in most preclinical settings might be mediated through engagement with downstream targets of mTOR. My data show that the effects of HMGB1 are crucially dependent on mTOR signalling. Upstream modulators of mTOR are the MAP kinases MEK1 and ERK, as well as Akt. I found that all these kinases were upregulated by HMGB1. Furthermore, I confirmed the pivotal role of mTOR signalling in mediating the effects of HMGB1 by abolishing these effects using rapamycin.

Activation of mTOR by HMGB1 was associated with improved cardiomyocyte function following cycles of hypoxia-normoxia. This was at least in part mediated by downregulation of pathways associated with cell stress and death, including JNK1/2, p38, HIF-1α, and p53. Concomitantly with reducing cell stress and injury, HMGB1 treatment enhanced

mitochondrial function and promoted cellular survival pathways. I found that HMGB1 treatment resulted in reduced levels of BNIP3 and ROS. Additionally, HMGB1 enhanced PGC-1α and YAP protein levels. Interestingly, rapamycin abolished the effects of HMGB1 on PGC-1α. The siRNA-mediated knockdown of PGC-1α confirmed its pivotal role in cardioprotection observed in this study, aligning with other research that has demonstrated similar protective effects by PGC-1α [206, 207]. One of the limitations of siRNA- PGC-1α knockdown is that the downregulation was temporary and limited to 7 days. Therefore, I was only able to assess the effects on cardiomyocytes exposed to one cycle of hypoxia-normoxia. In the future, this could be extended to the full four cycles using CRISPR-Cas gene deletion.

4.4. **Conclusion**

In summary, my data show that HMGB1 rescues cardiomyocytes exposed to multiple cycles of hypoxia-normoxia by upregulating pathways related to preservation of mitochondrial function. I confirmed that these effects were mediated through mTORC and PGC-1α (Fig. 10).

In the next chapter I will explore the effects of an improved HMGB1 construct and efficacy in doxorubicin-induced cardiotoxicit

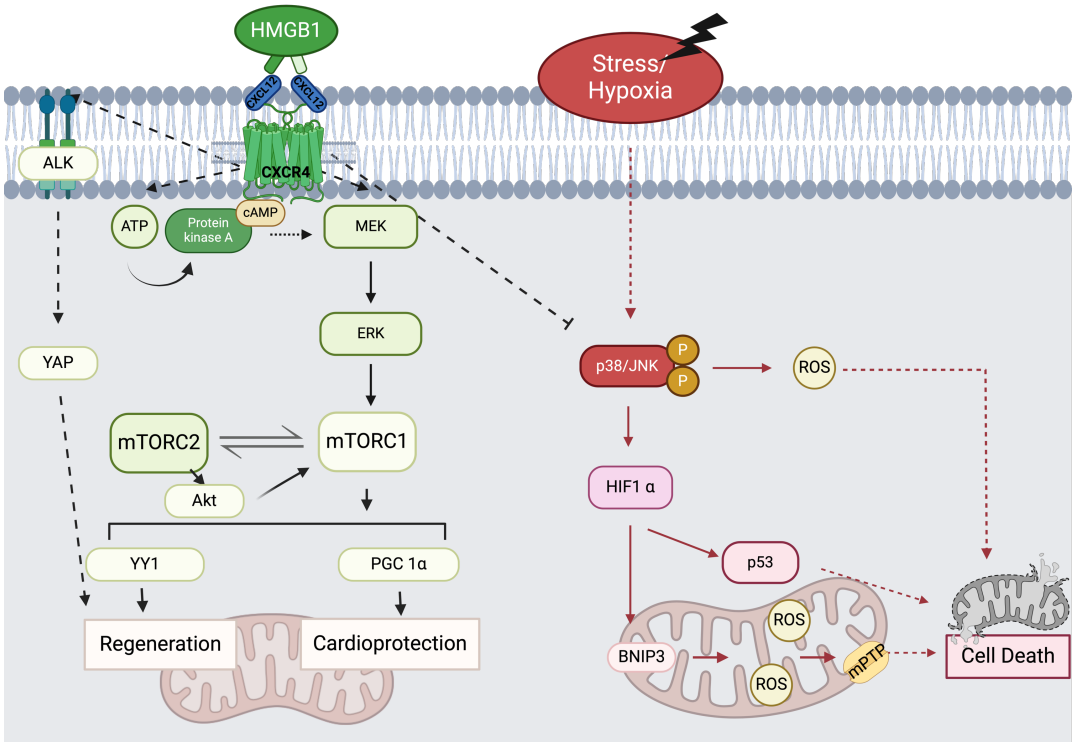

Figure 10: Schematic representation of the proposed HMGB1 signaling pathway

Chapter 5. The effect of HMGB1 and dBB in Ischaemia-Reperfusion (I/R) Injury and Doxorubicin-Induced Cardiotoxicity (DIC)

5.1. Introduction

In the previous chapter, I showed that FR-HMGB1 can improve cardiomyocyte viability following hypoxia-induced injury by preserving and upregulating mitochondrial pathways. I also showed that four cycles of hypoxia followed by normoxia mimic the effects of ischaemia reperfusion in vivo following acute myocardial infarction. [208]About one-third of patients who suffer an MI develop heart failure [208], and my data would suggest that FR-HMGB1 has the potential to prevent the development of ischaemic heart failure.

In the USA, about 2.5% of the population are affected by heart failure, with around 6.7 million people affected during the period 2017-2020 [209]. In the USA, the costs associated with heart failure in 2012 were $31 billion, two thirds of which were direct healthcare costs. The overall costs are projected to increase to $70 billion in 2030 as the number of people affected increases to > 8 million [210]. Approximately 46% of patients are affected by heart failure with preserved (>50%) ejection fraction (HFpEF), 8% have heart failure with mid-range (40-49%) ejection fraction, and another 46% heart failure with reduced (<40%) ejection fraction (HFrEF) [211]. Regardless of sub-type, 5-year survival remains low at around 50%, although there has been some improvement over recent years due to the use of evidence-based treatments [10, 11]. This reflects the relatively limited efficacy of current therapeutic modalities [11].

Factors associated with the development of heart failure include diabetes mellitus, obesity, hypertension, coronary artery disease. Numerous drugs can also exacerbate or cause heart failure, including analgesics, anaesthetic agents, drugs used to treat diabetes, arrhythmias, hypertension, fungal infections, neurological and psychiatric conditions, rheumatological diseases, pulmonary and urological conditions [212]. The largest class of drugs that cause cardiotoxicity are those used to treat cancer and include the anthracyclines, alkylating agents, anti-metabolites, taxanes, as well as targeted treatments such as some monoclonal

antibodies and kinase inhibitors [212]. Amongst the best known is the anthracycline doxorubicin. Chronic cardiotoxicity after doxorubicin treatment usually develops after a median of 7 years, and is characterised by cardiac dilatation, thinning of ventricular wall, progressive decline in left ventricular ejection fraction and eventually heart failure. Development of heart failure is dose-related, at 5% with a cumulative dose of 400 mg/m^2 and increases to 48% at a dose of 700 mg/m^2 [213]. Despite advancements in targeted therapies, such as tyrosine kinase inhibitors and monoclonal antibodies, anthracyclines continue to be prescribed to 40-50% of breast cancer patients and other cancer patients [214, 215], although predicting which patients will develop doxorubicin-induced cardiotoxicity and adequately protecting those at risk remains a significant challenge [216].

5.1.1. Mechanism of Doxorubicin-Induced Cardiotoxicity (DIC)

Reactive oxygen species (ROS) and mitochondrial dysfunction are major drivers of doxorubicin-induced cardiotoxicity (DIC) [213, 217]. The aetiology of DIC is multifaceted, including the generation of ROS leading to membrane damage [218], inhibition of topoisomerase II-β (TOP2B) and topoisomerase I mitochondrial (TOP1MT) [219, 220], and altered intracellular calcium [221]. Doxorubicin-induced ROS, through redox cycling within cardiomyocytes, leads to lipid peroxidation, mitochondrial dysfunction, DNA damage and protein carbonylation. Under normal conditions, ROS are neutralised by endogenous antioxidants like glutathione peroxidase, catalase, and superoxide dismutase. However, doxorubicin impairs these antioxidants, exacerbating oxidative stress and leading to DIC [222]. Mitochondria are particularly susceptible to doxorubicin-induced ROS due to the affinity of doxorubicin for cardiolipin, a component of the inner mitochondrial membrane [223, 224]. Additionally, TOP2B and TOP1MT inhibition disrupts nuclear and mitochondrial gene expression and triggers DNA-damage-induced apoptosis, with TOP2B implicated in reduced mitochondrial biogenesis mediated by PGC-1α and PGC-1β [219]. Finally, doxorubicin and its metabolite, doxorubicinol, induce Ca^{2+} release from the sarcoplasmic reticulum, leading to Ca^{2+} overload, sarcomeric disarray and myofibril deterioration [221, 225].

5.1.2. Engineered HMGB1

As described in my introductory chapter, FR-HMGB1 can be oxidised to the disulfide form (DS-HMGB1), [87]which has no reparative effects and instead promotes inflammation by

signalling through TLR-2, TLR-4 and RAGE [76, 226]. DS-HMGB1 is also the most potent platelet activator through RAGE signalling [89]. This has prompted the development of engineered variants that retain regenerative potential whilst avoiding potential deleterious proinflammatory effects [76]. One approach comprised substituting three cysteines in FR-HMGB1 with serines (3S-HMGB1) to inhibit disulfide bond formation between the two cysteines within the Box A domain, which leads to the formation of DS-HMGB1 [76]. Whilst in skeletal muscle, bone, bone marrow and liver the 3S-HMGB1 had similar effects to FR-HMGB1 [78, 87], when injected into the myocardium 4 hours after permanent ligation of the LAD, it resulted in increased fibrosis compared to placebo whilst FR-HMGB1 injection resulted in improved function [88].

During the course of my DPhil a member of our group (Alvaro Vinals Guitart) developed a different engineered form of HMGB1 comprising two Box B domains in tandem (dBB) [227]. FR-HMGB1 binds CXCL12 and the heterocomplex signals via the cell surface receptor CXCR4 [78]. DS-HMGB1 does not bind CXCL12 and instead signals via TLR-2, TLR-4 and RAGE. Dr Vinals Guitart mapped the epitopes on HMGB1 that bind CXCL12, TLR-2, TLR-4 and RAGE to design dBB.

In this chapter I will describe the effects of FR-HMGB1 on cardiomyocytes before or after doxorubicin-induced injury and also compare the effects of dBB with FR-HMGB1 on hESC-derived cardiomyocytes.

5.2. Results

5.2.1. dBB Retains Full Regenerative Capacity While Remaining Non-Oxidisable

In the previous chapter I showed that the fully reduced HMGB1 (FR-HMGB1) reduces hypoxia-induced injury by enhancing mitochondrial function and reducing cellular stress signalling *in vitro*. However, the potential conversion of FR-HMGB1 to its disulfide (DS) form in the extracellular environment, which can provoke an inflammatory response, has not been adequately addressed. In order to overcome these limitations, Dr Vinals Guitart developed an engineered HMGB1 variant, dBB, which does not include a Box A domain whilst retaining the capacity to bind CXCL12. dBB comprises two Box B domains in tandem, linked by a

short peptide bridge. I investigated the regenerative properties of various dBB constructs with different linker lengths and amino acid composition by assessing their effects on promoting the differentiation of endodermal cells derived from H9 human embryonic stem cells (hESC). I used the expression of the early endoderm progenitor marker, CXCR4, as a marker of differentiation. dBB12L led to a significant increase in the proportion of CXCR4-positive cells compared to control (Fig. 11A), and significantly outperformed almost all the other variants ($p < 0.0001$). Although dBB did not statistically differ from FR-HMGB1 to dBB167-172D, it showed a higher trend (Fig. 11A).

Next, I explored whether dBB could induce an inflammatory response in human MI macrophages differentiated from human monocytes by assessing tumour necrosis factor (TNF) expression. DS-HMGB1 increased TNF production, which was further enhanced by the addition of TLR-2 ligand lipoteichoic acid (LTA) (Fig. 11B) ($p<0.0001$). DS-HMGB1 also led to a significant increase in TNF production, with no synergistic effect observed with the TLR-4 ligand lipopolysaccharide (LPS) (Fig. 11B) ($p<0.0001$), whereas addition of dBB or FR-HMGB1 did not result in increased TNF production, even in the presence of the co-ligands. (Fig. 11B).

Given the importance of DS-HMGB1 to promote platelet activation, which accelerates thrombosis *in vivo*, I also assessed the prothrombotic response to dBB. A human blood clotting assay using a PFA-100 with Collagen/EPI cartridge, Collagen/ADP cartridge, and P2Y cartridge revealed no change in closure times after pre-exposure of whole blood from healthy donors to dBB for 30 minutes, compared to untreated controls. In contrast, pre-incubation with DS-HMGB1 significantly decreased closure times in all three assays (Fig. 11C), underscoring the non-thrombogenic nature of dBB.

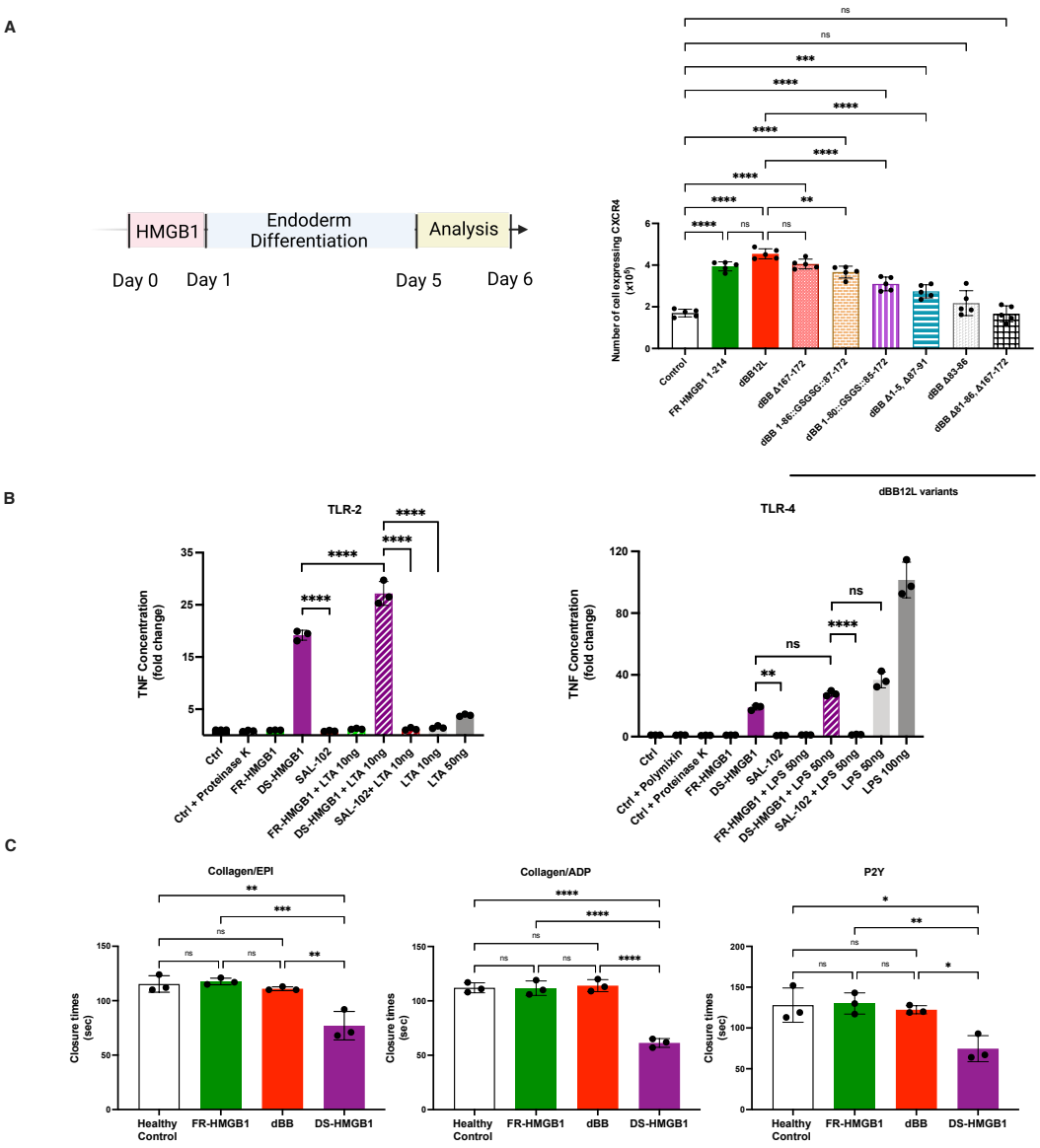

Figure 11. Engineered HMGB1 Construct dBB Retains Regenerative Effect Without Inducing Proinflammatory Cytokine Production or Platelet Activation

(A) Left: Schematic of experimental design for H9 endoderm differentiation with HMGB1 treatment. Right: Gene expression analysis of endodermal markers following HMGB1 treatment, showing dBB promotes differentiation of endodermal progenitor cells. **(B)** TNF production by human monocytes in response to various HMGB1 forms. Left: TLR-2 activation. Right: TLR-4 activation. Disulfide HMGB1 (DS-HMGB1) leads to increased production of TNF, which is enhanced by the presence of the TLR-2 ligand lipoteichoic acid (LTA) or the TLR-4 ligand LPS. dBB (dBB12L) and fully reduced HMGB1 (FR-HMGB1) show no increase in TNF production compared to control, even in the presence of co-ligands. **(C)** Platelet activation assays showing dBB and HMGB1 do not promote platelet activation. Left: Collagen/EPI closure time. Middle: Collagen/ADP closure time. Right: PFA-100 closure time. Data presented as mean ± SD. Statistical significance was determined by one-way ANOVA (A, B, C) followed by the Sidak post-hoc test. ns: not significant, *p≤0.0186, **p≤0.0081, ****p<0.0001. (A) n = 5, (B, C) n= 3 biological replicates, and each repeated in triplicate.

5.2.2. HMGB1 Reduces Doxorubicin-Induced Cardiotoxicity (DIC)

Having found that FR-HMGB1 ameliorates the injury induced by four cycles of hypoxia-normoxia, I investigated the effects on doxorubicin-induced cardiotoxicity. The doxorubicin model was selected for testing HMGB1 due to extensive literature on the role of reactive oxygen species (ROS), mitochondrial dysfunction and apoptosis-mediated loss of cardiomyocytes in doxorubicin-induced cardiotoxicity [228]. In the previous chapter I described my data showing FR-HMGB1 reduced all these effects following hypoxia-normoxia. Treatment with FR-HMGB1, administered either before or after doxorubicin exposure, significantly reduced cTnI levels, indicating a reduction in cellular stress and death (Fig. 2A). Interestingly, no significant differences were observed between pre- and post-doxorubicin exposure treatments with HMGB1 (Fig. 12A). HMGB1 also resulted in enhanced ATP production and reduced mitochondrial proton leak, suggesting improvements in mitochondrial function (Fig. 12B and 12C) ($p <= 0.0041$). Notably, HMGB1 treatment prior to doxorubicin exposure resulted in a greater reduction in no difference in ATP and mitochondrial leak compared to post-treatment (Fig. 12C).

As I approached the conclusion of my experiments with HMGB1 and my DPhil studies, dBB became available for testing. I then repeated key experiments with dBB along with HMGB1 to investigate the critical role of PGC-1α in doxorubicin-induced cardiotoxicity. Employing siRNA-mediated knockdown of PGC-1α in cardiomyocytes, I observed a significant reduction in PGC-1α expression, reaching its lowest levels two days post-siRNA treatment as described in the previous chapter (Fig. 9E). Given that ATP production and cell damage appeared consistent between HMGB1 treatments before and after doxorubicin exposure, I decided to focus solely on administration of HMGB1 constructs after post-doxorubicin-induced injury for these experiments. Knockdown of PGC-1α resulted in complete loss of the reduction in cardiomyocyte injury as assessed by levels of cTnI in the media (Fig. 12D) and restoration of ATP production (Fig. 12E).

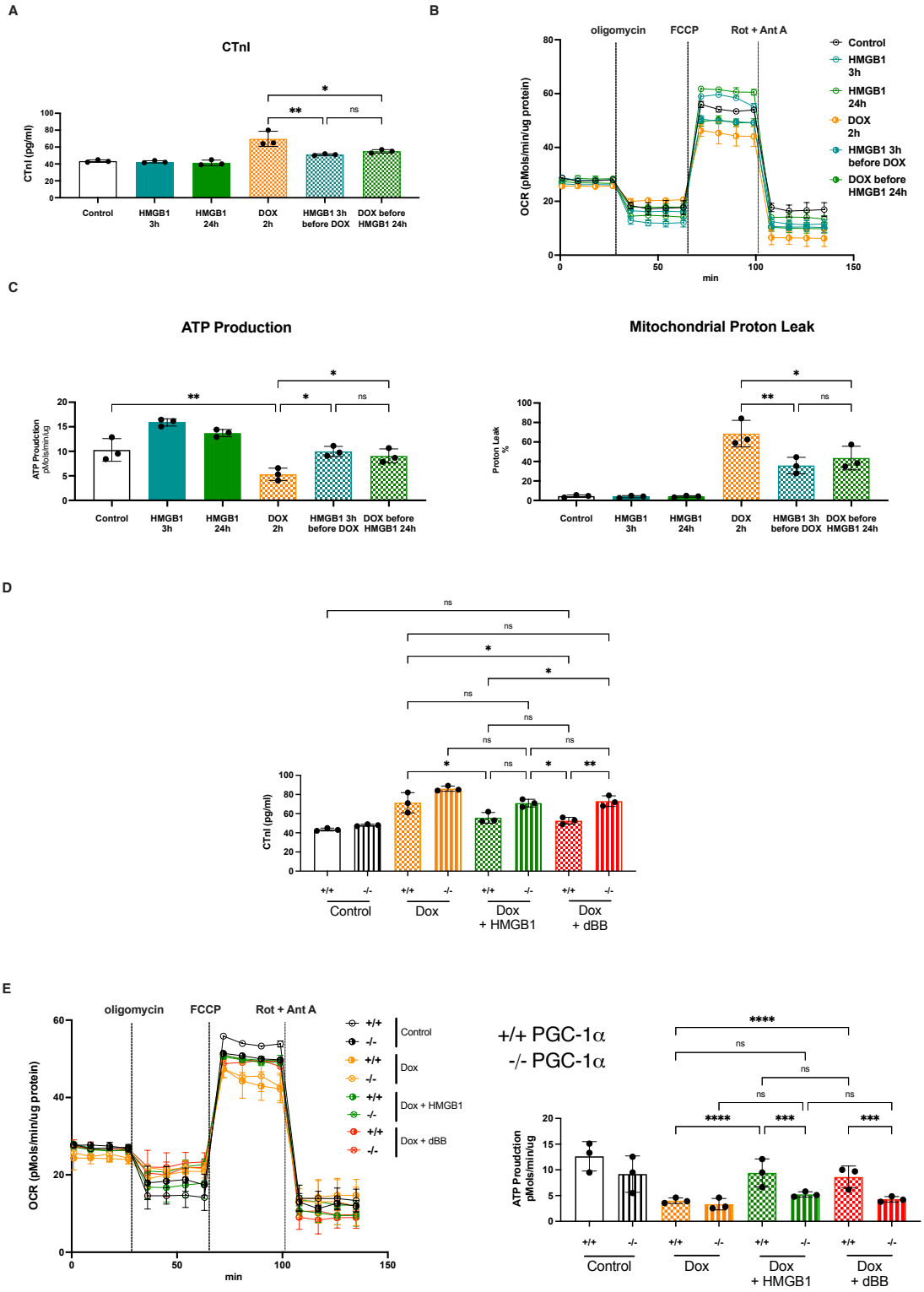
A
CTnI
CTnI (pg/ml)
Control
HMGB1 3h
HMGB1 24h
DOX 2h
HMGB1 3h before DOX
DOX before HMGB1 24h
B
oligomycin
FCCP
Rot + Ant A
OCR (pMols/min/ug protein)
min
C
ATP Production
ATP Proudction pMols/min/ug
Mitochondrial Proton Leak
Proton Leak %
D
CTnI (pg/ml)
Control
Dox
Dox + HMGB1
Dox + dBB
E
OCR (pMols/min/ug protein)
+/+ PGC-1α
-/- PGC-1α
ATP Proudction pMols/min/ug

Figure 12. FR-HMGB1 and dBB Reduce Doxorubicin-Induced Cardiotoxicity by Preserving Mitochondrial Function through PGC-1α

(A) Cardiac Troponin I (cTnI) levels in culture medium as a marker of cardiomyocyte injury. Treatment with FR-HMGB1 (1.2 mg/kg) either 3 hours before or 24 hours after doxorubicin (DOX, 5 μM) administration significantly reduces cTnI release compared to DOX alone, indicating a protective effect against doxorubicin-induced cardiotoxicity. **(B)** Real-time oxygen consumption rate (OCR) measurements under various treatment conditions. **(C)** Left: ATP production as measured by the Seahorse analyzer. FR-HMGB1 treatment, both before and after DOX exposure, significantly enhanced ATP production compared to DOX alone. Right: Mitochondrial proton leak. FR-HMGB1 treatment significantly reduced the DOX-induced increase in proton leak, suggesting preservation of mitochondrial integrity. **(D)** Effect of PGC-1α knockdown on cTnI levels. The +/- notation indicates the presence or absence of PGC-1α. PGC-1α knockdown abolished the protective effects of both FR-HMGB1 or dBB on DOX-induced cTnI release. **(E)** Impact of PGC-1α knockdown on ATP production following doxorubicin-induced cardiotoxicity. Both FR-HMGB1 and dBB failed to upregulate ATP production following PGC-1α knockdown , supporting the essential role of PGC-1α in mediating the protective effects against DOX-induced mitochondrial dysfunction. Data presented as mean ± SD. Statistical significance was determined by one-way ANOVA (A, C), and two-way ANOVA (D, E). ns: not significant *p≤0.0347, **p≤0.0079, ***p≤0.0003, ****p<0.0001. n= 3 biological replicates, each repeated in triplicate

5.2.3. dBB Demonstrates Comparable or Superior Efficacy in Reducing Hypoxia-Induced Injury Relative to HMGB1

In subsequent experiments, I assessed the efficacy of dBB on cardiomyocytes subjected to four cycles of hypoxia-normoxia, again focusing on selected key experiments. Treatment with dBB significantly decreased cTnI levels, indicative of a reduction in cellular stress and death (Fig. 13A). There was no difference in the reduction of cTnI levels between dBB and HMGB1 treatments (Fig. 13A). Additionally, dBB treatment resulted in enhanced ATP production and reduced mitochondrial proton leak and was significantly better than FR-HMGB1 (Fig. 13B, 13C and 13D).

Next, I investigated the effects of dBB on the gene expression profile of cardiomyocytes after four cycles of hypoxia-normoxia using bulk RNA sequencing. A volcano plot revealed differential gene expression, with upregulation of genes associated with cardiac mitochondrial function. These findings were consistent with those described for FR-HMGB1 in the previous chapter. Genes upregulated by dBB included *ATF5*, involved in maintaining mitochondrial homeostasis; *NPPA*, which regulates mechanical stress; *ATP2A2*,

responsible for calcium transport; *PPARGC1α* (PGC-1α), which is critical for mitochondrial function and biogenesis; and *CALM1*, which is involved in calcium signalling (Fig. 13E). Conversely, genes associated with cell stress and death pathways, such as *ATF3* and *TRIB3* (related to cellular stress and inflammatory responses), were downregulated by dBB (Fig. 13E). Gene Ontology Enrichment Analysis confirmed these findings, with upregulation of pathways associated with mitochondrial function and biogenesis and concurrent downregulation of pathways involved in cell stress and death (Fig. 13E).

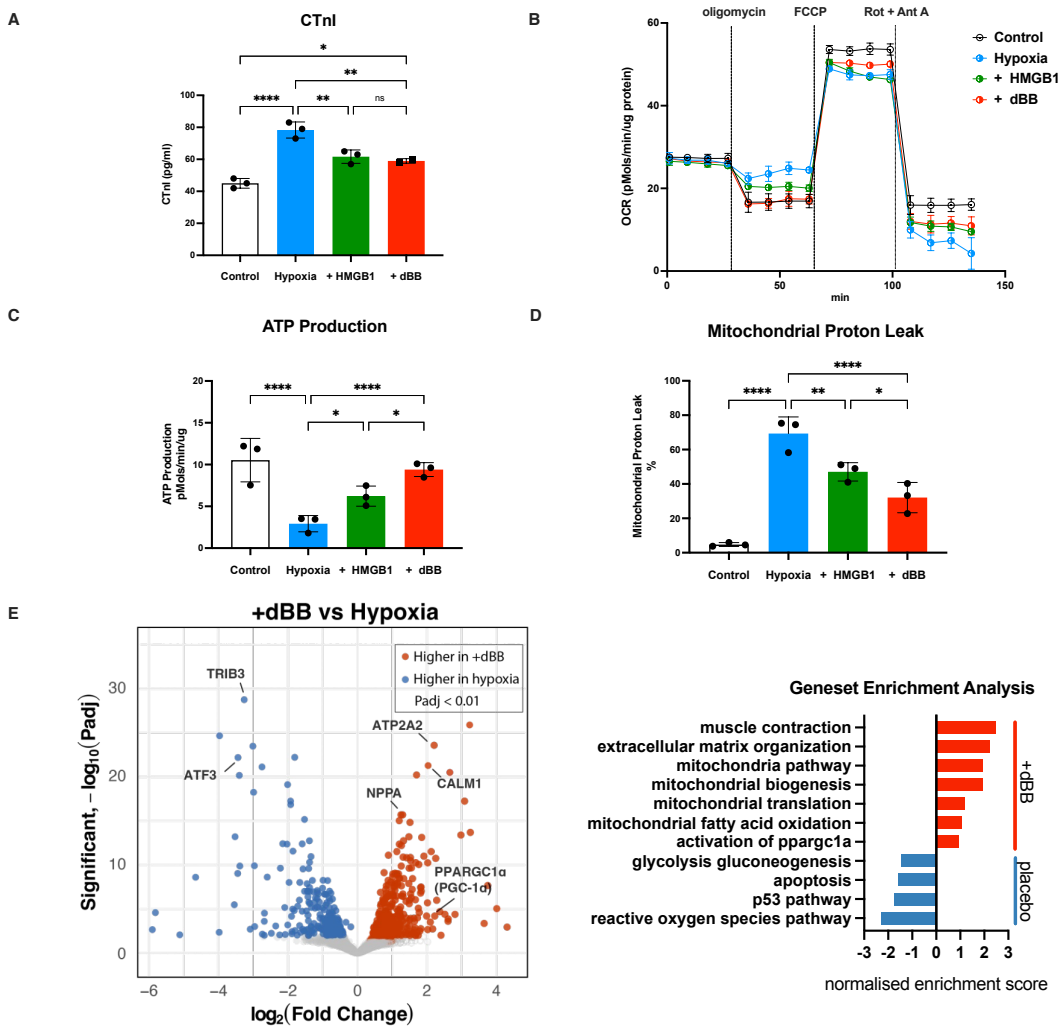

Figure 13. dBB Matches or Exceeds HMGB1 in Improving Viability and Mitochondrial Function of Cardiomyocytes Exposed to Four Cycles of Hypoxia-Normoxia

(A) Cardiac Troponin I (cTnI) levels in culture medium under various treatment conditions. Both dBB and HMGB1 treatment significantly reduce cTnI release compared to hypoxia alone, with comparable protection against hypoxia-induced cardiomyocyte injury. **(B-C)** ATP production as measured by Seahorse extracellular flux analyzer. dBB treatment increased ATP production to a higher level compared to HMGB1

treatment, both showing significant improvement over hypoxia alone. **(D)** Mitochondrial proton leak assessment. dBB treatment further reduces hypoxia-induced mitochondrial proton leak compared to HMGB1, suggesting superior preservation of mitochondrial integrity. **(E)** Left: Volcano plot displaying differential gene expression following dBB treatment compared to hypoxia. Notable genes involved in mitochondrial function, including *ATP2A2*, *PPARGC1α,* are upregulated (red), while genes associated with cell death pathways are downregulated (blue). Right: Geneset Enrichment Analysis showing that dBB treatment leads to upregulation of pathways associated with mitochondrial function and biogenesis, as well as fatty acid oxidation, and downregulation of glycolysis, cell death, p53 pathway and reactive oxygen species pathways. n = 3 biological replicates, each repeated in triplicate. Data presented as mean ± SD. Statistical significance determined by one-way ANOVA followed by Tukey's post-hoc test. ns: not significant,**p≤0.0064, ***p≤0.0002, ****p<0.0001. For the volcano plot, differential expression determined using a threshold of Padj < 0.01.

5.2.4. dBB Facilitates Shifts of Energy Production and Enhances Mitochondrial Function

Gene Ontology Enrichment Analysis revealed that dBB upregulates mitochondrial fatty acid oxidation while concurrently downregulating glycolysis. As before, I validated these observations by utilising the Seahorse XF Real-Time ATP Rate Assay Kit to examine the effects of dBB on ATP production derived from glycolysis and mitochondrial fatty acid oxidation at selected time points. I observed that dBB restored mitochondrial fatty acid oxidation and reduced glycolysis-derived ATP production to near control levels within 7-10 hours, with these effects sustained up to 48 hours. There were no significant differences in the metabolic profiles between dBB, FR-HMGB1 and the control group (Fig. 14A).

As discussed in the previous chapter, the mammalian target of rapamycin complex (mTORC1/2) is a critical regulator of cardiomyocyte metabolism, with phosphorylation indicating activation. Treatment with dBB in cardiomyocytes subjected to four cycles of hypoxia-normoxia resulted in an upregulation of phospho-mTORC1 (Fig. 14B). dBB also exhibited higher levels of Akt and MAP kinases ERK, which are upstream of mTOR, compared to HMGB1, although there was no significant difference in the expression of MEK between the treatments (Fig. 14B).

Concurrently, dBB treatment downregulated pathways associated with cellular stress and apoptosis. This included reduction in p53 expression, confirmed at both the gene and protein levels, with downregulation also observed in other stress-related pathways, including

JNK1/2, p38, and HIF-1α. dBB resulted in lower levels of HIF-1α compared to FR-HMGB1 (Fig. 14C).

Gene Ontology Enrichment Analysis also indicated that dBB enhances pathways associated with PGC-1α. I confirmed that dBB increased PGC-1α protein levels and upregulated YAP expression, with a concurrent reduction in BNIP3 and ROS levels. Overall, dBB showed improved effects on these markers compared to FR-HMGB1 (Fig. 14D). Knockdown of PGC-1α, as described in the previous chapter (Fig. 9E), completely abolished the beneficial effects mediated by dBB, including increase in ATP production (Fig. 14E).

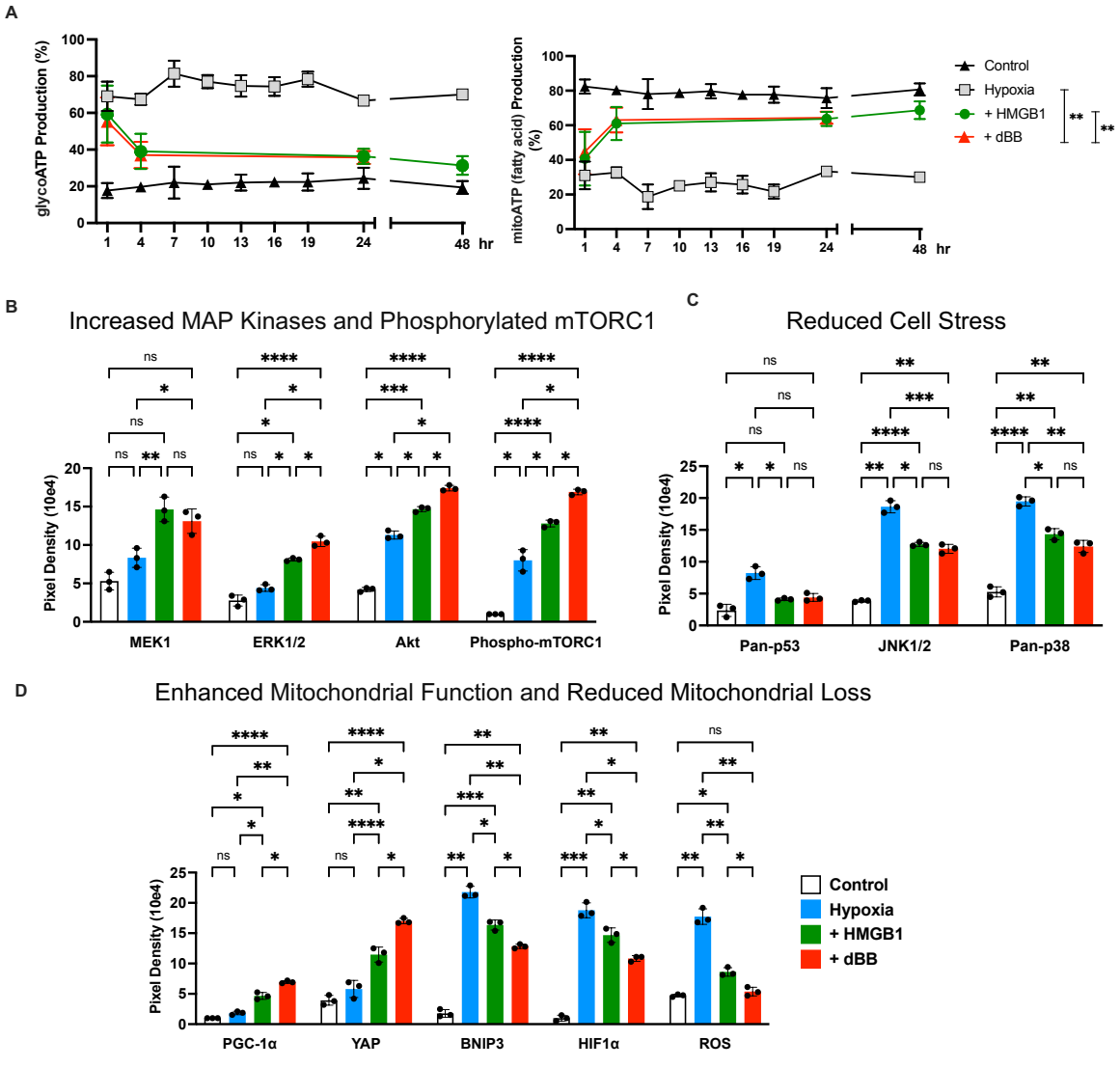

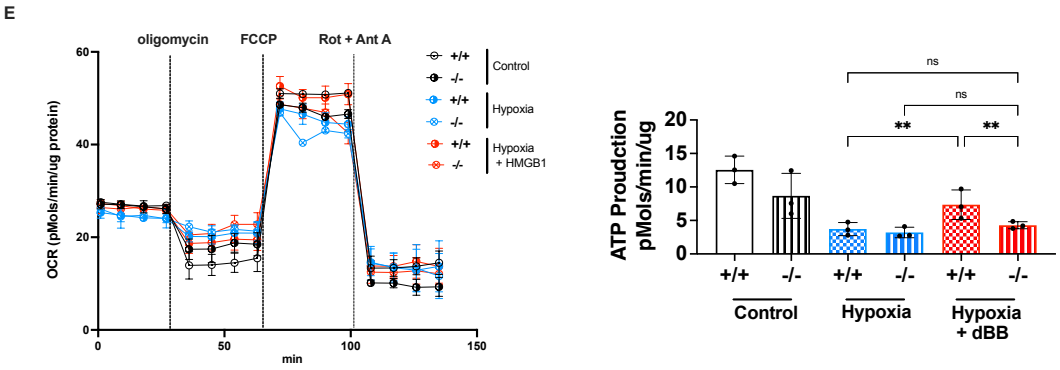

Figure 14. dBB Matches or Exceeds HMGB1 in Restoring Mitochondrial Function and Reducing Cellular Stress in Cardiomyocytes Exposed to Hypoxia-Normoxia Cycles

(A) Metabolic shift in cardiomyocytes exposed to three cycles of hypoxia-normoxia. Left: Glycolytic ATP production (glycoATP) over time. Right: Mitochondrial fatty acid oxidation-derived ATP production (mitoATP) over time. dBB treatment shifts metabolism from glycolysis back to mitochondrial fatty acid oxidation, matching the effect of HMGB1. **(B)** Upregulation of phosphorylated mTORC1 and upstream MAP kinases (MEK1, ERK1/2, and Akt) by dBB and HMGB1 treatments, indicating enhanced cellular growth and survival pathways. **(C)** Downregulation of proteins associated with cell stress (pan-p53, JNK1/2, pan-p38) by dBB and HMGB1 treatments, suggesting reduced cellular stress response. **(D)** Effects on mitochondrial function-related proteins. dBB and HMGB1 upregulate proteins associated with enhanced mitochondrial function (PGC-1α, YAP, BNIP3) and downregulate markers associated with mitochondrial loss (HIF1α, ROS), indicating improved mitochondrial health and reduced oxidative stress. **(E)** Impact of PGC-1α knockdown on dBB effects. Left: ATP production. Right: Mitochondrial proton leak. siRNA-mediated knockdown of PGC-1α abolishes the upregulation of ATP production by dBB, demonstrating the crucial role of PGC-1α in mediating effects of dBB effects. Data presented as mean ± SD. Statistical significance determined by one-way ANOVA followed by Tukey's post-hoc test. ns: not significant, *p<0.011, **p<0.0015, ***p<0.00015, ****p<0.0001; n= 3 biological replicate, each repeated in triplicate

5.3. Discussion

In this chapter, the investigation focused on the efficacy of the engineered HMGB1 construct dBB in mitigating both doxorubicin-induced and hypoxia-induced cardiotoxicity. The results demonstrated that dBB was comparable or superior compared to FR-HMGB1 in reducing both doxorubicin-induced cardiotoxicity and hypoxia-induced injury. dBB effectively reduced cardiac troponin I levels, enhanced ATP production and improved mitochondrial function. These findings underscore the potential of engineered HMGB1 constructs like dBB for therapeutic applications to prevent drug-related cardiotoxicity and ameliorate the effects of

ischaemia reperfusion following MI, provide insights into their mechanisms of action and highlighting the pivotal role of mitochondrial pathways in mediating these effects.

5.3.1. Engineered HMGB1 Variant, dBB

HMGB1, when oxidised to its disulfide form, promotes inflammation signalling via TLR-2, TLR-4 and RAGE via NF-kB [76, 84, 226]. In contrast, FR-HMGB1 binds to CXCL12 and the heterocomplex signals via CXCR4 to promote cell migration [76] and tissue repair [78, 87]. DS-HMGB1 is also the most important activator of platelets via RAGE [89]. Moreover, the HMGB1-TLR-2/TLR-4 signalling cascade has been shown to induce M1 macrophage polarisation, leading to cardiac dysfunction in mice prone to development of senescence [229]. Additionally, the HMGB1-TLR-4 axis plays a crucial role in inflammatory diseases, affecting the expression of major histocompatibility complex class I (MHC-I), TNF and IL-6, thereby amplifying the inflammatory response [230, 231]. If HMGB1 is to be used as a therapeutic, it is essential that we use a construct that cannot be oxidised to promote deleterious proinflammatory signalling or further thrombosis.

Another group has attempted to engineer a non-oxidisable HMGB1 variant, 3S-HMGB1, by replacing three cysteines in FR-HMGB1 (two in Box A and one in Box B) with serines to prevent disulfide bond formation within the Box A domain [76]. Although exogenous administration of 3S-HMGB1 has been shown to enhance regeneration in skeletal muscle and cell replication in the liver following injury [87], it proved deleterious in the heart, leading to increased fibrosis compared to placebo [88]. The data presented in this study showed that 3S-HMGB1 was more effective in promoting the migration of cardiac fibroblasts and interacted with CXCR4 differently from FR-HMGB1-CXCL12 as the effects on fibroblast migration could not be inhibited by AMD3100, a specific clinically approved inhibitor of CXCL12-CXCR4, or a CXCL12 antibody [88]. Given the deleterious effects of 3S-HMGB1 following MI, our group engineered an HMGB1 construct comprising two Box B domains in tandem that retained the binding of both Boxes to CXCL12. We called this dBB12L (abbreviated to dBB).

I confirmed that unlike DS-HMGB1, dBB did not induce or promote inflammation as evidenced by TNF expression by primary human MI macrophages. I also showed that, like FR-HMGB1, it did not promote clotting of human blood through platelet activation.

5.3.2. Doxorubicin-Induced Cardiotoxicity

Chronic cardiotoxicity after doxorubicin exposure is characterised by cardiac dilatation, thinning of ventricular wall, progressive decline in left ventricular ejection fraction and eventually heart failure. Development of heart failure is dose-related. The dose-dependent cardiotoxicity of doxorubicin has been shown to be caused by the generation of ROS, which leads to increased oxidative stress due to the innate inefficiency of mitochondrial iron efflux, ultimately resulting in heart failure in a subset of patients [110, 217, 232]. Moreover, doxorubicin can also lead to mitochondrial dysfunction through excess ROS production by damage to mitochondrial DNA and decrease mitochondrial transmembrane potential [233]. Furthermore, doxorubicin can suppress the electron transport chain, leading to a reduction in ATP production. This is consistent with my finding that addition of doxorubicin to cardiomyocytes resulted in increased mitochondrial proton leak and reduced ATP production. The impairment of mitochondrial function resulted in cell stress and death as evidenced by elevated levels of cTnI in the culture medium.

Studies indicate that doxorubicin treatment significantly suppresses SIRT3 expression, a mitochondrial NAD^+-dependent protein deacetylase responsible for the deacetylation of histone and non-histone lysine residues, both *in vivo* (mouse hearts) and *in vitro* (primary cardiomyocytes) [234, 235]. SIRT3 plays a pivotal role in regulating mitochondrial bioenergetics by enhancing fatty acid oxidation and pyruvate utilisation, thus maintaining oxidative phosphorylation [236]. It also modulates ROS production within the electron transport chain by upregulating the expression and activity of antioxidant enzymes and supports mitochondrial dynamics by targeting OPA1 [237, 238]. The overexpression of SIRT3 has been shown to mitigate ROS levels and preserve mitochondrial function following doxorubicin treatment [234, 237]. Similarly, SIRT1, another member of the sirtuin family, serves as a multifunctional regulator of numerous biological processes and has been shown to protect the heart from myocardial ischaemia-reperfusion (I/R) injury [239]. It also counters doxorubicin-induced mitochondrial dysfunction and cell death [240, 241]. Both SIRT1 and SIRT3 are known to deacetylate PGC-1α, activating a suite of genes involved in mitochondrial biogenesis and function, such as nuclear respiratory factor-1 (Nrf1) [242-244]. These data align with my findings and may explain why the knockdown of PGC-1α diminished the effects of HMGB1 and dBB.

I found that HMGB1 protects cardiomyocytes if administered before treatment with doxorubicin and could act as a therapeutic if administered after doxorubicin exposure. It was also effective when administered after exposure to doxorubicin. In both cases, HMGB1 resulted in reduced cellular damage, restoration of ATP production and decreased mitochondrial proton leak. Interestingly, pre-treatment with HMGB1 before doxorubicin resulted in trend toward less mitochondrial damage and more ATP production compared to post-treatment, although these differences did not reach statistical significance. This was likely due to HMGB1 not being able to reverse all the effects of doxorubicin-induced cardiotoxicity after injury. Cancer cells have inherent resistance or are able to develop resistance to chemotherapy drugs. This has prompted the use of combination therapy for some cancers [6]. Increasing the dose of chemotherapy may also be used but is limited by off target toxic effects, such as the cumulative dose-dependent cardiotoxicity seen with doxorubicin [245, 246]. Therefore, it would be interesting to determine if HMGB1 could enable higher-dose doxorubicin treatments without the drug resistance often observed in other studies.

5.3.3. dBB in Hypoxia Induced Injury

Similar to the effects seen with HMGB1, dBB also enhanced mitochondrial function following hypoxia-normoxia, as evidenced by increased ATP level and reduced mitochondrial proton leak. These changes were accompanied by the upregulation of genes associated with mitochondrial function and biogenesis, similar to those observed with HMGB1 treatment, and a concomitant downregulation of genes related to cell stress, apoptosis, and loss of mitochondrial function. One of the genes most highly upregulated by dBB was *CALM1*, which is known for modulating the calcium signal transduction pathway by regulating the function of cardiac ion channels. Knockout of *Calm1* in mice has been linked to arrhythmogenesis [247]. Increased expression of PGC-1α, which leads to mitochondrial biogenesis, can improve the contractile function of cardiomyocytes by enhancing calcium handling (clearance) while maintaining calcium homeostasis in cardiomyocytes[190]. This is consistent with the observed upregulation of muscle contraction and mitochondrial biogenesis, and the activation of *PPARGC1A*, the gene that encodes PGC-1α, as seen in the Gene Set Enrichment Analysis.

Both dBB and HMGB1 activated the mTORC pathways leading to reduced mitochondrial and cardiomyocyte injury following four cycles of hypoxia-normoxia. There are multiple upstream regulators of mTORC1 [28]. Amongst the best characterised of these are Akt and AMPK. Akt acts by phosphorylating and inhibiting tuberous sclerosis protein 1/2 (TSC1/2) and the protein rich Akt substrate of 40 kDa (PRAS40), both of which inhibit mTORC1 [28]. Akt activation in turn is typically associated with nutrient-rich conditions [28]. ERK1/2 also inhibits TSC1/2, as do IKK and NF-kB [28]. MEK1 upregulates activation of ERK1/2 through phosphorylation to inhibit cardiomyocyte apoptosis in vitro [28] and cardiomyocyte specific upregulation of MEK1 resulted in physiological hypertrophy of cardiomyocytes via ERK1/2 signalling and the MEK1 transgenic mice were resistant to I/R-induced apoptosis [248]. PI3K upregulates the activity of mTORC2, which in turn promotes the activity of Akt [28]. mTORC1 triggers the activation of genes involved in fatty acids metabolism by upregulating sterol responsive element-binding protein 1/2 (SREBP 1/2). mTORC1 also upregulates expression of yin-yan 1 (YY1) and PGC-1a.

Taken together, these findings underscore the critical role of Akt and MEK1 and its downstream targets, ERK1/2, to enhance cardiomyocyte survival, and are consistent with my observations using HMGB1 constructs. Interestingly, treatment with dBB resulted in higher expression levels of key markers like Akt and MAP kinases ERK, compared to HMGB1, while there was no significant difference in the expression of MEK between the treatments. This variation could potentially be attributed to MEK being upstream of the other two kinases and the time at which I collected the cells may be important. This would need to be tested in future experiments.

The major effects of both HMGB1 and dBB were on mitochondrial function. Factors I identified as being significantly regulated included those directly upstream of mitochondrial function (HIF-1α, PGC-1α, and YAP) or located within the mitochondria (BNIP3 and ROS). YAP is known to regulate and interact with the Wnt signalling pathways and insulin-like growth factor [63, 249]. Several studies have demonstrated that deregulation of the Hippo pathway in the adult heart leads to cardiac failures and ischaemic cardiac diseases. YAP and Taz have been reported to be required for cardiac regeneration, the effects being closely related to their levels [250-252]. Additionally, cardiomyocyte-specific overexpression of YAP has been reported to promote cardiac regeneration after myocardial injury, in part by

stimulating IGF and Akt signalling [252]. Although cardiac regeneration has now been discounted due to the very low numbers of c-kit$^+$ stem cell presents in the adult heart, leveraging this pathway to reduce injury and promote recovery remains important [37, 100, 102]. Interestingly, YAP also plays a role in regulating gene expression and the enzymatic activity of the glycolytic pathway and gluconeogenesis [253]. In the heart, the glucose transporter and its transcription are enhanced through the cooperation of YAP, TGF-b activated kinase and HIF-1α, which regulate the progression of cardiomyocyte hypertrophy [254]. YAP has also been shown to suppress expression of gluconeogenic genes via PGC-1α [255].

Concomitantly, both HMGB1 and dBB downregulated pathways associated with cell stress and death, including JNK1/2, p38, HIF-1α and p53. Both p38 and JNK play significant roles in apoptosis. JNK-mediated apoptosis of cardiomyocyte involves the ubiquitination and degradation of p53, which is regulated by JNK-mediated phosphorylation [256, 257]. Whereas p38 can induce apoptosis through its effects on cyclin D1 expression during the cell cycle, co-expression of MKK3 along with p38 inhibited mitogen-induced cyclin D1 expression [258, 259]. Furthermore, in a model of I/R with administration of SB203580, a p38 inhibitor, over the 1 hour of reperfusion led to improved cardiac function, which directly correlated with the reduction of apoptosis [260].

Treatment with dBB also led to lower levels of HIF-1α and Bnip3 compared to HMGB1 following four cycles of hypoxia-normoxia. Bnip3, a proapoptotic Bcl2 family member that is transcriptionally upregulated by HIF-1α during ischaemia in the heart and other tissues [261, 262]. Bnip3 is localised to the outer membrane of mitochondria. Increased expression results in cell death by opening of the mitochondrial permeability transition pore [263, 264]. Bnip3 is also involved in apoptosis, Bnip3 inhibition or knockout diminishes hypoxic cardiomyocyte death in vitro and *in vivo*, whereas adenovirus-mediated delivery of BNIP3 to cardiomyocyte expression provokes apoptosis [262, 265, 266]. As described above, Bnip3 expression is critically regulated by hypoxia through the HIF-1α transcription factor pathway [262, 267]. In accordance with this, transgenic overexpression of Bnip3 in the healthy mouse did not lead to excess cardiomyocyte apoptosis[266].

While reperfusion following MI results in improved outcomes, including survival, it paradoxically also results in a second wave of oxidative damage, cell death and deleterious

immune response through the generation of mitochondrial ROS [268, 269]. Chouchani et al. [21] demonstrated that during reperfusion, accumulated succinate is rapidly re-oxidised by succinate dehydrogenase, leading to excessive ROS generation via reverse electron transport at mitochondrial complex I. The authors also showed that pharmacological inhibition of ischaemic succinate accumulation significantly reduced cardiac ischaemia-reperfusion injury in murine models. An additional source of ROS is the NADPH oxidases (NOX) family [270]. Mice deficient in NOX4 exhibited reduced ROS production and a marked attenuation of infarct size following I/R, suggesting that NOX4-mediated ROS specifically in cardiomyocytes plays a pivotal role in mediating I/R injury [271]. Whilst high levels of ROS are detrimental, at physiological levels in the nanomolar range, ROS are important mediators of signalling, modulating metabolism and adaptation of stress [272]. dBB and FR-HMGB1 restored ROS to near physiological levels following hypoxia-normoxia, leading to improved cardiomyocyte health as evidenced by reduced levels of cTnI in the culture medium.

Finally, PGC-1α plays a critical role in cardiac health. Both HMGB1 and dBB helped restore cardiomyocyte cellular homeostasis by upregulating PGC-1α. Conversely, the effects of HMGB1 and dBB were negated by siRNA-mediated knockdown of PGC-1α, underscoring its essential function in these protective responses (Fig. 15).

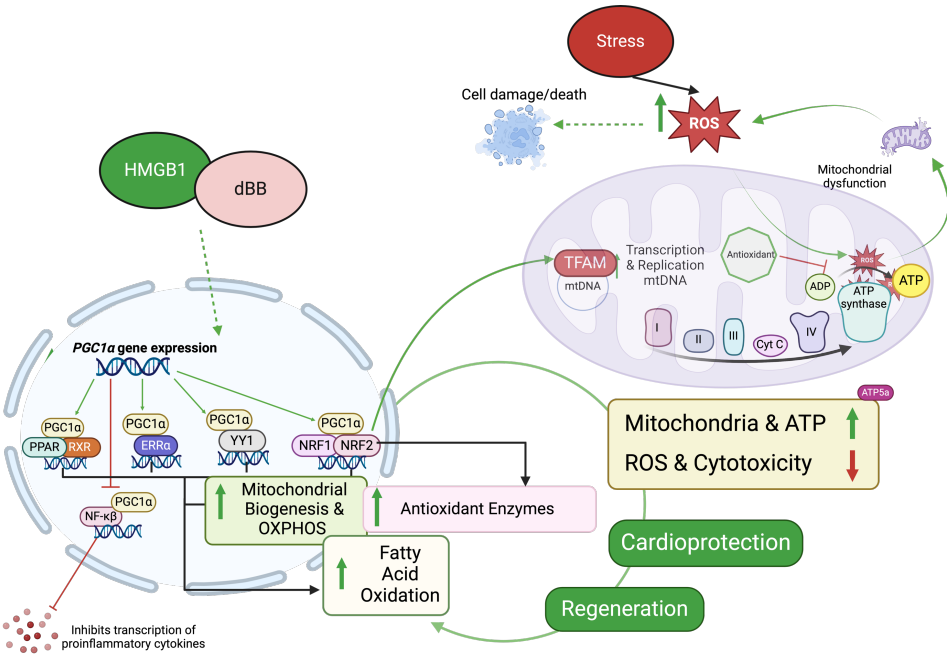

Fig. 15: Schematic representation of the proposed HMGB1 and dBB mediated signalling pathway via PGC-1α.

5.4. **Conclusion**

In summary, the data presented in this chapter show that both dBB and HMGB1 reduce doxorubicin-induced cardiotoxicity. Additionally, dBB exhibited comparable or superior efficacy in reducing hypoxia-induced injury compared to HMGB1. I also confirmed that these effects of dBB were mediated through the mTOR and PGC-1α pathway.

Chapter 6. Concluding Discussion

6.1. Discussion

6.1.1. Summary

Human embryonic stem cell-derived cardiomyocytes (hESC-CM) and human induced pluripotent stem cell-derived cardiomyocytes (hiPSC-CM) are used extensively for modelling drug-induced toxicity and mechanism validation. However, the relative immaturity of hESC-CM and hiPSC-CM poses significant challenges in emulating the complex functionalities of adult human cardiomyocytes. For instance, in contrast clinical data showing that dexrazoxane administration was associated with fewer serious adverse cardiovascular outcomes [273], Burridge et al. [110] observed that dexrazoxane did not confer cardioprotection in their hiPSC-CM model. They suggested that this discrepancy might be due to the lower mitochondrial density in their cells compared to adult human cardiomyocytes, emphasising the need for enhanced model fidelity.

In order to address this major challenge associated with the use of stem cell derived cardiomyocytes, I started my DPhil by investigating strategies to induce and accelerate the maturation of hESC-CM. My initial results showed that traditional culture methods predominantly yielded immature cardiomyocyte populations. These immature hESC-CM were relatively resistant to hypoxia-induced damage, in contrast to the responses of mature cardiomyocytes.

I investigated the effects of prolonged culture in fatty-acid-enriched media and electrical stimulation. These approaches proved effective, as evidenced by the enhanced expression of markers of mature cardiomyocyte and improved mitochondrial function. Combining both modalities significantly reduced the culture time required to achieve similar levels of maturation as observed with fatty-acid-enriched media alone. The resulting mature cells also demonstrated greater sensitivity to hypoxic conditions, better aligning with the expected response of adult human cardiomyocytes.

Next, I optimised the model of hypoxia followed by normoxia to emulate the *in vivo* effects of ischaemia reperfusion following myocardial infarction. Although short cycles are

associated with improved cell yields for downstream, assays the cardiomyocytes exhibit adaptive responses consistent with improved outcomes. Prolonging the duration of hypoxia and normoxia better emulates the effects seen *in vivo* but is associated with poor cell survival. Therefore, I explored the alternative approach of subjecting the mature cardiomyocytes to repeated cycles of hypoxia-normoxia. This also has the advantage of better emulating the fluctuating oxygen levels characteristic of non-ST-elevation myocardial infarction (NSTEMI), which now comprises around 70% of patients affected by myocardial infarction. I found that successive cycles progressively impaired cardiomyocyte viability and increased cellular stress, with four cycles proving to be optimal.

Having established a reproducible protocol that would optimally model the clinical scenario of ischaemia reperfusion, I was able to proceed to testing potential novel therapeutic modalities. Our group has previously shown that the alarmin HMGB1 can promote healing of multiple tissues by priming resident stem cells through upregulation of mitochondrial pathways as evidenced by increased mitochondrial DNA and ATP [78]. Given the reliance of normal cardiomyocytes on mitochondrial oxidative phosphorylation, we hypothesised that HMGB1 may be beneficial following myocardial infarction despite the absence of stem cells in the heart.

I found that administration of HMGB1 after four cycles of hypoxia-normoxia not only reduced cellular stress markers but also enhanced mitochondrial function. HMGB1 also upregulated expression of genes associated with fatty oxidation and downregulated those associated with glycolysis. I confirmed that HMGB1 facilitated a metabolic shift from glycolysis to fatty acid oxidation, crucial for energy production under stress. Consistent with the effects of HMGB1 on metabolism, I found that it upregulated pathways associated with the mammalian target of rapamycin complex (mTORC), including the upstream MAP kinases. Both rapamycin and siRNA inhibition of mTORC abolished the effects of HMGB1.

Having found that HMGB1 upregulated ATP levels, I investigated key pathways involved in mitochondrial function and biogenesis. I found that HMGB1 upregulated levels of PGC-1α, a key regulator of mitochondrial function and biogenesis. I confirmed the key role of PGC-1α through siRNA knockdown, which abolished the effects of HMGB1. In parallel, HMGB1 downregulated key mediators of injury, including ROS.

Next, I investigated the effects of HMGB1 on doxorubicin-induced cardiotoxicity. I found that HMGB1 improved doxorubicin-induced cardiotoxicity. Finally, I confirmed that the engineered variant of HMGB1 we called dBB does not lead to proinflammatory signalling or promote thrombosis. In the hypoxia-normoxia and doxorubicin models of cardiomyocyte injury, it resulted in improved outcomes, with several parameters being better than the native fully reduced HMGB1.

Overall, my research highlights the potential of using HMGB1 or dBB for the treatment of myocardial infarction and drug-related cardiotoxicity.

6.1.2. Limitation and Ethical Issue Relating to The Use of Human Embryonic Stem Cells

While the optimised protocols I developed represent an advance in generating mature hESC-CM suitable for testing the efficacy of potential therapeutic and their mechanism of action, there are significant limitations. Despite reducing the maturation time to 60 days, the scalability of these maturation protocols remains a significant challenge. Emerging technologies are beginning to address this limitation. The development of micro physiological systems, commonly referred to as “organs-on-a-chip”, represents a significant advance in this direction. These systems utilise hESC-derived cells to construct miniature models of human organs, which can mimic the complex interactions of human physiology at the microscale [274, 275]. Looking forward, the integration of hESC-CM into body-on-a-chip (BOC) systems presents a promising frontier. These systems aim to replicate human organ interactions within a single platform, offering a sophisticated tool for exploring the nuanced behaviours of mature cardiomyocytes in a controlled yet complex environment. Such advancements not only hold the potential to refine our understanding of cardiac physiology and pathology but also propel the development of personalized medicine approaches, reducing the reliance on traditional hESC models.

Pure cultures of CM facilitate the interrogation of pathways through a reductive approach. However, they suffer from the limitation of being a single cell type and *in vivo* outcomes following MI are determined by complex interrelated pathways involving multiple other cell types, including cardiac fibroblasts, vascular and immune cells. Additionally, inherent variability among different hESC lines and the complexity of induced pluripotent stem cells

(iPSCs) can complicate comparisons across studies, potentially skewing reproducibility and the ability to generalise the findings.

The use of hESC continues stimulate ethical debates, given their origin from human embryos. Consequently, the field is witnessing a gradual shift towards using iPSC which, despite their limitations such as variability and the risk of mutations, offer a more ethically acceptable and patient-specific model for cardiac research in some circles.

6.1.3. Future Work.

Impairment of mitochondrial function plays a key role in ischaemia-reperfusion injury. However, there are no approved therapeutics for targeting these pathways. PGC-1α plays a crucial role in upregulating mitochondrial function and exerts a myriad of downstream effects, including the regulation of bioenergetics, antioxidant response and mitochondrial biogenesis [188, 189]. However, targeting the PGC-1α pathway has proven challenging and successful translation to the clinic has proved elusive [33]. Whilst knockout of PGC-1α was detrimental in mouse models of heart failure [276], transgenic cardiomyocyte-specific upregulation of PGC-1α was also detrimental in a murine model of thoracic artery constriction model of heart failure [277], with even moderate upregulation resulting in reduced function [278]. This suggest that PGC-1α targeting should be optimised both in magnitude and temporally. Furthermore, clinical trials targeting individual components of the mitochondrial pathway have proven unsuccessful [23]. A meta-analysis of randomised controlled trials of drugs that at least in part function by targeting mitochondrial pathways, found that those with a broad spectrum of activity were more likely to be associated with reduction in adverse events [279]. Impairment of mitochondrial function plays a key role in ischaemia-reperfusion injury.

My data would suggest that treatment with HMGB1 or dBB triggers a physiologically optimised cascade to upregulate mitochondrial function and offers an alternative strategy to upregulating individual components such as PGC-1α. My data also suggest that dBB may be superior to native FR-HMGB1. However, the reasons for this remain unclear as the lack of proinflammatory signalling and promotion of thrombosis would not be relevant in my in vitro models. It is possible that dBB may lead to more rapid target engagement and hence more rapid restoration of ROS levels and fatty acid-derived ATP production. Excessively

high levels of ROS lead to mitochondrial dysfunction, resulting in damage to mitochondrial DNA, impairment of ATP production and cell death [191, 280]. If dBB can more efficiently restore mitochondrial function and enhance fatty acid metabolism, it would be able to salvage more critically injured cardiomyocytes. A widely adopted method for investigating the efficiency of this process is through fluorescence resonance energy transfer or bioluminescence resonance energy transfer [281]. These techniques allow for real-time interrogation of target engagement within intact cells and have been extensively used to monitor cGMP and cAMP signalling in cardiomyocytes [281-283].

My work has been limited to in vitro models. An important next step would be to test whether HMGB1 and dBB reduce I/R induced injury *in vivo*. This could be explored in mouse models as they would also permit elucidation of mechanism *in vivo* due to the wide availability of reagents and genetic models. Mice tend to be resistant to I/R- induced heart failure [121, 124] and whether the HMGB1 constructs prevent this could be explored over a prolonged period of time following permanent ligation.

The potential for the prophylactic use of HMGB1 or dBB to prevent the development of doxorubicin-induced cardiotoxicity should also be explored *in vivo*.

My data showing improvement following administration of HMGB1 or dBB after the cardiomyocytes had been damaged with doxorubicin raises the intriguing possibility that these constructs could potentially be used for established heart failure. Heart failure represents a huge unmet medical need, with 67 million people affected worldwide and annual costs in the USA totalling over $30 billion [1] [2-4]. Current treatments are restricted to reducing energy demand and blocking adverse compensatory pathways. A consensus opinion, including clinicians, academics, and industry, highlighted the importance of developing a new generation of therapeutic aimed at restoring mitochondrial function and improving mitochondrial biogenesis [284]. Samples from patients, including those with ischaemic and non-ischaemic heart failure, compared to normal controls showed that most downregulated genes in the heart failure patients were those associated with PGC-1α and ERRα signalling [284]. As described above, transgenic upregulation of PGC-1α paradoxically resulted in further impairment of function in a mouse model of thoracic artery constriction (TAC) [285]. A recent publication described the beneficial effects of pan ERR agonists both in *in vivo* (TAC) and in vitro through their effects on improving fatty acid

metabolism[286]. My data suggest that the HMGB1 constructs result in a physiologically optimised cascade that upregulate both PGC-1α-mediated pathways as well as restoring the metabolic activity of cardiomyocytes back to fatty acid metabolism.

My work exploring the mechanism of action of HMGB1 and dBB was based on my bulk RNA sequencing data supplemented by a hypothesis driven approach to examine the effects on pathways known to be involved in cardiomyocyte metabolism and mitochondrial function. Gene expression does not necessarily correlate with protein levels. Therefore, an important next step would be to explore the proteome of hESC-CM exposed to cycles of hypoxia-normoxia, with and without HMGB1 treatment. The findings could then be validated *in vivo* using multiplexed mass spectrometry-based imaging.

A combination of *in vivo* experiments with in vitro approaches using human cardiomyocytes would provide the ideal platform for advancing our understanding of ischaemia reperfusion and heart failure, as well as investigating novel therapeutics based that trigger upregulation of mitochondrial pathways to promote cell survival and function.

Chapter 7. Reference

1. Reed GW, Rossi JE, Cannon CP: **Acute myocardial infarction**. *Lancet* 2017, **389**(10065):197-210.
2. Prevention CfDCa: **CDC Wide-ranging ONline Data for Epidemiologic Research (WONDER) online database**. In.; 2021.
3. Foundation BH: **Heart & Circulatory Disease Statistics**. In., 2023 Compendium edn; 2023.
4. Tsao CW, Aday AW, Almarzooq ZI, Anderson CAM, Arora P, Avery CL, Baker-Smith CM, Beaton AZ, Boehme AK, Buxton AE *et al*: **Heart Disease and Stroke Statistics-2023 Update: A Report From the American Heart Association**. *Circulation* 2023, **147**(8):e93-e621.
5. Luengo-Fernandez R, Walli-Attaei M, Gray A, Torbica A, Maggioni AP, Huculeci R, Bairami F, Aboyans V, Timmis AD, Vardas P *et al*: **Economic burden of cardiovascular diseases in the European Union: a population-based cost study**. *Eur Heart J* 2023, **44**(45):4752-4767.
6. Bayat Mokhtari R, Homayouni TS, Baluch N, Morgatskaya E, Kumar S, Das B, Yeger H: **Combination therapy in combating cancer**. *Oncotarget* 2017, **8**(23):38022-38043.
7. Camacho X, Nedkoff L, Wright FL, Nghiem N, Buajitti E, Goldacre R, Rosella LC, Seminog O, Tan EJ, Hayes A *et al*: **Relative contribution of trends in myocardial infarction event rates and case fatality to declines in mortality: an international comparative study of 1·95 million events in 80·4 million people in four countries**. *Lancet Public Health* 2022, **7**(3):e229-e239.
8. Szummer K, Jernberg T, Wallentin L: **From Early Pharmacology to Recent Pharmacology Interventions in Acute Coronary Syndromes: JACC State-of-the-Art Review**. *J Am Coll Cardiol* 2019, **74**(12):1618-1636.
9. Gheorghe A, Griffiths U, Murphy A, Legido-Quigley H, Lamptey P, Perel P: **The economic burden of cardiovascular disease and hypertension in low- and middle-income countries: a systematic review**. *BMC Public Health* 2018, **18**(1):975.

10. Shahim B, Kapelios CJ, Savarese G, Lund LH: **Global Public Health Burden of Heart Failure: An Updated Review**. *Card Fail Rev* 2023, **9**:e11.
11. Jasinska-Piadlo A, Campbell P: **Management of patients with heart failure and preserved ejection fraction**. *Heart* 2023, **109**(11):874-883.
12. Askoxylakis V, Thieke C, Pleger ST, Most P, Tanner J, Lindel K, Katus HA, Debus J, Bischof M: **Long-term survival of cancer patients compared to heart failure and stroke: a systematic review**. *BMC Cancer* 2010, **10**:105.
13. Heusch G: **Myocardial ischemia/reperfusion: Translational pathophysiology of ischemic heart disease**. *Med* 2024, **5**(1):10-31.
14. French BA, Kramer CM: **Mechanisms of Post-Infarct Left Ventricular Remodeling**. *Drug Discov Today Dis Mech* 2007, **4**(3):185-196.
15. Hall C, Gehmlich K, Denning C, Pavlovic D: **Complex Relationship Between Cardiac Fibroblasts and Cardiomyocytes in Health and Disease**. *J Am Heart Assoc* 2021, **10**(5):e019338.
16. Eijgenraam TR, Silljé HHW, de Boer RA: **Current understanding of fibrosis in genetic cardiomyopathies**. *Trends Cardiovasc Med* 2020, **30**(6):353-361.
17. Neubauer S: **The failing heart--an engine out of fuel**. *N Engl J Med* 2007, **356**(11):1140-1151.
18. Lyra-Leite DM, Petersen AP, Ariyasinghe NR, Cho N, McCain ML: **Mitochondrial architecture in cardiac myocytes depends on cell shape and matrix rigidity**. *J Mol Cell Cardiol* 2021, **150**:32-43.
19. Hernandez-Resendiz S, Prunier F, Girao H, Dorn G, Hausenloy DJ, (CA16225) E-CCA: **Targeting mitochondrial fusion and fission proteins for cardioprotection**. *J Cell Mol Med* 2020, **24**(12):6571-6585.
20. Ibanez B, James S, Agewall S, Antunes MJ, Bucciarelli-Ducci C, Bueno H, Caforio ALP, Crea F, Goudevenos JA, Halvorsen S *et al*: **2017 ESC Guidelines for the management of acute myocardial infarction in patients presenting with ST-segment elevation: The Task Force for the management of acute myocardial infarction in patients presenting with ST-segment elevation of the European Society of Cardiology (ESC)**. *Eur Heart J* 2018, **39**(2):119-177.
21. Chouchani ET, Pell VR, Gaude E, Aksentijević D, Sundier SY, Robb EL, Logan A, Nadtochiy SM, Ord ENJ, Smith AC *et al*: **Ischaemic accumulation of succinate**

controls reperfusion injury through mitochondrial ROS. *Nature* 2014, **515**(7527):431-435.

22. Del Re DP, Amgalan D, Linkermann A, Liu Q, Kitsis RN: **Fundamental Mechanisms of Regulated Cell Death and Implications for Heart Disease**. *Physiol Rev* 2019, **99**(4):1765-1817.
23. Murphy MP, Hartley RC: **Mitochondria as a therapeutic target for common pathologies**. *Nat Rev Drug Discov* 2018, **17**(12):865-886.
24. Cung TT, Morel O, Cayla G, Rioufol G, Garcia-Dorado D, Angoulvant D, Bonnefoy-Cudraz E, Guérin P, Elbaz M, Delarche N *et al*: **Cyclosporine before PCI in Patients with Acute Myocardial Infarction**. *N Engl J Med* 2015, **373**(11):1021-1031.
25. Kelly DP, Scarpulla RC: **Transcriptional regulatory circuits controlling mitochondrial biogenesis and function**. *Genes Dev* 2004, **18**(4):357-368.
26. Ventura-Clapier R, Garnier A, Veksler V: **Transcriptional control of mitochondrial biogenesis: the central role of PGC-1alpha**. *Cardiovasc Res* 2008, **79**(2):208-217.
27. Riehle C, Abel ED: **PGC-1 proteins and heart failure**. *Trends Cardiovasc Med* 2012, **22**(4):98-105.
28. Sciarretta S, Forte M, Frati G, Sadoshima J: **New Insights Into the Role of mTOR Signaling in the Cardiovascular System**. *Circ Res* 2018, **122**(3):489-505.
29. Cunningham JT, Rodgers JT, Arlow DH, Vazquez F, Mootha VK, Puigserver P: **mTOR controls mitochondrial oxidative function through a YY1-PGC-1alpha transcriptional complex**. *Nature* 2007, **450**(7170):736-740.
30. Laplante M, Sabatini DM: **mTOR signaling in growth control and disease**. *Cell* 2012, **149**(2):274-293.
31. Lehman JJ, Barger PM, Kovacs A, Saffitz JE, Medeiros DM, Kelly DP: **Peroxisome proliferator-activated receptor gamma coactivator-1 promotes cardiac mitochondrial biogenesis**. *J Clin Invest* 2000, **106**(7):847-856.
32. Dorn GW, Vega RB, Kelly DP: **Mitochondrial biogenesis and dynamics in the developing and diseased heart**. *Genes Dev* 2015, **29**(19):1981-1991.
33. Chen L, Qin Y, Liu B, Gao M, Li A, Li X, Gong G: **PGC-1**. *Front Cell Dev Biol* 2022, **10**:871357.
34. Handschin C: **The biology of PGC-1α and its therapeutic potential**. *Trends Pharmacol Sci* 2009, **30**(6):322-329.

35. Wilmot KA, O'Flaherty M, Capewell S, Ford ES, Vaccarino V: **Coronary Heart Disease Mortality Declines in the United States From 1979 Through 2011**. *Circulation* 2015, **132**(11):997-1002.
36. Weissman IL: **Stem cells: units of development, units of regeneration, and units in evolution**. *Cell* 2000, **100**(1):157-168.
37. Chien KR, Frisén J, Fritsche-Danielson R, Melton DA, Murry CE, Weissman IL: **Regenerating the field of cardiovascular cell therapy**. *Nat Biotechnol* 2019, **37**(3):232-237.
38. Cahill TJ, Choudhury RP, Riley PR: **Heart regeneration and repair after myocardial infarction: translational opportunities for novel therapeutics**. *Nat Rev Drug Discov* 2017, **16**(10):699-717.
39. Rosen MR, Myerburg RJ, Francis DP, Cole GD, Marbán E: **Translating stem cell research to cardiac disease therapies: pitfalls and prospects for improvement**. *J Am Coll Cardiol* 2014, **64**(9):922-937.
40. Brooks A, Futrega K, Liang X, Hu X, Liu X, Crawford DHG, Doran MR, Roberts MS, Wang H: **Concise Review: Quantitative Detection and Modeling the In Vivo Kinetics of Therapeutic Mesenchymal Stem/Stromal Cells**. *Stem Cells Transl Med* 2018, **7**(1):78-86.
41. Forbes SJ, Rosenthal N: **Preparing the ground for tissue regeneration: from mechanism to therapy**. *Nat Med* 2014, **20**(8):857-869.
42. MacArthur JW, Purcell BP, Shudo Y, Cohen JE, Fairman A, Trubelja A, Patel J, Hsiao P, Yang E, Lloyd K *et al*: **Sustained release of engineered stromal cell-derived factor 1-α from injectable hydrogels effectively recruits endothelial progenitor cells and preserves ventricular function after myocardial infarction**. *Circulation* 2013, **128**(11 Suppl 1):S79-86.
43. Bollini S, Smart N, Riley PR: **Resident cardiac progenitor cells: at the heart of regeneration**. *J Mol Cell Cardiol* 2011, **50**(2):296-303.
44. Nguyen PK, Neofytou E, Rhee JW, Wu JC: **Potential Strategies to Address the Major Clinical Barriers Facing Stem Cell Regenerative Therapy for Cardiovascular Disease: A Review**. *JAMA Cardiol* 2016, **1**(8):953-962.
45. Vagnozzi RJ, Maillet M, Sargent MA, Khalil H, Johansen AKZ, Schwanekamp JA, York AJ, Huang V, Nahrendorf M, Sadayappan S *et al*: **An acute immune response**

underlies the benefit of cardiac stem cell therapy. *Nature* 2020, **577**(7790):405-409.

46. Chong JJ, Yang X, Don CW, Minami E, Liu YW, Weyers JJ, Mahoney WM, Van Biber B, Cook SM, Palpant NJ *et al*: **Human embryonic-stem-cell-derived cardiomyocytes regenerate non-human primate hearts**. *Nature* 2014, **510**(7504):273-277.
47. Menasché P, Alfieri O, Janssens S, McKenna W, Reichenspurner H, Trinquart L, Vilquin JT, Marolleau JP, Seymour B, Larghero J *et al*: **The Myoblast Autologous Grafting in Ischemic Cardiomyopathy (MAGIC) trial: first randomized placebo-controlled study of myoblast transplantation**. *Circulation* 2008, **117**(9):1189-1200.
48. Trainor N, Pietak A, Smith T: **Rethinking clinical delivery of adult stem cell therapies**. *Nat Biotechnol* 2014, **32**(8):729-735.
49. Dimmeler S, Ding S, Rando TA, Trounson A: **Translational strategies and challenges in regenerative medicine**. *Nat Med* 2014, **20**(8):814-821.
50. Lane SW, Williams DA, Watt FM: **Modulating the stem cell niche for tissue regeneration**. *Nat Biotechnol* 2014, **32**(8):795-803.
51. Eschenhagen T, Bolli R, Braun T, Field LJ, Fleischmann BK, Frisén J, Giacca M, Hare JM, Houser S, Lee RT *et al*: **Cardiomyocyte Regeneration: A Consensus Statement**. *Circulation* 2017, **136**(7):680-686.
52. Bergmann O, Bhardwaj RD, Bernard S, Zdunek S, Barnabé-Heider F, Walsh S, Zupicich J, Alkass K, Buchholz BA, Druid H *et al*: **Evidence for cardiomyocyte renewal in humans**. *Science* 2009, **324**(5923):98-102.
53. Soonpaa MH, Field LJ: **Survey of studies examining mammalian cardiomyocyte DNA synthesis**. *Circ Res* 1998, **83**(1):15-26.
54. Zhang Y, Gago-Lopez N, Li N, Zhang Z, Alver N, Liu Y, Martinson AM, Mehri A, MacLellan WR: **Single-cell imaging and transcriptomic analyses of endogenous cardiomyocyte dedifferentiation and cycling**. *Cell Discov* 2019, **5**:30.
55. Zhang Y, Li TS, Lee ST, Wawrowsky KA, Cheng K, Galang G, Malliaras K, Abraham MR, Wang C, Marbán E: **Dedifferentiation and proliferation of mammalian cardiomyocytes**. *PLoS One* 2010, **5**(9):e12559.

56. Wang WE, Li L, Xia X, Fu W, Liao Q, Lan C, Yang D, Chen H, Yue R, Zeng C *et al*: **Dedifferentiation, Proliferation, and Redifferentiation of Adult Mammalian Cardiomyocytes After Ischemic Injury**. *Circulation* 2017, **136**(9):834-848.

57. Hein S, Arnon E, Kostin S, Schönburg M, Elsässer A, Polyakova V, Bauer EP, Klövekorn WP, Schaper J: **Progression from compensated hypertrophy to failure in the pressure-overloaded human heart: structural deterioration and compensatory mechanisms**. *Circulation* 2003, **107**(7):984-991.

58. Beohar N, Rapp J, Pandya S, Losordo DW: **Rebuilding the damaged heart: the potential of cytokines and growth factors in the treatment of ischemic heart disease**. *J Am Coll Cardiol* 2010, **56**(16):1287-1297.

59. Giacca M, Zacchigna S: **Harnessing the microRNA pathway for cardiac regeneration**. *J Mol Cell Cardiol* 2015, **89**(Pt A):68-74.

60. Diez-Cuñado M, Wei K, Bushway PJ, Maurya MR, Perera R, Subramaniam S, Ruiz-Lozano P, Mercola M: **miRNAs that Induce Human Cardiomyocyte Proliferation Converge on the Hippo Pathway**. *Cell Rep* 2018, **23**(7):2168-2174.

61. Eulalio A, Mano M, Dal Ferro M, Zentilin L, Sinagra G, Zacchigna S, Giacca M: **Functional screening identifies miRNAs inducing cardiac regeneration**. *Nature* 2012, **492**(7429):376-381.

62. Aguirre A, Montserrat N, Zacchigna S, Nivet E, Hishida T, Krause MN, Kurian L, Ocampo A, Vazquez-Ferrer E, Rodriguez-Esteban C *et al*: **In vivo activation of a conserved microRNA program induces mammalian heart regeneration**. *Cell Stem Cell* 2014, **15**(5):589-604.

63. Heallen T, Zhang M, Wang J, Bonilla-Claudio M, Klysik E, Johnson RL, Martin JF: **Hippo pathway inhibits Wnt signaling to restrain cardiomyocyte proliferation and heart size**. *Science* 2011, **332**(6028):458-461.

64. Gabisonia K, Prosdocimo G, Aquaro GD, Carlucci L, Zentilin L, Secco I, Ali H, Braga L, Gorgodze N, Bernini F *et al*: **MicroRNA therapy stimulates uncontrolled cardiac repair after myocardial infarction in pigs**. *Nature* 2019, **569**(7756):418-422.

65. Atluri P, Woo YJ: **Pro-angiogenic cytokines as cardiovascular therapeutics: assessing the potential**. *BioDrugs* 2008, **22**(4):209-222.

66. Henry TD, Annex BH, McKendall GR, Azrin MA, Lopez JJ, Giordano FJ, Shah PK, Willerson JT, Benza RL, Berman DS *et al*: **The VIVA trial: Vascular endothelial**

growth factor in Ischemia for Vascular Angiogenesis. *Circulation* 2003, **107**(10):1359-1365.

67. Yang ZJ, Xu SL, Chen B, Zhang SL, Zhang YL, Wei W, Ma DC, Wang LS, Zhu TB, Li CJ *et al*: **Hepatocyte growth factor plays a critical role in the regulation of cytokine production and induction of endothelial progenitor cell mobilization: a pilot gene therapy study in patients with coronary heart disease**. *Clin Exp Pharmacol Physiol* 2009, **36**(8):790-796.
68. Chung ES, Miller L, Patel AN, Anderson RD, Mendelsohn FO, Traverse J, Silver KH, Shin J, Ewald G, Farr MJ *et al*: **Changes in ventricular remodelling and clinical status during the year following a single administration of stromal cell-derived factor-1 non-viral gene therapy in chronic ischaemic heart failure patients: the STOP-HF randomized Phase II trial**. *Eur Heart J* 2015, **36**(33):2228-2238.
69. Panahi M, Papanikolaou A, Torabi A, Zhang JG, Khan H, Vazir A, Hasham MG, Cleland JGF, Rosenthal NA, Harding SE *et al*: **Immunomodulatory interventions in myocardial infarction and heart failure: a systematic review of clinical trials and meta-analysis of IL-1 inhibition**. *Cardiovasc Res* 2018, **114**(11):1445-1461.
70. Kang R, Chen R, Zhang Q, Hou W, Wu S, Cao L, Huang J, Yu Y, Fan XG, Yan Z *et al*: **HMGB1 in health and disease**. *Mol Aspects Med* 2014, **40**:1-116.
71. Son M, Porat A, He M, Suurmond J, Santiago-Schwarz F, Andersson U, Coleman TR, Volpe BT, Tracey KJ, Al-Abed Y *et al*: **C1q and HMGB1 reciprocally regulate human macrophage polarization**. *Blood* 2016, **128**(18):2218-2228.
72. Andersson U, Wang H, Palmblad K, Aveberger AC, Bloom O, Erlandsson-Harris H, Janson A, Kokkola R, Zhang M, Yang H *et al*: **High mobility group 1 protein (HMG-1) stimulates proinflammatory cytokine synthesis in human monocytes**. *J Exp Med* 2000, **192**(4):565-570.
73. Andrassy M, Volz HC, Igwe JC, Funke B, Eichberger SN, Kaya Z, Buss S, Autschbach F, Pleger ST, Lukic IK *et al*: **High-mobility group box-1 in ischemia-reperfusion injury of the heart**. *Circulation* 2008, **117**(25):3216-3226.
74. Huang H, Nace GW, McDonald KA, Tai S, Klune JR, Rosborough BR, Ding Q, Loughran P, Zhu X, Beer-Stolz D *et al*: **Hepatocyte-specific high-mobility group box 1 deletion worsens the injury in liver ischemia/reperfusion: a role for intracellular high-mobility group box 1 in cellular protection**. *Hepatology* 2014, **59**(5):1984-1997.

75. Izuishi K, Tsung A, Jeyabalan G, Critchlow ND, Li J, Tracey KJ, Demarco RA, Lotze MT, Fink MP, Geller DA *et al*: **Cutting edge: high-mobility group box 1 preconditioning protects against liver ischemia-reperfusion injury**. *J Immunol* 2006, **176**(12):7154-7158.

76. Venereau E, Casalgrandi M, Schiraldi M, Antoine DJ, Cattaneo A, De Marchis F, Liu J, Antonelli A, Preti A, Raeli L *et al*: **Mutually exclusive redox forms of HMGB1 promote cell recruitment or proinflammatory cytokine release**. *J Exp Med* 2012, **209**(9):1519-1528.

77. Kitahara T, Takeishi Y, Harada M, Niizeki T, Suzuki S, Sasaki T, Ishino M, Bilim O, Nakajima O, Kubota I: **High-mobility group box 1 restores cardiac function after myocardial infarction in transgenic mice**. *Cardiovasc Res* 2008, **80**(1):40-46.

78. Lee G, Espirito Santo AI, Zwingenberger S, Cai L, Vogl T, Feldmann M, Horwood NJ, Chan JK, Nanchahal J: **Fully reduced HMGB1 accelerates the regeneration of multiple tissues by transitioning stem cells to G**. *Proc Natl Acad Sci U S A* 2018, **115**(19):E4463-E4472.

79. Askari AT, Unzek S, Popovic ZB, Goldman CK, Forudi F, Kiedrowski M, Rovner A, Ellis SG, Thomas JD, DiCorleto PE *et al*: **Effect of stromal-cell-derived factor 1 on stem-cell homing and tissue regeneration in ischaemic cardiomyopathy**. *Lancet* 2003, **362**(9385):697-703.

80. Deglurkar I, Mal N, Mills WR, Popovic ZB, McCarthy P, Blackstone EH, Laurita KR, Penn MS: **Mechanical and electrical effects of cell-based gene therapy for ischemic cardiomyopathy are independent**. *Hum Gene Ther* 2006, **17**(11):1144-1151.

81. Unzek S, Zhang M, Mal N, Mills WR, Laurita KR, Penn MS: **SDF-1 recruits cardiac stem cell-like cells that depolarize in vivo**. *Cell Transplant* 2007, **16**(9):879-886.

82. Dong F, Caplan AI: **Cell transplantation as an initiator of endogenous stem cell-based tissue repair**. *Curr Opin Organ Transplant* 2012, **17**(6):670-674.

83. Schiraldi M, Raucci A, Muñoz LM, Livoti E, Celona B, Venereau E, Apuzzo T, De Marchis F, Pedotti M, Bachi A *et al*: **HMGB1 promotes recruitment of inflammatory cells to damaged tissues by forming a complex with CXCL12 and signaling via CXCR4**. *J Exp Med* 2012, **209**(3):551-563.

84. Yang H, Hreggvidsdottir HS, Palmblad K, Wang H, Ochani M, Li J, Lu B, Chavan S, Rosas-Ballina M, Al-Abed Y *et al*: **A critical cysteine is required for HMGB1**

binding to Toll-like receptor 4 and activation of macrophage cytokine release. *Proc Natl Acad Sci U S A* 2010, **107**(26):11942-11947.

85. Limana F, Esposito G, D'Arcangelo D, Di Carlo A, Romani S, Melillo G, Mangoni A, Bertolami C, Pompilio G, Germani A *et al*: **HMGB1 attenuates cardiac remodelling in the failing heart via enhanced cardiac regeneration and miR-206-mediated inhibition of TIMP-3**. *PLoS One* 2011, **6**(6):e19845.
86. van Berlo JH, Maillet M, Molkentin JD: **Signaling effectors underlying pathologic growth and remodeling of the heart**. *J Clin Invest* 2013, **123**(1):37-45.
87. Tirone M, Tran NL, Ceriotti C, Gorzanelli A, Canepari M, Bottinelli R, Raucci A, Di Maggio S, Santiago C, Mellado M *et al*: **High mobility group box 1 orchestrates tissue regeneration via CXCR4**. *J Exp Med* 2018, **215**(1):303-318.
88. Di Maggio S, Milano G, De Marchis F, D'Ambrosio A, Bertolotti M, Palacios BS, Badi I, Sommariva E, Pompilio G, Capogrossi MC *et al*: **Non-oxidizable HMGB1 induces cardiac fibroblasts migration via CXCR4 in a CXCL12-independent manner and worsens tissue remodeling after myocardial infarction**. *Biochim Biophys Acta Mol Basis Dis* 2017, **1863**(11):2693-2704.
89. Stark K, Philippi V, Stockhausen S, Busse J, Antonelli A, Miller M, Schubert I, Hoseinpour P, Chandraratne S, von Brühl ML *et al*: **Disulfide HMGB1 derived from platelets coordinates venous thrombosis in mice**. *Blood* 2016, **128**(20):2435-2449.
90. Zhu X, Shen W, Yao K, Wang H, Liu B, Li T, Song L, Diao D, Mao G, Huang P *et al*: **Fine-Tuning of PGC1α Expression Regulates Cardiac Function and Longevity**. *Circ Res* 2019, **125**(7):707-719.
91. Takahashi K, Fukushima S, Yamahara K, Yashiro K, Shintani Y, Coppen SR, Salem HK, Brouilette SW, Yacoub MH, Suzuki K: **Modulated inflammation by injection of high-mobility group box 1 recovers post-infarction chronically failing heart**. *Circulation* 2008, **118**(14 Suppl):S106-114.
92. He YY, Wen Y, Zheng XX, Jiang XJ: **Intramyocardial delivery of HMGB1 by a novel thermosensitive hydrogel attenuates cardiac remodeling and improves cardiac function after myocardial infarction**. *J Cardiovasc Pharmacol* 2013, **61**(4):283-290.
93. Bauzá MDR, Giménez CS, Locatelli P, De Lorenzi A, Hnatiuk A, Capogrossi MC, Crottogini A, Cuniberti L, Olea FD: **High-dose intramyocardial HMGB1 induces**

long-term cardioprotection in sheep with myocardial infarction. *Drug Deliv Transl Res* 2019, **9**(5):935-944.

94. Zhou YH, Han QF, Gao L, Sun Y, Tang ZW, Wang M, Wang W, Yao HC: **HMGB1 Protects the Heart Against Ischemia-Reperfusion Injury via PI3K/AkT Pathway-Mediated Upregulation of VEGF Expression**. *Front Physiol* 2019, **10**:1595.

95. Limana F, Germani A, Zacheo A, Kajstura J, Di Carlo A, Borsellino G, Leoni O, Palumbo R, Battistini L, Rastaldo R *et al*: **Exogenous high-mobility group box 1 protein induces myocardial regeneration after infarction via enhanced cardiac C-kit+ cell proliferation and differentiation**. *Circ Res* 2005, **97**(8):e73-83.

96. Limana F, Esposito G, Fasanaro P, Foglio E, Arcelli D, Voellenkle C, Di Carlo A, Avitabile D, Martelli F, Russo MA *et al*: **Transcriptional profiling of HMGB1-induced myocardial repair identifies a key role for Notch signaling**. *Mol Ther* 2013, **21**(10):1841-1851.

97. Liu FY, Fan D, Yang Z, Tang N, Guo Z, Ma SQ, Ma ZG, Wu HM, Deng W, Tang QZ: **TLR9 is essential for HMGB1-mediated post-myocardial infarction tissue repair through affecting apoptosis, cardiac healing, and angiogenesis**. *Cell Death Dis* 2019, **10**(7):480.

98. Beltrami AP, Barlucchi L, Torella D, Baker M, Limana F, Chimenti S, Kasahara H, Rota M, Musso E, Urbanek K *et al*: **Adult cardiac stem cells are multipotent and support myocardial regeneration**. *Cell* 2003, **114**(6):763-776.

99. van Berlo JH, Kanisicak O, Maillet M, Vagnozzi RJ, Karch J, Lin SC, Middleton RC, Marbán E, Molkentin JD: **c-kit+ cells minimally contribute cardiomyocytes to the heart**. *Nature* 2014, **509**(7500):337-341.

100. Sultana N, Zhang L, Yan J, Chen J, Cai W, Razzaque S, Jeong D, Sheng W, Bu L, Xu M *et al*: **Resident c-kit(+) cells in the heart are not cardiac stem cells**. *Nat Commun* 2015, **6**:8701.

101. Liu Q, Yang R, Huang X, Zhang H, He L, Zhang L, Tian X, Nie Y, Hu S, Yan Y *et al*: **Genetic lineage tracing identifies in situ Kit-expressing cardiomyocytes**. *Cell Res* 2016, **26**(1):119-130.

102. He L, Nguyen NB, Ardehali R, Zhou B: **Heart Regeneration by Endogenous Stem Cells and Cardiomyocyte Proliferation: Controversy, Fallacy, and Progress**. *Circulation* 2020, **142**(3):275-291.

103. Goto T, Miyagawa S, Tamai K, Matsuura R, Kido T, Kuratani T, Shimamura K, Sakaniwa R, Harada A, Sawa Y: **High-mobility group box 1 fragment suppresses adverse post-infarction remodeling by recruiting PDGFRα-positive bone marrow cells**. *PLoS One* 2020, **15**(4):e0230392.

104. Wu X, Reboll MR, Korf-Klingebiel M, Wollert KC: **Angiogenesis after acute myocardial infarction**. *Cardiovasc Res* 2021, **117**(5):1257-1273.

105. Nakada Y, Canseco DC, Thet S, Abdisalaam S, Asaithamby A, Santos CX, Shah AM, Zhang H, Faber JE, Kinter MT *et al*: **Hypoxia induces heart regeneration in adult mice**. *Nature* 2017, **541**(7636):222-227.

106. Zhang Q, Wang L, Wang S, Cheng H, Xu L, Pei G, Wang Y, Fu C, Jiang Y, He C *et al*: **Signaling pathways and targeted therapy for myocardial infarction**. *Signal Transduct Target Ther* 2022, **7**(1):78.

107. Zhao SQ, Xue ZZ, Wang LZ: **HMGB1, TGF-β and NF-κB are associated with chronic allograft nephropathy**. *Exp Ther Med* 2017, **14**(6):6138-6146.

108. Fassi EMA, Sgrignani J, D'Agostino G, Cecchinato V, Garofalo M, Grazioso G, Uguccioni M, Cavalli A: **Oxidation State Dependent Conformational Changes of HMGB1 Regulate the Formation of the CXCL12/HMGB1 Heterocomplex**. *Comput Struct Biotechnol J* 2019, **17**:886-894.

109. Hoes MF, Bomer N, van der Meer P: **Concise Review: The Current State of Human In Vitro Cardiac Disease Modeling: A Focus on Gene Editing and Tissue Engineering**. *Stem Cells Transl Med* 2019, **8**(1):66-74.

110. Burridge PW, Li YF, Matsa E, Wu H, Ong SG, Sharma A, Holmström A, Chang AC, Coronado MJ, Ebert AD *et al*: **Human induced pluripotent stem cell-derived cardiomyocytes recapitulate the predilection of breast cancer patients to doxorubicin-induced cardiotoxicity**. *Nat Med* 2016, **22**(5):547-556.

111. Guo XM, Zhao YS, Chang HX, Wang CY, E LL, Zhang XA, Duan CM, Dong LZ, Jiang H, Li J *et al*: **Creation of engineered cardiac tissue in vitro from mouse embryonic stem cells**. *Circulation* 2006, **113**(18):2229-2237.

112. Martin TP, MacDonald EA, Elbassioni AAM, O'Toole D, Zaeri AAI, Nicklin SA, Gray GA, Loughrey CM: **Preclinical models of myocardial infarction: from mechanism to translation**. *Br J Pharmacol* 2022, **179**(5):770-791.

113. Gao E, Lei YH, Shang X, Huang ZM, Zuo L, Boucher M, Fan Q, Chuprun JK, Ma XL, Koch WJ: **A novel and efficient model of coronary artery ligation and myocardial infarction in the mouse**. *Circ Res* 2010, **107**(12):1445-1453.

114. Gharacholou SM, Lopes RD, Washam JB, Newby LK, James SK, Alexander JH: **Antithrombotic therapy in acute coronary syndromes: guidelines translated for the clinician**. *J Thromb Thrombolysis* 2010, **29**(4):516-528.

115. Sicklinger F, Zhang Y, Lavine KJ, Simon N, Bucher V, Jugold M, Lehmann L, Konstandin MH, Katus HA, Leuschner F: **A Minimal-Invasive Approach for Standardized Induction of Myocardial Infarction in Mice**. *Circ Res* 2020, **127**(9):1214-1216.

116. Sun Q, Wang KK, Pan M, Zhou JP, Qiu XT, Wang ZY, Yang Z, Chen Y, Shen H, Gu QL *et al*: **A minimally invasive approach to induce myocardial infarction in mice without thoracotomy**. *J Cell Mol Med* 2018, **22**(11):5208-5219.

117. Heusch G, Gersh BJ: **The pathophysiology of acute myocardial infarction and strategies of protection beyond reperfusion: a continual challenge**. *Eur Heart J* 2017, **38**(11):774-784.

118. Burke AP, Virmani R: **Pathophysiology of acute myocardial infarction**. *Med Clin North Am* 2007, **91**(4):553-572; ix.

119. Heusch G, Rassaf T: **Time to Give Up on Cardioprotection? A Critical Appraisal of Clinical Studies on Ischemic Pre-, Post-, and Remote Conditioning**. *Circ Res* 2016, **119**(5):676-695.

120. Reimer KA, Lowe JE, Rasmussen MM, Jennings RB: **The wavefront phenomenon of ischemic cell death. 1. Myocardial infarct size vs duration of coronary occlusion in dogs**. *Circulation* 1977, **56**(5):786-794.

121. De Villiers C, Riley PR: **Mouse models of myocardial infarction: comparing permanent ligation and ischaemia-reperfusion**. *Dis Model Mech* 2020, **13**(11).

122. Frantz S, Bauersachs J, Ertl G: **Post-infarct remodelling: contribution of wound healing and inflammation**. *Cardiovasc Res* 2009, **81**(3):474-481.

123. Dewald O, Frangogiannis NG, Zoerlein MP, Duerr GD, Taffet G, Michael LH, Welz A, Entman ML: **A murine model of ischemic cardiomyopathy induced by repetitive ischemia and reperfusion**. *Thorac Cardiovasc Surg* 2004, **52**(5):305-311.

124. van den Borne SW, van de Schans VA, Strzelecka AE, Vervoort-Peters HT, Lijnen PM, Cleutjens JP, Smits JF, Daemen MJ, Janssen BJ, Blankesteijn WM: **Mouse strain determines the outcome of wound healing after myocardial infarction**. *Cardiovasc Res* 2009, **84**(2):273-282.

125. Lindsey ML, Bolli R, Canty JM, Du XJ, Frangogiannis NG, Frantz S, Gourdie RG, Holmes JW, Jones SP, Kloner RA *et al*: **Guidelines for experimental models of myocardial ischemia and infarction**. *Am J Physiol Heart Circ Physiol* 2018, **314**(4):H812-H838.

126. Hanf A, Oelze M, Manea A, Li H, Münzel T, Daiber A: **The anti-cancer drug doxorubicin induces substantial epigenetic changes in cultured cardiomyocytes**. *Chem Biol Interact* 2019, **313**:108834.

127. Steinhelper ME, Field LJ: **Cardiac tumors and dysrhythmias in transgenic mice**. *Toxicol Pathol* 1990, **18**(4 Pt 1):464-469.

128. Li M, Hu J, Heermeier K, Hennighausen L, Furth PA: **Expression of a viral oncoprotein during mammary gland development alters cell fate and function: induction of p53-independent apoptosis is followed by impaired milk protein production in surviving cells**. *Cell Growth Differ* 1996, **7**(1):3-11.

129. Claycomb WC, Lanson NA, Stallworth BS, Egeland DB, Delcarpio JB, Bahinski A, Izzo NJ: **HL-1 cells: a cardiac muscle cell line that contracts and retains phenotypic characteristics of the adult cardiomyocyte**. *Proc Natl Acad Sci U S A* 1998, **95**(6):2979-2984.

130. Wilson KD, Hu S, Venkatasubrahmanyam S, Fu JD, Sun N, Abilez OJ, Baugh JJ, Jia F, Ghosh Z, Li RA *et al*: **Dynamic microRNA expression programs during cardiac differentiation of human embryonic stem cells: role for miR-499**. *Circ Cardiovasc Genet* 2010, **3**(5):426-435.

131. Hoekstra M, Mummery CL, Wilde AA, Bezzina CR, Verkerk AO: **Induced pluripotent stem cell derived cardiomyocytes as models for cardiac arrhythmias**. *Front Physiol* 2012, **3**:346.

132. Stack JP, Moslehi J, Sayed N, Wu JC: **Cancer therapy-induced cardiomyopathy: can human induced pluripotent stem cell modelling help prevent it?** *Eur Heart J* 2019, **40**(22):1764-1770.

133. Yu J, Vodyanik MA, Smuga-Otto K, Antosiewicz-Bourget J, Frane JL, Tian S, Nie J, Jonsdottir GA, Ruotti V, Stewart R *et al*: **Induced pluripotent stem cell lines derived from human somatic cells**. *Science* 2007, **318**(5858):1917-1920.

134. Narsinh KH, Plews J, Wu JC: **Comparison of human induced pluripotent and embryonic stem cells: fraternal or identical twins?** *Mol Ther* 2011, **19**(4):635-638.

135. Williams TL, Colzani MT, Macrae RGC, Robinson EL, Bloor S, Greenwood EJD, Zhan JR, Strachan G, Kuc RE, Nyimanu D *et al*: **Human embryonic stem cell-derived cardiomyocyte platform screens inhibitors of SARS-CoV-2 infection**. *Commun Biol* 2021, **4**(1):926.

136. Navarrete EG, Liang P, Lan F, Sanchez-Freire V, Simmons C, Gong T, Sharma A, Burridge PW, Patlolla B, Lee AS *et al*: **Screening drug-induced arrhythmia [corrected] using human induced pluripotent stem cell-derived cardiomyocytes and low-impedance microelectrode arrays**. *Circulation* 2013, **128**(11 Suppl 1):S3-13.

137. Gherghiceanu M, Barad L, Novak A, Reiter I, Itskovitz-Eldor J, Binah O, Popescu LM: **Cardiomyocytes derived from human embryonic and induced pluripotent stem cells: comparative ultrastructure**. *J Cell Mol Med* 2011, **15**(11):2539-2551.

138. Lundy SD, Zhu WZ, Regnier M, Laflamme MA: **Structural and functional maturation of cardiomyocytes derived from human pluripotent stem cells**. *Stem Cells Dev* 2013, **22**(14):1991-2002.

139. Cao F, Wagner RA, Wilson KD, Xie X, Fu JD, Drukker M, Lee A, Li RA, Gambhir SS, Weissman IL *et al*: **Transcriptional and functional profiling of human embryonic stem cell-derived cardiomyocytes**. *PLoS One* 2008, **3**(10):e3474.

140. Correia C, Koshkin A, Duarte P, Hu D, Carido M, Sebastião MJ, Gomes-Alves P, Elliott DA, Domian IJ, Teixeira AP *et al*: **3D aggregate culture improves metabolic maturation of human pluripotent stem cell derived cardiomyocytes**. *Biotechnol Bioeng* 2018, **115**(3):630-644.

141. Eder A, Vollert I, Hansen A, Eschenhagen T: **Human engineered heart tissue as a model system for drug testing**. *Adv Drug Deliv Rev* 2016, **96**:214-224.

142. Drawnel FM, Boccardo S, Prummer M, Delobel F, Graff A, Weber M, Gérard R, Badi L, Kam-Thong T, Bu L *et al*: **Disease modeling and phenotypic drug screening**

for diabetic cardiomyopathy using human induced pluripotent stem cells. *Cell Rep* 2014, **9**(3):810-821.

143. Yang X, Rodriguez ML, Leonard A, Sun L, Fischer KA, Wang Y, Ritterhoff J, Zhao L, Kolwicz SC, Pabon L *et al*: **Fatty Acids Enhance the Maturation of Cardiomyocytes Derived from Human Pluripotent Stem Cells**. *Stem Cell Reports* 2019, **13**(4):657-668.
144. Machiraju P, Greenway SC: **Current methods for the maturation of induced pluripotent stem cell-derived cardiomyocytes**. *World J Stem Cells* 2019, **11**(1):33-43.
145. Piccini I, Rao J, Seebohm G, Greber B: **Human pluripotent stem cell-derived cardiomyocytes: Genome-wide expression profiling of long-term in vitro maturation in comparison to human heart tissue**. *Genom Data* 2015, **4**:69-72.
146. Simon MC, Keith B: **The role of oxygen availability in embryonic development and stem cell function**. *Nat Rev Mol Cell Biol* 2008, **9**(4):285-296.
147. Kamakura T, Makiyama T, Sasaki K, Yoshida Y, Wuriyanghai Y, Chen J, Hattori T, Ohno S, Kita T, Horie M *et al*: **Ultrastructural maturation of human-induced pluripotent stem cell-derived cardiomyocytes in a long-term culture**. *Circ J* 2013, **77**(5):1307-1314.
148. Braam SR: **Culture medium composition for maturating cardiomyocytes derived from pluripotent mammalian stem cells**. In. Edited by Office USPaT: PLURIOMICS B.V; 2014.
149. Chung S, Dzeja PP, Faustino RS, Perez-Terzic C, Behfar A, Terzic A: **Mitochondrial oxidative metabolism is required for the cardiac differentiation of stem cells**. *Nat Clin Pract Cardiovasc Med* 2007, **4 Suppl 1**(Suppl 1):S60-67.
150. Rana P, Anson B, Engle S, Will Y: **Characterization of human-induced pluripotent stem cell-derived cardiomyocytes: bioenergetics and utilization in safety screening**. *Toxicol Sci* 2012, **130**(1):117-131.
151. Miki K, Deguchi K, Nakanishi-Koakutsu M, Lucena-Cacace A, Kondo S, Fujiwara Y, Hatani T, Sasaki M, Naka Y, Okubo C *et al*: **ERRγ enhances cardiac maturation with T-tubule formation in human iPSC-derived cardiomyocytes**. *Nat Commun* 2021, **12**(1):3596.
152. Wei W, Liu Y, Zhang Q, Wang Y, Zhang X, Zhang H: **Danshen-Enhanced Cardioprotective Effect of Cardioplegia on Ischemia Reperfusion Injury in a**

Human-Induced Pluripotent Stem Cell-Derived Cardiomyocytes Model. *Artif Organs* 2017, **41**(5):452-460.

153. Nunes SS, Miklas JW, Liu J, Aschar-Sobbi R, Xiao Y, Zhang B, Jiang J, Massé S, Gagliardi M, Hsieh A *et al*: **Biowire: a platform for maturation of human pluripotent stem cell-derived cardiomyocytes**. *Nat Methods* 2013, **10**(8):781-787.
154. Ronaldson-Bouchard K, Ma SP, Yeager K, Chen T, Song L, Sirabella D, Morikawa K, Teles D, Yazawa M, Vunjak-Novakovic G: **Advanced maturation of human cardiac tissue grown from pluripotent stem cells**. *Nature* 2018, **556**(7700):239-243.
155. Wallace KB, Sardão VA, Oliveira PJ: **Mitochondrial Determinants of Doxorubicin-Induced Cardiomyopathy**. *Circ Res* 2020, **126**(7):926-941.
156. Saleh M, Ambrose JA: **Understanding myocardial infarction**. *F1000Res* 2018, **7**.
157. Wu D, Yotnda P: **Induction and testing of hypoxia in cell culture**. *J Vis Exp* 2011(54).
158. Keeley TP, Mann GE: **Defining Physiological Normoxia for Improved Translation of Cell Physiology to Animal Models and Humans**. *Physiol Rev* 2019, **99**(1):161-234.
159. Rinderknecht H, Ehnert S, Braun B, Histing T, Nussler AK, Linnemann C: **The Art of Inducing Hypoxia**. *Oxygen* 2021, **1**(1):46-61.
160. Newby D, Marks L, Lyall F: **Dissolved oxygen concentration in culture medium: assumptions and pitfalls**. *Placenta* 2005, **26**(4):353-357.
161. Zhang H, Yang Q, Lian X, Jiang P, Cui J: **Hypoxia-Inducible Factor-1α (HIF-1α) Promotes Hypoxia-Induced Invasion and Metastasis in Ovarian Cancer by Targeting Matrix Metallopeptidase 13 (MMP13)**. *Med Sci Monit* 2019, **25**:7202-7208.
162. Li Y, Zhao L, Li XF: **Hypoxia and the Tumor Microenvironment**. *Technol Cancer Res Treat* 2021, **20**:15330338211036304.
163. Hidalgo A, Glass N, Ovchinnikov D, Yang SK, Zhang X, Mazzone S, Chen C, Wolvetang E, Cooper-White J: **Modelling ischemia-reperfusion injury (IRI)**. *APL Bioeng* 2018, **2**(2):026102.
164. Peters MC, Maas RGC, van Adrichem I, Doevendans PAM, Mercola M, Šarić T, Buikema JW, van Mil A, Chamuleau SAJ, Sluijter JPG *et al*: **Metabolic Maturation**

Increases Susceptibility to Hypoxia-induced Damage in Human iPSC-derived Cardiomyocytes. *Stem Cells Transl Med* 2022, **11**(10):1040-1051.

165. Häkli M, Kreutzer J, Mäki AJ, Välimäki H, Lappi H, Huhtala H, Kallio P, Aalto-Setälä K, Pekkanen-Mattila M: **Human induced pluripotent stem cell-based platform for modeling cardiac ischemia**. *Sci Rep* 2021, **11**(1):4153.
166. Acosta D, Puckett M: **Ischemic myocardial injury in cultured heart cells: preliminary observations on morphology and beating activity**. *In Vitro* 1977, **13**(12):818-823.
167. Portal L, Martin V, Assaly R, d'Anglemont de Tassigny A, Michineau S, Berdeaux A, Ghaleb B, Pons S: **A model of hypoxia-reoxygenation on isolated adult mouse cardiomyocytes: characterization, comparison with ischemia-reperfusion, and application to the cardioprotective effect of regular treadmill exercise**. *J Cardiovasc Pharmacol Ther* 2013, **18**(4):367-375.
168. Ward MC, Gilad Y: **A generally conserved response to hypoxia in iPSC-derived cardiomyocytes from humans and chimpanzees**. *Elife* 2019, **8**.
169. Richards DJ, Li Y, Kerr CM, Yao J, Beeson GC, Coyle RC, Chen X, Jia J, Damon B, Wilson R *et al*: **Human cardiac organoids for the modelling of myocardial infarction and drug cardiotoxicity**. *Nat Biomed Eng* 2020, **4**(4):446-462.
170. Bader SB, Dewhirst MW, Hammond EM: **Cyclic Hypoxia: An Update on Its Characteristics, Methods to Measure It and Biological Implications in Cancer**. *Cancers (Basel)* 2020, **13**(1).
171. Hou J, Wang L, Long H, Wu H, Wu Q, Zhong T, Chen X, Zhou C, Guo T, Wang T: **Hypoxia preconditioning promotes cardiac stem cell survival and cardiogenic differentiation in vitro involving activation of the HIF-1α/apelin/APJ axis**. *Stem Cell Res Ther* 2017, **8**(1):215.
172. Bourdier G, Détrait M, Bouyon S, Lemarié E, Brasseur S, Doutreleau S, Pépin JL, Godin-Ribuot D, Belaidi E, Arnaud C: **Intermittent Hypoxia Triggers Early Cardiac Remodeling and Contractile Dysfunction in the Time-Course of Ischemic Cardiomyopathy in Rats**. *J Am Heart Assoc* 2020, **9**(16):e016369.
173. Davis CK, Jain SA, Bae ON, Majid A, Rajanikant GK: **Hypoxia Mimetic Agents for Ischemic Stroke**. *Front Cell Dev Biol* 2018, **6**:175.
174. Isaja L, Mucci S, Vera J, Rodríguez-Varela MS, Marazita M, Morris-Hanon O, Videla-Richardson GA, Sevlever GE, Scassa ME, Romorini L: **Chemical hypoxia induces**

apoptosis of human pluripotent stem cells by a NOXA-mediated HIF-1α and HIF-2α independent mechanism. *Sci Rep* 2020, **10**(1):20653.

175. Muñoz-Sánchez J, Chánez-Cárdenas ME: **The use of cobalt chloride as a chemical hypoxia model**. *J Appl Toxicol* 2019, **39**(4):556-570.
176. Wang P, Guan D, Zhang XP, Liu F, Wang W: **Modeling the regulation of p53 activation by HIF-1 upon hypoxia**. *FEBS Lett* 2019, **593**(18):2596-2611.
177. Saxton RA, Sabatini DM: **mTOR Signaling in Growth, Metabolism, and Disease**. *Cell* 2017, **168**(6):960-976.
178. Nair R, Johnson M, Kravitz K, Huded C, Rajeswaran J, Anabila M, Blackstone E, Menon V, Lincoff AM, Kapadia S *et al*: **Characteristics and Outcomes of Early Recurrent Myocardial Infarction After Acute Myocardial Infarction**. *J Am Heart Assoc* 2021, **10**(16):e019270.
179. Eckle T, Köhler D, Lehmann R, El Kasmi K, Eltzschig HK: **Hypoxia-inducible factor-1 is central to cardioprotection: a new paradigm for ischemic preconditioning**. *Circulation* 2008, **118**(2):166-175.
180. Cai Z, Zhong H, Bosch-Marce M, Fox-Talbot K, Wang L, Wei C, Trush MA, Semenza GL: **Complete loss of ischaemic preconditioning-induced cardioprotection in mice with partial deficiency of HIF-1 alpha**. *Cardiovasc Res* 2008, **77**(3):463-470.
181. Hölscher M, Schäfer K, Krull S, Farhat K, Hesse A, Silter M, Lin Y, Pichler BJ, Thistlethwaite P, El-Armouche A *et al*: **Unfavourable consequences of chronic cardiac HIF-1α stabilization**. *Cardiovasc Res* 2012, **94**(1):77-86.
182. Nguyen BY, Ruiz-Velasco A, Bui T, Collins L, Wang X, Liu W: **Mitochondrial function in the heart: the insight into mechanisms and therapeutic potentials**. *Br J Pharmacol* 2019, **176**(22):4302-4318.
183. Chaanine AH, Joyce LD, Stulak JM, Maltais S, Joyce DL, Dearani JA, Klaus K, Nair KS, Hajjar RJ, Redfield MM: **Mitochondrial Morphology, Dynamics, and Function in Human Pressure Overload or Ischemic Heart Disease With Preserved or Reduced Ejection Fraction**. *Circ Heart Fail* 2019, **12**(2):e005131.
184. Lai P, Hille SS, Subramanian H, Wiegmann R, Roser P, Müller OJ, Nikolaev VO, De Jong KA: **Remodelling of cAMP dynamics within the SERCA2a microdomain in heart failure with preserved ejection fraction caused by obesity and type 2 diabetes**. *Cardiovasc Res* 2024, **120**(3):273-285.

185. Ver Heyen M, Heymans S, Antoons G, Reed T, Periasamy M, Awede B, Lebacq J, Vangheluwe P, Dewerchin M, Collen D *et al*: **Replacement of the muscle-specific sarcoplasmic reticulum Ca(2+)-ATPase isoform SERCA2a by the nonmuscle SERCA2b homologue causes mild concentric hypertrophy and impairs contraction-relaxation of the heart**. *Circ Res* 2001, **89**(9):838-846.
186. Slavin MB, Kumari R, Hood DA: **ATF5 is a regulator of exercise-induced mitochondrial quality control in skeletal muscle**. *Mol Metab* 2022, **66**:101623.
187. Rowe GC, Jiang A, Arany Z: **PGC-1 coactivators in cardiac development and disease**. *Circ Res* 2010, **107**(7):825-838.
188. Houten SM, Auwerx J: **PGC-1alpha: turbocharging mitochondria**. *Cell* 2004, **119**(1):5-7.
189. Jannig PR, Dumesic PA, Spiegelman BM, Ruas JL: **SnapShot: Regulation and biology of PGC-1α**. *Cell* 2022, **185**(8):1444-1444.e1441.
190. Chen M, Wang Y, Qu A: **PGC-1 alpha accelerates cytosolic Ca2+ clearance without disturbing Ca2+ homeostasis in cardiac myocytes**. *Biochem Biophys Res Commun* 2010, **396**(4):894-900.
191. Lopaschuk GD, Karwi QG, Tian R, Wende AR, Abel ED: **Cardiac Energy Metabolism in Heart Failure**. *Circ Res* 2021, **128**(10):1487-1513.
192. Lopaschuk GD, Ussher JR, Folmes CD, Jaswal JS, Stanley WC: **Myocardial fatty acid metabolism in health and disease**. *Physiol Rev* 2010, **90**(1):207-258.
193. Neglia D, De Caterina A, Marraccini P, Natali A, Ciardetti M, Vecoli C, Gastaldelli A, Ciociaro D, Pellegrini P, Testa R *et al*: **Impaired myocardial metabolic reserve and substrate selection flexibility during stress in patients with idiopathic dilated cardiomyopathy**. *Am J Physiol Heart Circ Physiol* 2007, **293**(6):H3270-3278.
194. Zhang D, Contu R, Latronico MV, Zhang J, Rizzi R, Catalucci D, Miyamoto S, Huang K, Ceci M, Gu Y *et al*: **MTORC1 regulates cardiac function and myocyte survival through 4E-BP1 inhibition in mice**. *J Clin Invest* 2010, **120**(8):2805-2816.
195. Aoyama T, Matsui T, Novikov M, Park J, Hemmings B, Rosenzweig A: **Serum and glucocorticoid-responsive kinase-1 regulates cardiomyocyte survival and hypertrophic response**. *Circulation* 2005, **111**(13):1652-1659.

196. Völkers M, Konstandin MH, Doroudgar S, Toko H, Quijada P, Din S, Joyo A, Ornelas L, Samse K, Thuerauf DJ *et al*: **Mechanistic target of rapamycin complex 2 protects the heart from ischemic damage**. *Circulation* 2013, **128**(19):2132-2144.

197. Hasumi Y, Baba M, Hasumi H, Huang Y, Lang M, Reindorf R, Oh HB, Sciarretta S, Nagashima K, Haines DC *et al*: **Folliculin (Flcn) inactivation leads to murine cardiac hypertrophy through mTORC1 deregulation**. *Hum Mol Genet* 2014, **23**(21):5706-5719.

198. Stähli BE, Klingenberg R, Heg D, Branca M, Manka R, Kapos I, Müggler O, Denegri A, Kesterke R, Berger F *et al*: **Mammalian Target of Rapamycin Inhibition in Patients With ST-Segment Elevation Myocardial Infarction**. *J Am Coll Cardiol* 2022, **80**(19):1802-1814.

199. Berra E, Pagès G, Pouysségur J: **MAP Kinases and Hypoxia in the Control of VEGF Expression**. *Cancer and Metastasis Reviews* 2000, **19**(1):139-145.

200. Kulisz A, Chen N, Chandel NS, Shao Z, Schumacker PT: **Mitochondrial ROS initiate phosphorylation of p38 MAP kinase during hypoxia in cardiomyocytes**. *American Journal of Physiology-Lung Cellular and Molecular Physiology* 2002, **282**(6):L1324-L1329.

201. Wilson KS, Suveizdyt K, Liles JT, Budas GR, Peacock AJ, Welsh DJ: **Hypoxia-induced pulmonary artery fibroblast proliferation and migration is prevented by ASK1 inhibition in anin vitrocellular model of pulmonary hypertension**. *European Respiratory Journal* 2015, **46**.

202. Qin S-Z: **Protective Effect of Paeoniflorin on Hypoxia Reoxygenation Cardiomyocytes and its Mechanism Based on MAPK Signal Pathway**. *Pakistan Journal of Zoology* 2023.

203. Krylatov A, Maslov L, Tsibulnikov SY, Voronkov N, Boshchenko A, Downey J, Mentzer R: **The Role of Reactive Oxygen Species, Kinases, Hydrogen Sulfide, and Nitric Oxide in the Regulation of Autophagy and Their Impact on Ischemia and Reperfusion Injury in the Heart**. *Curr Cardiol Rev* 2021, **17**(4):e230421186874.

204. Yu C-j, Xia F, Ruan L, Hu S-p, Zhu W-j, Yang K: **Circ_0004771 Promotes Hypoxia/Reoxygenation Induced Cardiomyocyte Injury via Activation of Mitogen-Activated Protein Kinase Signaling Pathway**. *International Heart Journal* 2023, **64**(6):1125-1132.

205. Dhingra R, Gang H, Wang Y, Biala AK, Aviv Y, Margulets V, Tee A, Kirshenbaum LA: **Bidirectional regulation of nuclear factor-κB and mammalian target of rapamycin signaling functionally links Bnip3 gene repression and cell survival of ventricular myocytes**. *Circ Heart Fail* 2013, **6**(2):335-343.
206. Li YQ, Jiao Y, Liu YN, Fu JY, Sun LK, Su J: **PGC-1α protects from myocardial ischaemia-reperfusion injury by regulating mitonuclear communication**. *J Cell Mol Med* 2022, **26**(3):593-600.
207. Wang C, Li Z, Zhao B, Wu Y, Fu Y, Kang K, Li Y, Dong L, Li X, Zhang B *et al*: **PGC-1**. *Oxid Med Cell Longev* 2021, **2021**:6677955.
208. Sulo G, Igland J, Vollset SE, Nygård O, Ebbing M, Sulo E, Egeland GM, Tell GS: **Heart Failure Complicating Acute Myocardial Infarction; Burden and Timing of Occurrence: A Nation-wide Analysis Including 86 771 Patients From the Cardiovascular Disease in Norway (CVDNOR) Project**. *J Am Heart Assoc* 2016, **5**(1).
209. Tsao CW, Aday AW, Almarzooq ZI, Anderson CAM, Arora P, Avery CL, Baker-Smith CM, Beaton AZ, Boehme AK, Buxton AE *et al*: **Heart Disease and Stroke Statistics-2023 Update: A Report From the American Heart Association**. *Circulation* 2023, **147**(8):e93-e621.
210. Heidenreich PA, Albert NM, Allen LA, Bluemke DA, Butler J, Fonarow GC, Ikonomidis JS, Khavjou O, Konstam MA, Maddox TM *et al*: **Forecasting the impact of heart failure in the United States: a policy statement from the American Heart Association**. *Circ Heart Fail* 2013, **6**(3):606-619.
211. Savarese G, Stolfo D, Sinagra G, Lund LH: **Heart failure with mid-range or mildly reduced ejection fraction**. *Nat Rev Cardiol* 2022, **19**(2):100-116.
212. Page RL, O'Bryant CL, Cheng D, Dow TJ, Ky B, Stein CM, Spencer AP, Trupp RJ, Lindenfeld J, Cardiology AHACPaHFaTCotCoC *et al*: **Drugs That May Cause or Exacerbate Heart Failure: A Scientific Statement From the American Heart Association**. *Circulation* 2016, **134**(6):e32-69.
213. Wu L, Wang L, Du Y, Zhang Y, Ren J: **Mitochondrial quality control mechanisms as therapeutic targets in doxorubicin-induced cardiotoxicity**. *Trends Pharmacol Sci* 2023, **44**(1):34-49.
214. bc.overview@ctsu.ox.ac.uk EBCTCGEEa, (EBCTCG) EBCTCG: **Anthracycline-containing and taxane-containing chemotherapy for early-stage operable**

breast cancer: a patient-level meta-analysis of 100 000 women from 86 randomised trials. *Lancet* 2023, **401**(10384):1277-1292.

215. Giordano SH, Temin S, Kirshner JJ, Chandarlapaty S, Crews JR, Davidson NE, Esteva FJ, Gonzalez-Angulo AM, Krop I, Levinson J *et al*: **Systemic therapy for patients with advanced human epidermal growth factor receptor 2-positive breast cancer: American Society of Clinical Oncology clinical practice guideline**. *J Clin Oncol* 2014, **32**(19):2078-2099.
216. Granger CB: **Prediction and prevention of chemotherapy-induced cardiomyopathy: can it be done?** *Circulation* 2006, **114**(23):2432-2433.
217. Ling G, Wang X, Tan N, Cao J, Li W, Zhang Y, Jiang J, Sun Q, Jiang Y, Wang W *et al*: **Mechanisms and Drug Intervention for Doxorubicin-Induced Cardiotoxicity Based on Mitochondrial Bioenergetics**. *Oxid Med Cell Longev* 2022, **2022**:7176282.
218. Deavall DG, Martin EA, Horner JM, Roberts R: **Drug-induced oxidative stress and toxicity**. *J Toxicol* 2012, **2012**:645460.
219. Zhang S, Liu X, Bawa-Khalfe T, Lu LS, Lyu YL, Liu LF, Yeh ET: **Identification of the molecular basis of doxorubicin-induced cardiotoxicity**. *Nat Med* 2012, **18**(11):1639-1642.
220. Khiati S, Dalla Rosa I, Sourbier C, Ma X, Rao VA, Neckers LM, Zhang H, Pommier Y: **Mitochondrial topoisomerase I (top1mt) is a novel limiting factor of doxorubicin cardiotoxicity**. *Clin Cancer Res* 2014, **20**(18):4873-4881.
221. Hanna AD, Lam A, Tham S, Dulhunty AF, Beard NA: **Adverse effects of doxorubicin and its metabolic product on cardiac RyR2 and SERCA2A**. *Mol Pharmacol* 2014, **86**(4):438-449.
222. Shakir DK, Rasul KI: **Chemotherapy induced cardiomyopathy: pathogenesis, monitoring and management**. *J Clin Med Res* 2009, **1**(1):8-12.
223. Goormaghtigh E, Huart P, Praet M, Brasseur R, Ruysschaert JM: **Structure of the adriamycin-cardiolipin complex. Role in mitochondrial toxicity**. *Biophys Chem* 1990, **35**(2-3):247-257.
224. Ichikawa Y, Ghanefar M, Bayeva M, Wu R, Khechaduri A, Naga Prasad SV, Mutharasan RK, Naik TJ, Ardehali H: **Cardiotoxicity of doxorubicin is mediated through mitochondrial iron accumulation**. *J Clin Invest* 2014, **124**(2):617-630.

225. Holmberg SR, Williams AJ: **Patterns of interaction between anthraquinone drugs and the calcium-release channel from cardiac sarcoplasmic reticulum**. *Circ Res* 1990, **67**(2):272-283.

226. Chen R, Kang R, Tang D: **The mechanism of HMGB1 secretion and release**. *Exp Mol Med* 2022, **54**(2):91-102.

227. Nanchahal J, Vinals Guitart A, Yue W, Burgess-Brown N, Lee T, Espirito Santo A: **Polypeptides related to hmgb1 useful for promoting tissue regeneration, compositions comprising same, and uses thereof**. In. Edited by Bureau I; 2021.

228. Zhao N, Li Q, Sui H, Zhang H: **Role of Oxidation-Dependent CaMKII Activation in the Genesis of Abnormal Action Potentials in Atrial Cardiomyocytes: A Simulation Study**. *Biomed Res Int* 2020, **2020**:1597012.

229. Karuppagounder V, Giridharan VV, Arumugam S, Sreedhar R, Palaniyandi SS, Krishnamurthy P, Quevedo J, Watanabe K, Konishi T, Thandavarayan RA: **Modulation of Macrophage Polarization and HMGB1-TLR2/TLR4 Cascade Plays a Crucial Role for Cardiac Remodeling in Senescence-Accelerated Prone Mice**. *PLoS One* 2016, **11**(4):e0152922.

230. Wan Z, Zhang X, Peng A, He M, Lei Z, Wang Y: **TLR4-HMGB1 signaling pathway affects the inflammatory reaction of autoimmune myositis by regulating MHC-I**. *Int Immunopharmacol* 2016, **41**:74-81.

231. Chen X, Li L, Khan MN, Shi L, Wang Z, Zheng F, Gong F, Fang M: **HMGB1 exacerbates experimental mouse colitis by enhancing innate lymphoid cells 3 inflammatory responses via promoted IL-23 production**. *Innate Immun* 2016, **22**(8):696-705.

232. Swain SM, Whaley FS, Ewer MS: **Congestive heart failure in patients treated with doxorubicin: a retrospective analysis of three trials**. *Cancer* 2003, **97**(11):2869-2879.

233. Marechal X, Montaigne D, Marciniak C, Marchetti P, Hassoun SM, Beauvillain JC, Lancel S, Neviere R: **Doxorubicin-induced cardiac dysfunction is attenuated by ciclosporin treatment in mice through improvements in mitochondrial bioenergetics**. *Clin Sci (Lond)* 2011, **121**(9):405-413.

234. Pillai VB, Bindu S, Sharp W, Fang YH, Kim G, Gupta M, Samant S, Gupta MP: **Sirt3 protects mitochondrial DNA damage and blocks the development of**

doxorubicin-induced cardiomyopathy in mice. *Am J Physiol Heart Circ Physiol* 2016, **310**(8):H962-972.

235. Zhang J, Xiang H, Liu J, Chen Y, He RR, Liu B: **Mitochondrial Sirtuin 3: New emerging biological function and therapeutic target**. *Theranostics* 2020, **10**(18):8315-8342.

236. He L, Liu F, Li J: **Mitochondrial Sirtuins and Doxorubicin-induced Cardiotoxicity**. *Cardiovasc Toxicol* 2021, **21**(3):179-191.

237. Cheung KG, Cole LK, Xiang B, Chen K, Ma X, Myal Y, Hatch GM, Tong Q, Dolinsky VW: **Sirtuin-3 (SIRT3) Protein Attenuates Doxorubicin-induced Oxidative Stress and Improves Mitochondrial Respiration in H9c2 Cardiomyocytes**. *J Biol Chem* 2015, **290**(17):10981-10993.

238. Samant SA, Zhang HJ, Hong Z, Pillai VB, Sundaresan NR, Wolfgeher D, Archer SL, Chan DC, Gupta MP: **SIRT3 deacetylates and activates OPA1 to regulate mitochondrial dynamics during stress**. *Mol Cell Biol* 2014, **34**(5):807-819.

239. Hsu CP, Zhai P, Yamamoto T, Maejima Y, Matsushima S, Hariharan N, Shao D, Takagi H, Oka S, Sadoshima J: **Silent information regulator 1 protects the heart from ischemia/reperfusion**. *Circulation* 2010, **122**(21):2170-2182.

240. Danz ED, Skramsted J, Henry N, Bennett JA, Keller RS: **Resveratrol prevents doxorubicin cardiotoxicity through mitochondrial stabilization and the Sirt1 pathway**. *Free Radic Biol Med* 2009, **46**(12):1589-1597.

241. Ruan Y, Dong C, Patel J, Duan C, Wang X, Wu X, Cao Y, Pu L, Lu D, Shen T *et al*: **SIRT1 suppresses doxorubicin-induced cardiotoxicity by regulating the oxidative stress and p38MAPK pathways**. *Cell Physiol Biochem* 2015, **35**(3):1116-1124.

242. Son SH, Lee SM, Lee MH, Son YK, Kim SE, An WS: **Omega-3 Fatty Acids Upregulate SIRT1/3, Activate PGC-1α via Deacetylation, and Induce Nrf1 Production in 5/6 Nephrectomy Rat Model**. *Mar Drugs* 2021, **19**(4).

243. Zhang J, Ren D, Fedorova J, He Z, Li J: **SIRT1/SIRT3 Modulates Redox Homeostasis during Ischemia/Reperfusion in the Aging Heart**. *Antioxidants (Basel)* 2020, **9**(9).

244. Naaz S, Mishra S, Pal PK, Chattopadhyay A, Das AR, Bandyopadhyay D: **Activation of SIRT1/PGC 1α/SIRT3 pathway by melatonin provides protection**

against mitochondrial dysfunction in isoproterenol induced myocardial injury. *Heliyon* 2020, **6**(10):e05159.

245. Renu K, V G A, P B TP, Arunachalam S: **Molecular mechanism of doxorubicin-induced cardiomyopathy - An update**. *Eur J Pharmacol* 2018, **818**:241-253.
246. Rawat PS, Jaiswal A, Khurana A, Bhatti JS, Navik U: **Doxorubicin-induced cardiotoxicity: An update on the molecular mechanism and novel therapeutic strategies for effective management**. *Biomed Pharmacother* 2021, **139**:111708.
247. Tsai WC, Guo S, Olaopa MA, Field LJ, Yang J, Shen C, Chang CP, Chen PS, Rubart M: **Complex Arrhythmia Syndrome in a Knock-In Mouse Model Carrier of the N98S**. *Circulation* 2020, **142**(20):1937-1955.
248. Bueno OF, De Windt LJ, Tymitz KM, Witt SA, Kimball TR, Klevitsky R, Hewett TE, Jones SP, Lefer DJ, Peng CF *et al*: **The MEK1-ERK1/2 signaling pathway promotes compensated cardiac hypertrophy in transgenic mice**. *EMBO J* 2000, **19**(23):6341-6350.
249. Xin M, Kim Y, Sutherland LB, Qi X, McAnally J, Schwartz RJ, Richardson JA, Bassel-Duby R, Olson EN: **Regulation of insulin-like growth factor signaling by Yap governs cardiomyocyte proliferation and embryonic heart size**. *Sci Signal* 2011, **4**(196):ra70.
250. Zhou Q, Li L, Zhao B, Guan KL: **The hippo pathway in heart development, regeneration, and diseases**. *Circ Res* 2015, **116**(8):1431-1447.
251. Matsuda T, Zhai P, Sciarretta S, Zhang Y, Jeong JI, Ikeda S, Park J, Hsu CP, Tian B, Pan D *et al*: **NF2 Activates Hippo Signaling and Promotes Ischemia/Reperfusion Injury in the Heart**. *Circ Res* 2016, **119**(5):596-606.
252. Xin M, Kim Y, Sutherland LB, Murakami M, Qi X, McAnally J, Porrello ER, Mahmoud AI, Tan W, Shelton JM *et al*: **Hippo pathway effector Yap promotes cardiac regeneration**. *Proc Natl Acad Sci U S A* 2013, **110**(34):13839-13844.
253. Shu ZP, Yi GW, Deng S, Huang K, Wang Y: **Hippo pathway cooperates with ChREBP to regulate hepatic glucose utilization**. *Biochem Biophys Res Commun* 2020, **530**(1):115-121.
254. Gao C, Wang Y: **YAP: The nexus between metabolism and cardiac remodeling**. *J Clin Invest* 2022, **132**(6).

255. Hu Y, Shin DJ, Pan H, Lin Z, Dreyfuss JM, Camargo FD, Miao J, Biddinger SB: **YAP suppresses gluconeogenic gene expression through PGC1α**. *Hepatology* 2017, **66**(6):2029-2041.

256. Sun A, Zou Y, Wang P, Xu D, Gong H, Wang S, Qin Y, Zhang P, Chen Y, Harada M *et al*: **Mitochondrial aldehyde dehydrogenase 2 plays protective roles in heart failure after myocardial infarction via suppression of the cytosolic JNK/p53 pathway in mice**. *J Am Heart Assoc* 2014, **3**(5):e000779.

257. Mazelin L, Panthu B, Nicot AS, Belotti E, Tintignac L, Teixeira G, Zhang Q, Risson V, Baas D, Delaune E *et al*: **mTOR inactivation in myocardium from infant mice rapidly leads to dilated cardiomyopathy due to translation defects and p53/JNK-mediated apoptosis**. *J Mol Cell Cardiol* 2016, **97**:213-225.

258. Romero-Becerra R, Santamans AM, Folgueira C, Sabio G: **p38 MAPK Pathway in the Heart: New Insights in Health and Disease**. *Int J Mol Sci* 2020, **21**(19).

259. Lavoie JN, L'Allemain G, Brunet A, Müller R, Pouysségur J: **Cyclin D1 expression is regulated positively by the p42/p44MAPK and negatively by the p38/HOGMAPK pathway**. *J Biol Chem* 1996, **271**(34):20608-20616.

260. Yue TL, Wang C, Gu JL, Ma XL, Kumar S, Lee JC, Feuerstein GZ, Thomas H, Maleeff B, Ohlstein EH: **Inhibition of extracellular signal-regulated kinase enhances Ischemia/Reoxygenation-induced apoptosis in cultured cardiac myocytes and exaggerates reperfusion injury in isolated perfused heart**. *Circ Res* 2000, **86**(6):692-699.

261. Bruick RK: **Expression of the gene encoding the proapoptotic Nip3 protein is induced by hypoxia**. *Proc Natl Acad Sci U S A* 2000, **97**(16):9082-9087.

262. Regula KM, Ens K, Kirshenbaum LA: **Inducible expression of BNIP3 provokes mitochondrial defects and hypoxia-mediated cell death of ventricular myocytes**. *Circ Res* 2002, **91**(3):226-231.

263. Webster KA, Graham RM, Bishopric NH: **BNip3 and signal-specific programmed death in the heart**. *J Mol Cell Cardiol* 2005, **38**(1):35-45.

264. Vande Velde C, Cizeau J, Dubik D, Alimonti J, Brown T, Israels S, Hakem R, Greenberg AH: **BNIP3 and genetic control of necrosis-like cell death through the mitochondrial permeability transition pore**. *Mol Cell Biol* 2000, **20**(15):5454-5468.

265. Hamacher-Brady A, Brady NR, Logue SE, Sayen MR, Jinno M, Kirshenbaum LA, Gottlieb RA, Gustafsson AB: **Response to myocardial ischemia/reperfusion injury involves Bnip3 and autophagy**. *Cell Death Differ* 2007, **14**(1):146-157.
266. Diwan A, Krenz M, Syed FM, Wansapura J, Ren X, Koesters AG, Li H, Kirshenbaum LA, Hahn HS, Robbins J *et al*: **Inhibition of ischemic cardiomyocyte apoptosis through targeted ablation of Bnip3 restrains postinfarction remodeling in mice**. *J Clin Invest* 2007, **117**(10):2825-2833.
267. Moslehi J, Minamishima YA, Shi J, Neuberg D, Charytan DM, Padera RF, Signoretti S, Liao R, Kaelin WG: **Loss of hypoxia-inducible factor prolyl hydroxylase activity in cardiomyocytes phenocopies ischemic cardiomyopathy**. *Circulation* 2010, **122**(10):1004-1016.
268. Murphy E, Steenbergen C: **Mechanisms underlying acute protection from cardiac ischemia-reperfusion injury**. *Physiol Rev* 2008, **88**(2):581-609.
269. Timmers L, Pasterkamp G, de Hoog VC, Arslan F, Appelman Y, de Kleijn DP: **The innate immune response in reperfused myocardium**. *Cardiovasc Res* 2012, **94**(2):276-283.
270. Bedard K, Krause KH: **The NOX family of ROS-generating NADPH oxidases: physiology and pathophysiology**. *Physiol Rev* 2007, **87**(1):245-313.
271. Matsushima S, Kuroda J, Ago T, Zhai P, Ikeda Y, Oka S, Fong GH, Tian R, Sadoshima J: **Broad suppression of NADPH oxidase activity exacerbates ischemia/reperfusion injury through inadvertent downregulation of hypoxia-inducible factor-1α and upregulation of peroxisome proliferator-activated receptor-α**. *Circ Res* 2013, **112**(8):1135-1149.
272. Sies H, Jones DP: **Reactive oxygen species (ROS) as pleiotropic physiological signalling agents**. *Nat Rev Mol Cell Biol* 2020, **21**(7):363-383.
273. Chow EJ, Aggarwal S, Doody DR, Aplenc R, Armenian SH, Baker KS, Bhatia S, Blythe N, Colan SD, Constine LS *et al*: **Dexrazoxane and Long-Term Heart Function in Survivors of Childhood Cancer**. *J Clin Oncol* 2023, **41**(12):2248-2257.
274. Novak R, Ingram M, Marquez S, Das D, Delahanty A, Herland A, Maoz BM, Jeanty SSF, Somayaji MR, Burt M *et al*: **Robotic fluidic coupling and interrogation of multiple vascularized organ chips**. *Nat Biomed Eng* 2020, **4**(4):407-420.
275. Huebsch N, Charrez B, Neiman G, Siemons B, Boggess SC, Wall S, Charwat V, Jæger KH, Cleres D, Telle Å *et al*: **Metabolically driven maturation of human-**

induced-pluripotent-stem-cell-derived cardiac microtissues on microfluidic chips. *Nat Biomed Eng* 2022, **6**(4):372-388.

276. Bhat S, Chin A, Shirakabe A, Ikeda Y, Ikeda S, Zhai P, Hsu CP, Sayed D, Abdellatif M, Byun J *et al*: **Recruitment of RNA Polymerase II to Metabolic Gene Promoters Is Inhibited in the Failing Heart Possibly Through PGC-1α (Peroxisome Proliferator-Activated Receptor-γ Coactivator-1α) Dysregulation**. *Circ Heart Fail* 2019, **12**(3):e005529.
277. Karamanlidis G, Garcia-Menendez L, Kolwicz SC, Lee CF, Tian R: **Promoting PGC-1α-driven mitochondrial biogenesis is detrimental in pressure-overloaded mouse hearts**. *Am J Physiol Heart Circ Physiol* 2014, **307**(9):H1307-1316.
278. Zhou B, Tian R: **Mitochondrial dysfunction in pathophysiology of heart failure**. *J Clin Invest* 2018, **128**(9):3716-3726.
279. Campo G, Pavasini R, Morciano G, Lincoff AM, Gibson CM, Kitakaze M, Lonborg J, Ahluwalia A, Ishii H, Frenneaux M *et al*: **Clinical benefit of drugs targeting mitochondrial function as an adjunct to reperfusion in ST-segment elevation myocardial infarction: A meta-analysis of randomized clinical trials**. *Int J Cardiol* 2017, **244**:59-66.
280. Sugamura K, Keaney JF: **Reactive oxygen species in cardiovascular disease**. *Free Radic Biol Med* 2011, **51**(5):978-992.
281. Lebakken CS, Riddle SM, Singh U, Frazee WJ, Eliason HC, Gao Y, Reichling LJ, Marks BD, Vogel KW: **Development and applications of a broad-coverage, TR-FRET-based kinase binding assay platform**. *J Biomol Screen* 2009, **14**(8):924-935.
282. Ghigo A, Mika D: **cAMP/PKA signaling compartmentalization in cardiomyocytes: Lessons from FRET-based biosensors**. *J Mol Cell Cardiol* 2019, **131**:112-121.
283. Calamera G, Li D, Ulsund AH, Kim JJ, Neely OC, Moltzau LR, Bjørnerem M, Paterson D, Kim C, Levy FO *et al*: **FRET-based cyclic GMP biosensors measure low cGMP concentrations in cardiomyocytes and neurons**. *Commun Biol* 2019, **2**:394.
284. Brown DA, Perry JB, Allen ME, Sabbah HN, Stauffer BL, Shaikh SR, Cleland JG, Colucci WS, Butler J, Voors AA *et al*: **Expert consensus document: Mitochondrial function as a therapeutic target in heart failure**. *Nat Rev Cardiol* 2017, **14**(4):238-250.

285. Oka S, Alcendor R, Zhai P, Park JY, Shao D, Cho J, Yamamoto T, Tian B, Sadoshima J: **PPARα-Sirt1 complex mediates cardiac hypertrophy and failure through suppression of the ERR transcriptional pathway**. *Cell Metab* 2011, **14**(5):598-611.

286. Xu W, Billon C, Li H, Wilderman A, Qi L, Graves A, Rideb JRDC, Zhao Y, Hayes M, Yu K *et al*: **Novel Pan-ERR Agonists Ameliorate Heart Failure Through Enhancing Cardiac Fatty Acid Metabolism and Mitochondrial Function**. *Circulation* 2024, **149**(3):227-250.